Università degli Studi di Padova

Dipartimento di Scienze Chirurgiche, Oncologiche e Gastroenterologiche

---

SCUOLA DI DOTTORATO DI RICERCA IN

ONCOLOGIA E ONCOLOGIA CHIRURGICA

XXIX CICLO

STUDY OF RHO GTPASES IN MULTIPLE MYELOMA: INVOLVEMENT OF RHOU IN DISEASE INITIATION AND PROGRESSION

Tesi redatta con il contributo finanziario della Fondazione Cariparo

Direttore della Scuola : Ch.ma Prof.ssa PAOLA ZANOVELLO

Supervisore : Dr. FRANCESCO PIAZZA

Dottorando : SARA JOSE' CANOVAS NUNES

INDEX

ABBREVIATIONS

B-ALL	B cell Acute Lymphocytic Leukemia
B-CLL	B cell Chronic Lymphocytic Leukemia
BM	Bone Marrow
BMECs	Bone Marrow Epithelial Cells
BMSC	Bone Marrow Stromal Cell
CCND2	Cyclin D2
CD	Cluster of Differentiation
Cdc42	Cell Division Control protein 42
CDC42SE1	Cdc42 Small Effector 1
Chp	Cdc42 homologous protein
CRAB	Calcium, Renal, Anemia and Bone abnormalities
DAPI	4′,6-diamidino-2-phenylindole
DAVID	Database for Annotation, Visualization and Integrated Discovery
DLBCL	Diffuse Large B Cell Lymphoma
DMEM	Dulbecco's Modified Eagle's Medium
ES	Enrichment Score
FISH	Fluorescence In Situ Hybridization
GAP	GTPase Activating Protein
GAPDH	Glyceraldehyde-3-phosphate dehydrogenase
GC	Germinal Center
GDP	Guanine nucleotide Diphosphate
GEF	Guanine nucleotide Exchange Factor
GO	Gene Ontology
GTP	Guanine nucleotide Triphosphate
GTPase	Guanosine Triphosphatase
HD	Hyperdiploid
HSCs	Hematopoietic Stem Cells
Ig	Immunoglobulin
IGH	Immunoglobulin Heavy chain
IL-6	Interleukin 6
IL-6R	Interleukin 6 Receptor
IMiDs	Immunomodulatory Drugs

JAK1	Janus kinase 1
JNK	c-Jun N-terminal kinase
MALT	Mucosa-Associated Lymphoid Tissue
MCL	Mantle Cell Lymphoma
MGUS	Monoclonal Gammopathy of Unknown Significance
miRNA21	Micro RNA 21
MM	Multiple Myeloma
OCs	Osteoclasts
PC	Plasma Cell
PCL	Plasma Cell Leukemia
PCP	Planar Cell Polarity
PIAS3	Protein Inhibitor of Activated STAT3
PIs	Proteasome Inhibitors
PTMs	Post-Translational Modifications
qRT-PCR	quantitative Real-Time PCR
RhoU	Ras homologue gene family member U
RhoV	Ras homologue gene family member V
RPMI	Roswell Park Memorial Institute 1640 Medium
SCR	Scrambled non-targeting siRNA
SH2	Src Homology 2
SH3	Src Homology 3
siRNA	small interfering RNA
sMM	Smoldering Multiple Myeloma
SMZL	Splenic Marginal Zone Lymphoma
SOCS3	Suppressor of Cytokine Signaling
STAT3	Signal Transducer and Activator of Transcription 3
T-ALL	T-cell Acute Lymphoblastic Leukemia
Wnt-1	Wnt family member 1
Wrch1	Wnt-responsive Cdc42 homologue 1

AMINO ACID ABBREVIATIONS

A	Ala	Alanine
C	Cys	Cysteine
D	Asp	Aspartic acid
E	Glu	Glutamic acid
F	Phe	Phenylalanine
G	Gly	Glycine
H	His	Histidine
I	Ile	Isoleucine
K	Lys	Lysine
L	Leu	Leucine
M	Met	Methionine
N	Asn	Asparagine
P	Pro	Proline
Q	Gln	Glutamine
R	Arg	Arginine
S	Ser	Serine
T	Thr	Threonine
V	Val	Valine
W	Trp	Tryptophan
Y	Tyr	Tyrosine
X	generic amino acid	

ABSTRACT

Multiple myeloma (MM) is a cancer of post-germinal center B cells characterized by a clonal proliferation of long-lived plasma cells inside the bone marrow. MM cells typically exhibit numerous structural and numerical chromosomal aberrations besides the presence of mutations in oncogenes and tumor-suppressor genes. Recently, a lot of attention has been drawn towards the tumor microenvironment. The interaction between malignant plasma cells and other cells inside the bone marrow is thought to be essential for the survival and expansion of MM. Indeed, stromal cells are able to produce growth factors that are important in sustaining the proliferation of MM cells, for example, interleukin-6 (IL-6).

IL-6 triggers the signal downstream of its receptor IL-6R, leading to the activation of the JAK/STAT pathway. An important target of this pathway is STAT3 transcription factor. STAT3 binds to the promotor region of a set of genes that regulate cell growth, proliferation, survival, mitosis, adhesion/migration, and are extremely important in controlling the inflammatory response.

RhoU is an atypical member of the Rho GTPase family that lies downstream of STAT3 activation. This GTPase is constitutively active whenever expressed and could mediate the effects of STAT3 in regulating the cytoskeleton dynamics. In MM nothing is known about this G protein. Here we demonstrate for the first time a role for RhoU in regulating the F-actin cytoskeleton of MM cells.

RhoU was found heterogeneously expressed in MM patients' cells, significantly modulated with disease progression, and expressed at higher levels in patients with bad prognosis mutations including t(4;14), del(13) and 1q gain. Different levels of RhoU mRNA correlate with a diverse gene expression profile in 557 genes. We have also found that it significantly clusters with cell cycle and DNA damage genes. Importantly, its expression positively correlates with cyclin D2 expression, and negatively correlates with the expression of cell cycle control and DNA damage response genes.

In MM cell lines, RhoU is over-expressed in IL-6 dependent cell lines, while its expression is down-modulated in those that can proliferate independently of IL-6 stimulus. MM cell lines were able to up-regulate RhoU mRNA expression in response to IL-6 stimulus through the activation of STAT3. RhoU silencing led to an accumulation of actin stress fibers, an increase in adhesion and a blockade in migration.

Lastly, immunomodulatory drugs (IMIDs) were recently found to control the activation of classical GTPases like Cdc42 and RhoA. In accordance with this, Lenalidomide positively regulated STAT3 activation leading to an increase in RhoU expression that resulted in a higher migration capability of MM cell lines, indicating that IMIDs can also alter the expression of atypical GTPases.

INTRUDUCTION

1. RHO GTPASES

The Rho family of small guanosine triphosphatases (GTPases) forms part of the Ras superfamily. Over 150 members comprise the Ras superfamily, which is divided into five major branches on the basis of sequence and functional similarities: Ras, Rho, Rab, Ran and Arf families (Wennerberg, Rossman and Der, 2005; Cox and Der, 2010). These GTPases share a common biochemical mechanism, acting as molecular switches to transduce the signal downstream to their effectors (Vetter and Wittinghofer, 2001).

It is important to note that the Ras family has been proven to profoundly influence cell growth and that activating mutations of Ras are associated with cancer (Aspenström, Ruusala and Pacholsky, 2007). In contrast with what happens with Ras oncogenes, Rho GTPases are hardly ever found mutated in cancer cells but often display altered activity in malignant cells when compared to healthy counterparts (Vega and Ridley, 2008). Rho GTPases are potent regulators of cytoskeleton dynamics and of the actin filament system, thereby affecting the morphologic and migratory properties of cells (Raftopoulou and Hall, 2004). Due to their important roles in controlling cell morphology, deregulated Rho GTPases could be at the basis of many tumorigenic processes and for this reason particular attention has been given to these proteins in the last few years.

To this moment, there are 21 identified GTPases in the Rho family, which can be further divided based on their sequence and functional resemblances and classified into eight subgroups (Figure 1). There are four groups of classical Rho GTPases: **Rho** that comprises RhoA, RhoB and RhoC; **Rac** that includes family members Rac1, Rac2, Rac3 and RhoG; **Cdc42** comprising Cdc42, RhoQ (also known as TC10) and RhoJ (also known as TC10-like protein, TCL); and **RhoD/F** with only two proteins, RhoF (also known as RAP1-interacting factor-1, RIF) and RhoD. And four groups of atypical GTPases: **Rnd** containing the members Rnd1, Rnd2 and Rnd3 (also known as RhoE); **RhoBTB** that comprises RhoBTB1, RhoBTB2 and RhoBTB3; **RhoH** that hosts RhoH alone; and lastly **RhoU/V** composed by RhoU (also known as WNT1-responsive Cdc42 homologue-1, Wrch1) and RhoV (also known as Cdc42 homologous protein, Chp).

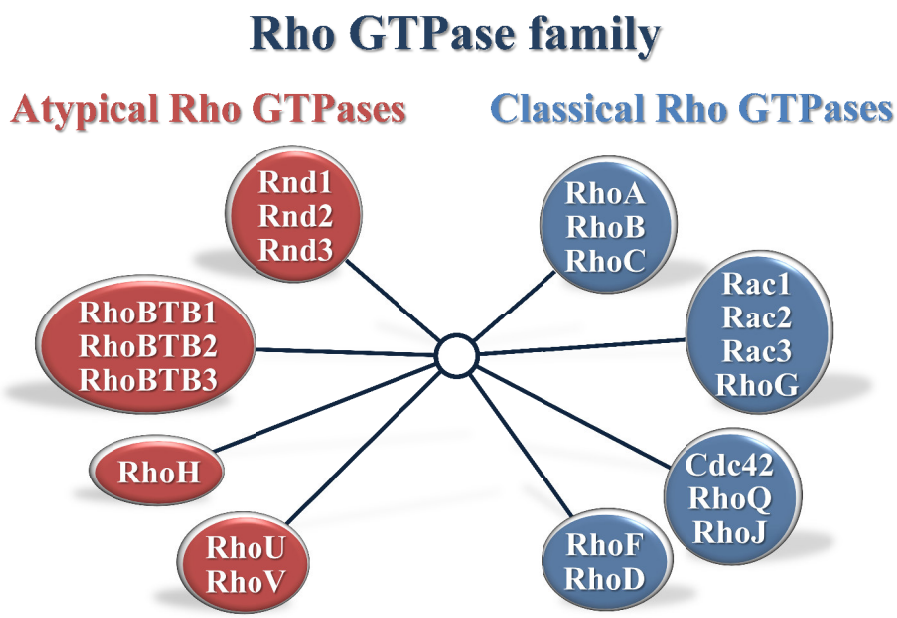

Figure 1: Illustration of the Rho GTPase family composed of its 8 subfamilies. The classical Rho GTPases cycle between active GTP-bound and inactive GDP-bound forms and are divided in four subfamilies: Rho (RhoA, RhoB and RhoC), Rac (Rac1, Rac2, Rac3 and RhoG), Cdc42 (Cdc42, RhoQ and RhoJ), RhoF/D (RhoF and RhoD). The atypical Rho GTPases, on the other hand, are prevalently GTP-bound and are thought to be regulated by other mechanisms, including phosphorylation and RNA expression levels. Atypical subfamilies are: Rnd (Rnd1, Rnd2 and Rnd3), RhoU/V (RhoU and RhoV), RhoH (RhoH alone) and RhoBTB (RhoBTB1, RhoBTB2 and RhoBTB3.

Classical Rho GTPases, like all other classical GTPases of the Ras superfamily, are activated by Guanine Nucleotide Exchange Factors (GEFs) that catalyze the exchange of GDP for GTP, whereas GTPase-Activating Proteins (GAPs) increase the intrinsic GTP hydrolysis rate, thereby inactivating them (Figure 2) (Fritz and Pertz, 2016). In this way, classical GTPases in different branches of the Ras superfamily keep cycling between active GTP-bound and inactive GDP-bound states and exhibit structurally distinct but mechanistically similar regulatory GAPs and GEFs (Vetter and Wittinghofer, 2001; Wennerberg, Rossman and Der, 2005).

In the active GTP-bound conformation, Rho GTPases interact with a range of effector proteins, including kinases, actin regulators and adaptor proteins, leading to changes in cell behavior(Fritz and Pertz, 2016). A single Rho GTPase can activate a broad range of cellular responses, depending on stimulus and cell type. For this reason the spatiotemporal regulation of each Rho GTPase is important to determine the outcome of its activity.

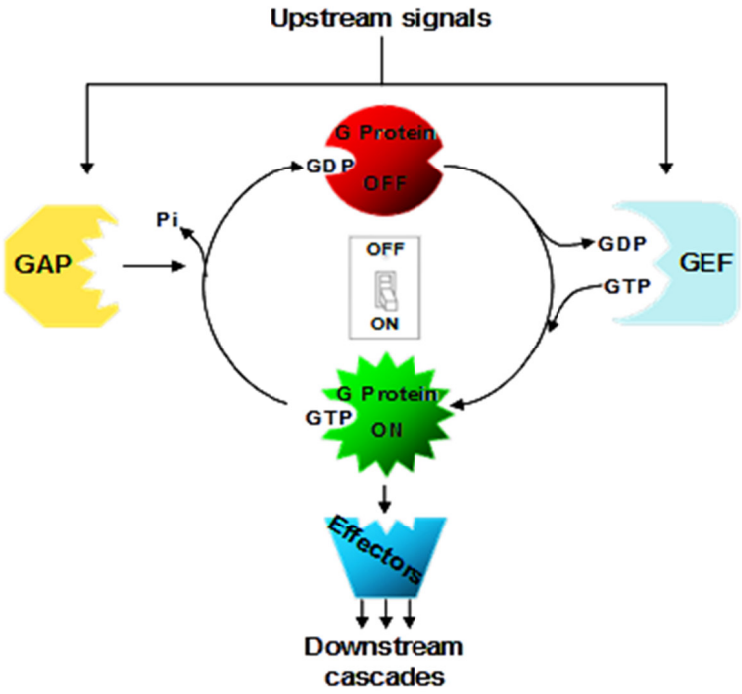

Figure 2: Classical Rho GTPase cycling. Rho GTPases act as "molecular switches" cycling between inactive GDP-bound and active GTP-bound state. Upstream signals act onto Rho GTPases through the activation of GEFs and GAPs. GEFs catalyze the exchange of GDP for GTP, activating Rho GTPases, and GAPs increase GTP hydrolysis thereby inactivating them. GTP-bound Rho GTPases are able to interact with effector proteins in activating downstream cascades.

Mechanisms other than cycling also affect Rho GTPase signaling. 'Atypical' GTPases, for example, are not generally regulated by GTP–GDP cycling and therefore do not require GEFs and GAPs. Instead, they are constitutively GTP-bound, because they either possess high intrinsic nucleotide exchange activity or have substitutions in their GTPase domain that prevent GTPase activity (Aspenström, Ruusala and Pacholsky, 2007). These atypical features strongly imply that members of these subgroups of GTPases need to be regulated by alternative mechanisms rather than just a simple switch of conformation (Chardin, 2006). Indeed, the expression of some atypical Rho GTPases has been shown to be tightly regulated at the transcriptional level, with a very rapid increase of its mRNA in response to upstream signals (Chardin, 2006; Aspenström, Ruusala and Pacholsky, 2007). Signaling by these GTPases is probably also controlled through other mechanisms, including post-translational modifications (PTMs) and gene expression alterations by microRNAs (Aspenström, Ruusala and Pacholsky, 2007).

Nowadays Rho GTPases are best known for their roles in regulating cytoskeletal rearrangements, cell motility, cell polarity, axon guidance, vesicle trafficking and recently the cell cycle (Hodge and Ridley, 2016). In fact, alterations in Rho GTPases signaling have been recently found to contribute to malignant transformation, neurological abnormalities and immunological diseases (Fritz and Henninger, 2015; Pajic *et al.*, 2015; Smithers and Overduin, 2016).

The knowledge on signaling networks involving Rho GTPases has increased in complexity and the studies on the atypical Rho GTPases have significantly broadened the concept of Rho-regulated biological pathways. Since disturbances in Rho GTPases functions are somehow related to oncogenic transformation, it is likely that dysfunctional atypical Rho GTPases could also play a role in this and several other disease conditions, which makes it important to increase our attention to these proteins and the biological processes in which they are involved.

2. RHOU/V SUBFAMILY

The two GTPases RhoU, also known as Wrch-1, and RhoV, also called Chp, form a distinct subfamily of Rho proteins related to Cdc42 and Rac1. In fact, human RhoU and RhoV proteins share 57% and 52% identity, respectively, with the well-known Cdc42 GTPase but they are functionally rather different (Aspenström, Ruusala and Pacholsky, 2007).

RhoU and RhoV are actually an example of Rho GTPases with atypical features but they do not exhibit amino acid substitutions which render them GTPase deficient like other atypical GTPases (Figure 3) (Shutes *et al.*, 2004; Vega and Ridley, 2008). These two GTPases display high intrinsic guanine nucleotide exchange activity and are thus thought to be constitutively active whenever expressed. Due to their spontaneous activation, they are expressed at very low levels in various tissues and organs (Boureux *et al.*, 2007).

Also, both proteins have an N-terminal proline-rich domain that is not present in any other Rho GTPase, enabling them to bind to Src homology 3 (SH3) domain-containing proteins (Figure 3). SH3 domains usually remain constitutively associated with their ligands and protein interactions connected to SH3 domains have been implicated in cytoskeletal alterations (Risse *et al.*, 2013). Interestingly, the presence of SH3 domain-

containing adaptors in Rac1 were found to be essential for its localization to focal adhesions but, opposite to Rac1, the N-terminal domain of RhoU was proved dispensable for its targeting to focal adhesions (Ory, Brazier and Blangy, 2007). Therefore, the functions of the N-terminal proline-rich domain of these two atypical GTPases still remain to be fully understood.

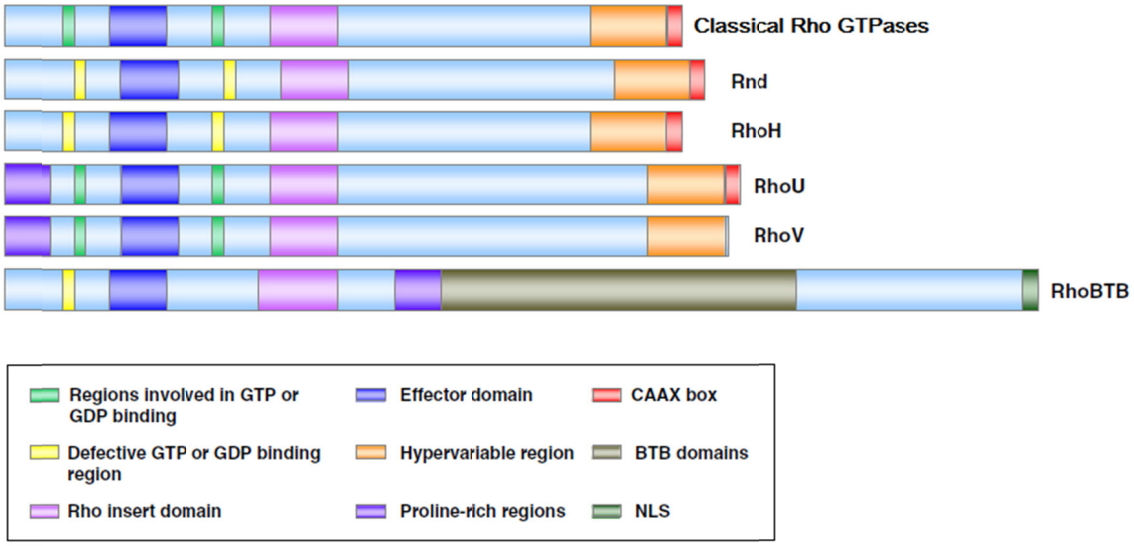

Figure 3: Domain organization of Rho GTPases. Classical Rho GTPases have similar basic protein structure while the Rnd and RhoH atypical proteins have modifications on the GTP/GDP binding region that make them lack GTPase activity. RhoU and RhoV have a structure similar to classical Rho GTPases with the addition of an N-terminal proline-rich region; also RhoV is missing the final CAAX box domain and instead has a unique 32 amino acid sequence. RhoBTB have the most divergent protein organization. (edited from: Vega and Ridley, 2008)

Besides their similarities, these proteins seem to have really different or even opposite roles in cytoskeleton regulation. Indeed, RhoU over-expression has been shown to highly increase cell motility (Ory, Brazier and Blangy, 2007) while RhoV over-expression had the opposite effect, negatively affecting the migratory phenotype of cells (Weisz Hubsman *et al.*, 2007).

3. RHOU

RhoU, as mentioned before, is an atypical G protein of the Rho GTPase family. Although it has no detectable GTPase activity, its very high intrinsic guanine nucleotide exchange activity is likely to ensure that the protein is predominantly in the GTP-loaded conformation (Dickover *et al.*, 2014). It is encoded by the *RHOU* gene at 1q42.13 (Figure 4). Its expression is mainly controlled at the RNA level downstream of 'Wnt family member 1' (Wnt-1) and 'signal transducer and activator of transcription 3' (STAT3) activation and it might mediate the effects of these signaling pathways in regulating cell morphology, cytoskeletal organization and proliferation (Schiavone *et al.*, 2009).

Figure 4: Location of *RHOU* gene in human chromosome 1. This gene present in the plus strand of chromosome 1 at 1q42.13, marked with the red arrow, is composed of 102023 bases and encodes for RhoU GTPase (*RHOU* gene in genomic location: bands according to Ensembl).

3.1. STRUCTURE

RhoU GTPase is a 258 amino acids' protein, with a molecular mass of around 28KDa (Gileadi *et al.*, 2007). The illustration of its secondary structure shows how alpha helices and beta sheets alternate to create its very complex secondary structure (Figure 5). The overall fold of RhoU resembles that of known GTPase structures but it possesses an extra helix between residues 168 and 177 (Gileadi *et al.*, 2007). As happens usually in GTPases, a magnesium ion is present in the nucleotide binding site and helps to stabilize phosphate groups.

RhoU also exhibits extended N- and C-terminal domains. The N-terminal extension promotes binding to SH3 domain-containing adaptors, whereas the C-terminal extension mediates membrane targeting through palmitoylation of its non-conventional CAAX box (Ory, Brazier and Blangy, 2007).

Its high intrinsic guanine nucleotide exchange activity suggests that this protein is constitutively GTP-bound, even though it has no measurable GTPase activity (Shutes *et al.*, 2004).

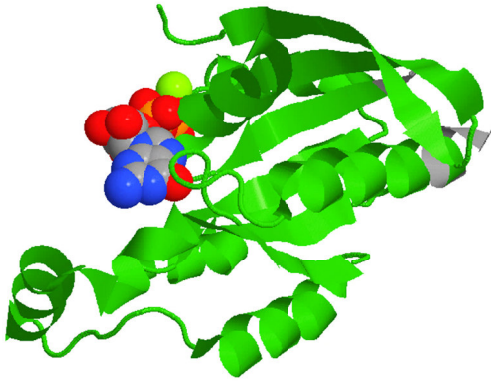

Figure 5: Structure of the GTPase RhoU in the inactive GDP-bound state (mutated RhoU Cys190Leu). Wild type *RHOU* produces a protein that is prone to aggregation and precipitation thus preventing further crystallographic analysis. A magnesium ion (green sphere) which helps to stabilize phosphate groups of the nucleotide is present in the guanine nucleotide binding site where GDP can be seen (Gileadi *et al.*, 2007).

3.2. FUNCTIONS

The biologic functions of this GTPase remain largely unknown. The most significant studies regarding the localization and functions of RhoU, after over-expression of GTP-bound protein, state that it localizes to focal adhesions in HeLa cells and to podosomes in osteoclasts, but it was also found to colocalize with the EGF receptor on endosomes after EGF stimulus in pancreatic cancer cells (Chuang *et al.*, 2007; Ory, Brazier and Blangy, 2007; Dickover *et al.*, 2014). Remarkably, all of these localizations led to the same output: a decrease in adhesion and an increase in cell migration rate. It is now clear that this protein acts on the actin cytoskeleton by stimulating filopodia formation and stress fiber dissolution, and that it also induces quiescent cells to re-enter the cell cycle (Tao *et al.*, 2001; Schiavone *et al.*, 2009).

In addition to experimental evidence, informatics tools as for example Gene Ontology (GO) predict that RhoU could be important for the following cell processes:

- G1/S transition of mitotic cell cycle (confirmed by experimental evidence in mice)

- Rac protein signal transduction
- actin cytoskeleton organization (confirmed by experimental evidence)
- regulation of cell shape (confirmed by experimental evidence)
- regulation of small GTPase mediated signal transduction (confirmed by experimental evidence)

and that it can localize to:

- Golgi membrane
- cell projections (confirmed by experimental evidence)
- cytosol
- focal adhesions (confirmed by experimental evidence)
- plasma membrane (confirmed by experimental evidence)
- podosomes (confirmed by experimental evidence)

The broad spectrum of localizations and processes where RhoU can intervene, call the attention to the impact this protein could have in cancer and autoimmunity, situations where these subcellular components are under stress and these processes are deregulated.

It is important to notice that different levels of this GTPase might lead to diverse outcomes in cell morphology. Indeed, during epithelial-mesenchymal transition of neural crest cells, high levels of RhoU have been described to influence cell polarity and migration while low levels were required for cell adhesion (Fort *et al.*, 2011).

3.3. REGULATION

RhoU protein, as stated before, is not regulated by GTP-GDP cycling and for this reason does not request the action of GEFs and GAPs. Instead, the expression of this protein is mostly regulated at the mRNA level.

Its gene is a common transcriptional target of both the gp130/STAT3 and Wnt-1/planar cell polarity (PCP) pathways (Schiavone *et al.*, 2009). Two functional STAT3-binding sites were identified on the *RHOU* promoter however, RhoU induction by Wnt-1 was proven to be independent of β-catenin (not involving STAT3) and seems to be mediated by the Wnt/PCP pathway through the activation of JNK (Schiavone *et al.*, 2009). Both the non-canonical Wnt and STAT3 pathways are therefore able to induce RhoU expression, which in turn might be involved in mediating their effects on cell migration and adhesion.

Even though the regulation of RhoU expression occurs mostly at the mRNA level, its membrane association, subcellular localization, and biological activity might be mediated by a novel membrane-targeting mechanism that differs from other GTPases. In fact, RhoU terminates in a CAAX tetrapeptide motif that is modified by the fatty acid palmitate (Berzat *et al.*, 2005). Palmitoylation of its non-conventional CAAX box regulates RhoU localization to the cell membrane and pharmacologic inhibition of CAAX palmitoylation leads to RhoU mislocalization, and could have an inhibitory effect on its function (Ory, Brazier and Blangy, 2007).

3.4. RHOU IN TUMORIGENESIS

Rho GTPases are involved directly or indirectly in most steps of cancer initiation and progression, from unlimited proliferation and apoptosis evasion, to migration, invasion and metastasis (Vega and Ridley, 2008). Unlike its close relative Ras, Rho proteins are rarely mutated in cancer cells but their expression and activity are frequently affected. Several GTPases are up-regulated in some human tumors and are thought to be pro-oncogenic, importantly Cdc42 and Rac1 that have been extensively studied in the last few years. In fact, they have been shown to be involved in tumor growth, progression, metastasis, and angiogenesis. In solid tumors it has recently become clear that cancer cells dynamically regulate Rac1 and Cdc42 activity to promote transformation, cancer development, invasion and metastasis (Pajic *et al.*, 2015). When it comes to the bone marrow (BM) microenvironment, adhesion and migration abnormalities in hematopoietic stem cells (HSCs) were also proven to be associated with increased Cdc42 and Rac1 activation that leads to an increased mobilization of HSCs out of the BM cavity (Yang *et al.*, 2001). Indeed, Cdc42−/− mice have increased numbers of HSCs circulating away from BM niches, as well as profound defects in homing activities (Yang *et al.*, 2007). Moreover, in accordance with its involvement in homing and mobilization, Rac1 expression was recently associated with leukemia cell chemotherapy resistance, quiescence and niche interaction (Wang *et al.*, 2013).

Even though RhoU is strictly related to Rac1 and Cdc42, little research has been conducted on this protein and its role in cancer biology and pathology remains still incognito. However, few papers seem to prove a role for this GTPase in altering cell morphology and migration capabilities that could be of great importance in understanding its role in blood tumorigenesis. For example, Brazier *et al.* (2006) showed that silencing

RhoU expression severely inhibited differentiation of BM macrophages and HSCs, and affected osteoclast morphology. Then again, van Helden *et al.* (2012) obtained contrasting results thus leaving some questions unanswered. Also, RhoU depletion in T-cell acute lymphoblastic leukemia (T-ALL) cell lines inhibited cell migration and chemotaxis; and T-ALL cell migration through RhoU up-regulation contributed to leukemia cell dissemination (Bhavsar *et al.*, 2013).

4. B CELL DIFFERENTIATION

B cells develop from hematopoietic precursor cells in the BM through a methodical maturation and selection process (Figure 6). B cell differentiation process involves two phases: an antigen-independent process that occurs in the BM, and an antigen-dependent process that occurs in the lymphoid tissue.

In the first, stem cells in the BM give rise to a common lymphoid progenitor that through multiple steps of differentiation will become an immature B cell (Pieper, Grimbacher and Eibel, 2013). This immature B cell will enter peripheral circulation and suffer alternative splicing that results in the production of new immunoglobulin (Ig) chains. In the primary lymphoid follicle, it will further differentiate into the so called mature naive B cell. By entering circulation this cell can now bind to a specific antigen in the lymphoid tissue and initiate the second phase of the maturation process (Fairfax *et al.*, 2008; Pieper, Grimbacher and Eibel, 2013). The activated B cell will enter a loop of proliferation, alternative splicing, isotype switching, and somatic hypermutations that give rise to short- and long-lived plasma cells (PCs) that secrete unspecific and specific antibodies, respectively, and to memory B cells (Fairfax *et al.*, 2008). Antibody producing PCs will fight the current infection while memory B cells recirculate and prepare for a future infection by the same antigen. Long-lived PCs can then migrate to the BM, where they will find a survival niche. There they remain alive and able to continue to produce antibodies, however they do not proliferate (Fairfax *et al.*, 2008).

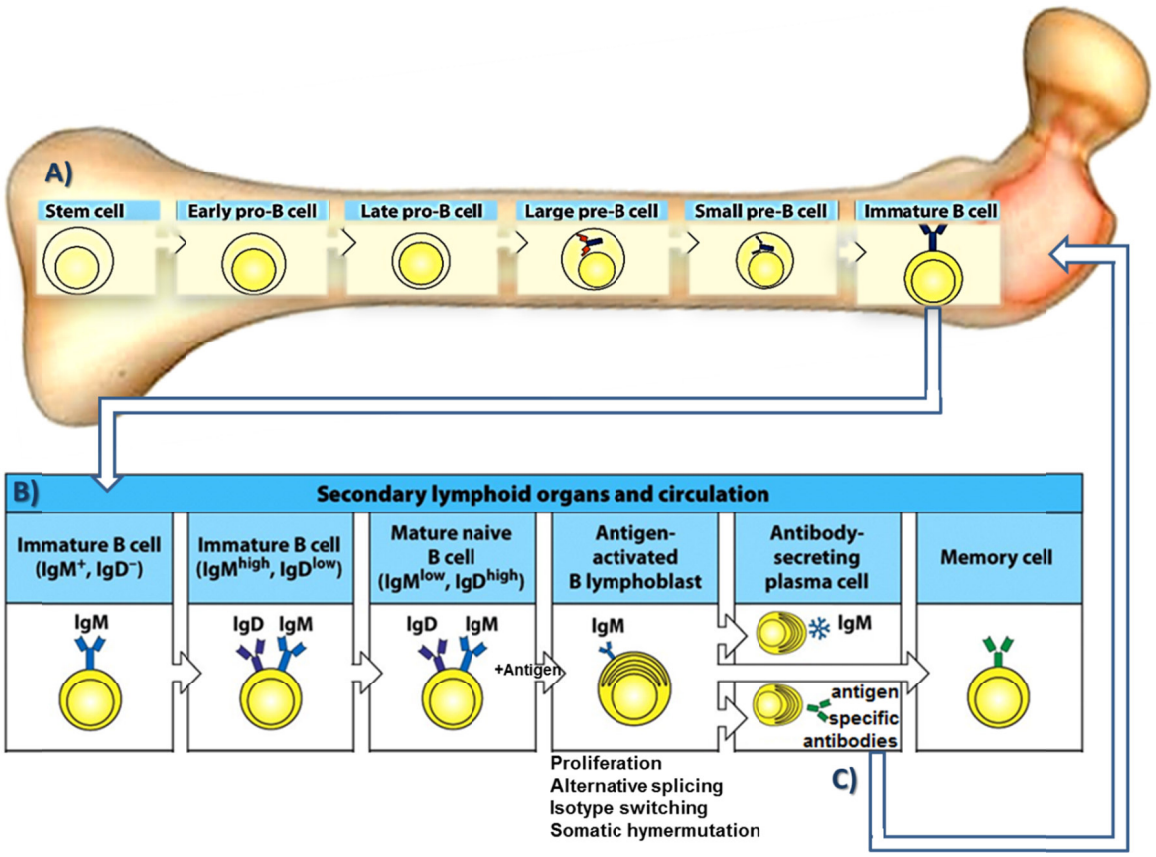

Figure 6: B cell maturation and differentiation process. A) In the BM, stem cells give rise to a common lymphoid progenitor that through multiple steps of differentiation will give rise to an immature B cell. B) The immature B cell will enter peripheral circulation, suffer alternative splicing that results in the production of new Ig chains and move to the primary lymphoid follicle where it will further differentiate into the so called mature naive B cell and enter circulation. If it binds to a specific antigen in the lymphoid tissue the second differentiation phase will begin where the activated B cell enters a loop of proliferation, alternative splicing, isotype switching, and somatic hypermutations, giving rise to short- and long-lived PCs and to memory B cells. C) Long-lived PCs can then migrate back into the BM where they will reside.

Specific cluster of differentiation (CD) markers such as: CD19, CD20, CD27, CD38 and CD138 are helpful to distinguish the transitional phases through which B cells pass during maturation (Dalakas, 2008). CD19 is expressed throughout B maturation from Pre-B cells to memory B cells but it is not expressed in PCs. The only difference between CD19 and CD20 is that the latter is not expressed in Pre-B cells. CD27 and CD38 on the other hand are expressed only at late stages of B cell development (after the transition of activated B cells) in memory B cells, early and late PCs. The surface marker present only in PCs and that allows their recognition is CD138.

B cell malignancies have been associated with distinct stages of B cell development (Rickert, 2013):

- B cell acute lymphocytic leukemia (B-ALL) arises from pre-B cells;
- B cell chronic lymphocytic leukemia (B-CLL) derives from mature B cells;
- Mantle cell lymphoma (MCL) also arises from circulating mature B cells;
- Splenic marginal zone lymphoma (SMZL) and mucosa-associated lymphoid tissue (MALT) lymphoma both derive from marginal zone B cells;
- Follicular lymphoma, diffuse large B cell lymphoma (DLBCL) and Burkitt's lymphoma are all derived from germinal center (GC) B cells;
- Multiple Myeloma (MM) is a GC-derived PC malignancy that persists in the BM and most of the times is dependent on BM stromal cell (BMSC) contact and cytokines such as interleukin-6 (IL-6).

Malignant cells often express CD markers that are not present or that are expressed at different stages in normal cells. Some malignant B cells can actually express T cell markers (Boyd *et al.*, 2013). Besides the expression of different cell surface markers, malignant cells can also express the same surface markers but at different densities, for example the majority of MM cells express higher CD138 and CD38 than normal PCs (Kumar, Kimlinger and Morice, 2010).

5. MULTIPLE MYELOMA

MM is a post-GC cancer characterized by a multifocal proliferation of clonal, long-lived PCs within the BM that can be clearly observed by the high amounts of $CD138^{+}$ cells in a BM biopsy (Figure 7). Overproliferation of malignant PCs leads to osteolytic bone lesions and hypercalcemia, and can cause BM suppression (pancytopenia) (Anderson and Carrasco, 2011). Malignant PCs produce defective antibodies, known as monoclonal M proteins. The production of M proteins by MM cells besides causing blood hyperviscosity and renal complications, leads also to a decrease of normal immunoglobulins levels, increasing the risk of infection (Landgren *et al.*, 2009).

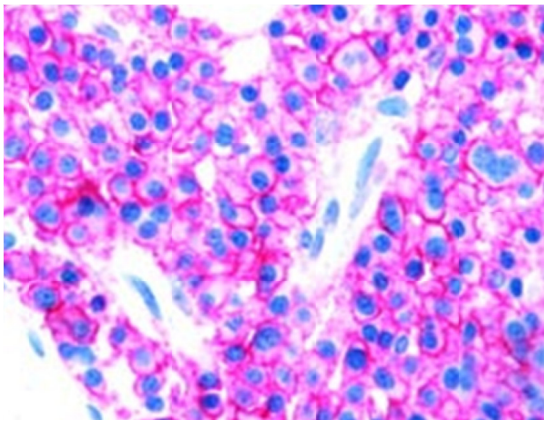

Figure 7: Anti CD138 staining in a BM biopsy of a MM patient (Bayer-Garner *et al.*, 2001)

MM cells, like normal long-lived PCs, are highly dependent on the BM microenvironment that activates multiple pathways that protect these cells from apoptosis (Noonan and Borrello, 2011). The BM microenvironment is composed of several cell types involved in the evolution and progression of MM: BMSCs, Osteoclasts (OCs), BM epithelial cells (BMECs), Osteoblasts, erythrocytes, HSCs, progenitors and precursor cells (Podar, Chauhan and Anderson, 2009). IL-6, primarily produced by BMSCs, is the best characterized MM growth factor and is highly responsible for cell homing, seeding, proliferation and survival (Morgan, Walker and Davies, 2012).

5.1. PROGRESSION AND PATHOBIOLOGY

MM is a multistep malignancy (Figure 8) preceded by an age-progressive premalignant condition called monoclonal gammopathy of unknown significance (MGUS) (Anderson and Carrasco, 2011; Morgan, Walker and Davies, 2012). However, MGUS is present in 1% of adults over the age of 25 and progresses to MM at a rate of 0.5-3% per year, with a 30% probability to develop MM over a 25 years follow-up (Bladé *et al.*, 2008; Landgren *et al.*, 2009).

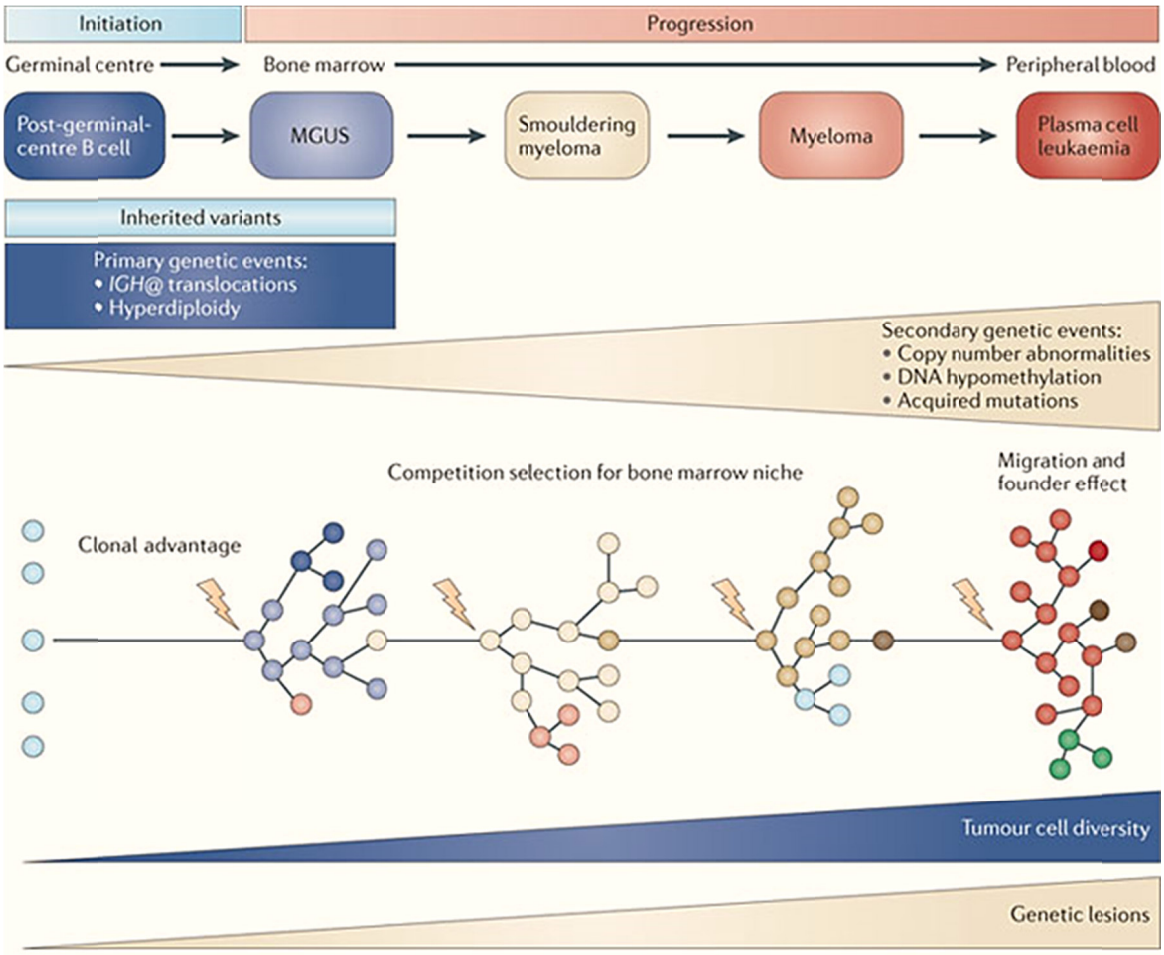

Figure 8: Initiation and progression of myeloma. MGUS is an indolent, asymptomatic condition that precedes MM malignancy; sMM is a myeloma that lacks clinical features; symptomatic MM, on the other hand, has various clinical features including osteolytic bone lesions; PCL is the last and most aggressive stage of this disease where cells can be found at extramedullary sites and as circulating cells (Morgan, Walker and Davies, 2012).

Some patients pass through a phase called smoldering myeloma (sMM), in which some of the diagnosis criteria for MM are met: serum M protein ≥ 3g per 100ml and BM PCs ≥ 10%, but there are no clinical manifestations. MM on the contrary, has various clinical features that are referred to as CRAB (calcium, renal, anemia and bone abnormalities) (Morgan, Walker and Davies, 2012). The last and most aggressive stage of the disease is called plasma cell leukemia (PCL) and at this point MM PCs are no longer restrained to grow within the BM and can be found at extramedullary sites and as circulating cells in the peripheral blood (Anderson and Carrasco, 2011; Morgan, Walker and Davies, 2012).

MM malignancy is characterized by markedly heterogeneous chromosomal aberrations, in particular, translocations involving the immunoglobulin heavy chain locus at 14q32 and different chromosomal partners occur in approximately 60% of MM cases (Fonseca *et al.*, 2004). The most recurrent of these translocations include t(11;14)(q13;q32), t(4;14)(p16.3;q32), t(6;14)(p21;q32), t(14;16)(q32; q23), and t(14;20)(q32;q11) that lead to a deregulation of *CCND1*, *FGFR3* and *MMSET*, *CCND3*, *MAF*, and *MAFB* genes respectively (Agnelli *et al.*, 2005).

After the evolution towards a malignant phenotype, MM cells can develop through two already described types of subclonal evolution: "linear" with the accumulation of genetic events or "branching" with early divergence of subclones with different mutations, which are differentially selected during disease progression (Morgan, Walker and Davies, 2012; Corre, Munshi and Avet-Loiseau, 2015). In fact, distinct phenotypic subclones can be observed in as much as 30% of newly diagnosed MM patients, supporting the existence of a branching evolution (Paíno *et al.*, 2015). This characteristic makes the disease even more heterogeneous and thus more difficult to study since different clones from the same patient can have different translocations and gene expression profiles.

5.2. PROGNOSIS

In the last few years a new way of dividing patients in subgroups that could allow doctors to better define strategies for risk-adapted therapy has been developed. It is the so called stratification into TC (translocations/cyclins) groups (Table 1).

Table 1: MM stratification into TC subgroups

TC Group	Primary translocation	D-Cyclin	Ploidy	Frequency in newly diagnosed MM
TC1	t(11;14) t(6;14)	D1 D3	NH	25%
TC2	None	D1 (low to moderate)	H	25%
TC3	None	D2	H/NH	30%
TC4	t(4;14)	D2	NH > H	15%
TC5	t(14;16) t(14;20)	D2	NH	5%

Patients can be stratified into 5 groups: TC1, characterized by the t(11;14) or t(6;14) translocation, with the consequent over-expression of CCND1 or CCND3, and a non-hyperdiploid status; TC2, showing low to moderate levels of the CCND1 gene in the absence of any primary Ig heavy chain (IGH) translocations but associated with a hyperdiploid status; TC3, including tumors that do not fall into any of the other groups, most of which express CCND2; TC4, showing high CCND2 levels and the presence of the t(4;14) translocation; and TC5, expressing the highest levels of CCND2 in association with either the t(14;16) or t(14;20) translocation (Hideshima *et al.*, 2004; Agnelli *et al.*, 2005).

This stratification can aid in the correct identification of patients at higher risk of early death, and is important in establishing proper treatment and a closer surveillance. Patients that fall into the TC4 and TC5 groups with t(4;14), t(4;16) or t(4;20) are designated "high-risk patients" (Fonseca, 2007). However, high levels of CCND2 have also been associated with a bad prognosis (Bergsagel *et al.*, 2005), and this renders all the patients with high CCND2 in the TC3 group high risk patients as well. Other high-risk factors are 1q gain, del(13) and hypodiploidy that can be used to further stratify patients into standard-risk or high-risk (Fonseca, 2007).

5.3. TREATMENT OPTIONS

In the last decade, several agents like proteasome inhibitors (PIs) and immunomodulatory drugs (IMiDs), with singular mechanisms of action have been discovered, developed and approved (Kumar *et al.*, 2008; Palumbo and Anderson, 2011).

Currently, the Food and Drug Administration (FDA) has approved 8 drugs for the treatment of MM and 9 others are currently in phase III clinical trials (Figure 9) (Ocio *et al.*, 2014). However, the most commonly used drugs for the treatment of MM remain Bortezomib, one of the two PIs approved, and Lenalidomide, one of the three IMIDs approved.

The advances made in the last decade in developing new treatments options for MM patients have resulted in a clear improvement in overall survival, but despite this MM remains incurable and patients who become refractory or ineligible to receive Bortezomib or IMIDs have a very poor prognosis (Kumar *et al.*, 2012).

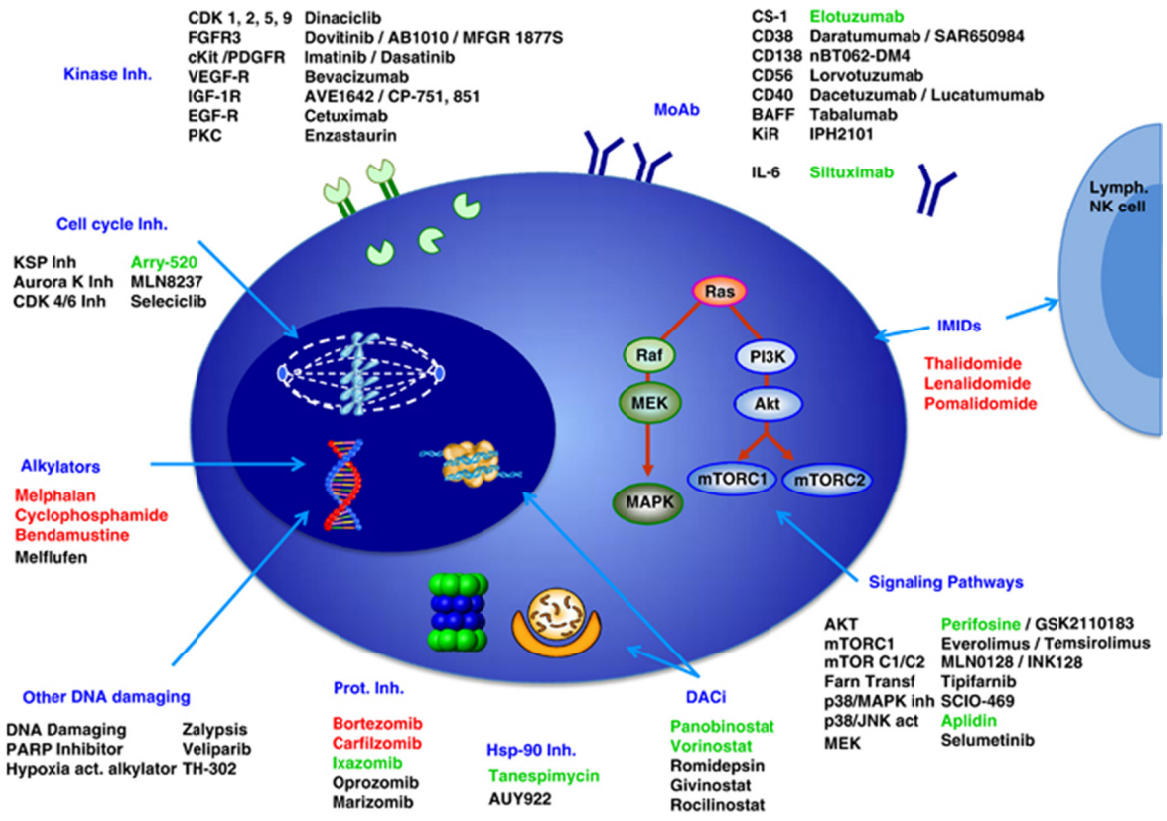

Figure 9: Targeted therapies in MM. Schematic representation of the main targets and drugs in MM: in red the approved drugs and in green those that have reached phase III clinical trials (Ocio *et al.*, 2014).

Long-term complete responses in MM patients are rare and the median survival with standard therapy is of about 3 years (Ocio *et al.*, 2014). Another relevant option for these patients is autologous stem cell transplantation that may prolong progression free survival, but it's not curative (Kumar *et al.*, 2008).

5.4. LENALIDOMIDE

Lenalidomide is a member of a class of molecules that have been termed IMiDs, and has significant therapeutic activity in diseases such as MM, myelodysplastic syndrome with del(5q) and MCL (Guirguis and Ebert, 2015).

Even though IMiDs represent an important class of anticancer and anti-inflammation drugs, the majority of the molecular mechanisms through which they exert their effects are currently undefined. IMiDs are Thalidomide derivatives that, although structurally

related, have their unique set of anti-inflammatory, immunomodulatory, anti-proliferative, antiangiogenic and toxicity profiles (Anderson, 2005). Thalidomide is a drug known by many because of its use as an oral sedative and anti-emetic in 1957 that had profound teratogenic effects. However, it found its use as a novel anti-myeloma drug for relapsed and refractory disease in 1999 (Strasser and Ludwig, 2002). Thalidomide, though effective, was associated with dose-limiting toxicities including somnolence, constipation, neuropathy, and increased incidence of venothromboembolism (Latif *et al.*, 2012). Two other FDA approved IMiDs for MM treatment are Lenalidomide and Pomalidomide that have very similar structural features (Figure 10).

IMiDs have been recently reported to be involved in the regulation of Rho GTPases as part of their mechanism of action. However, only a few classical Rho GTPases where studied in depth.

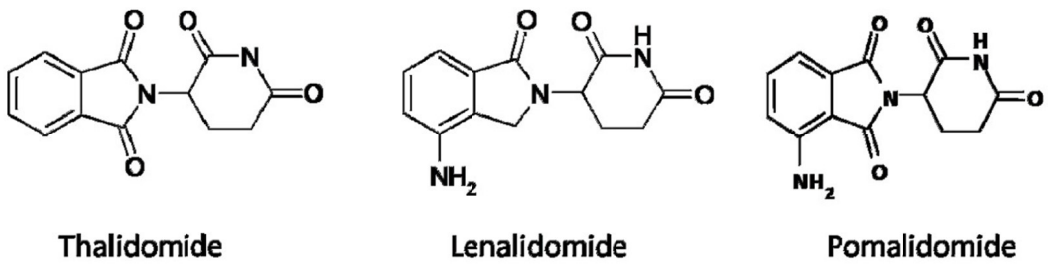

Figure 10: Molecular structures of Thalidomide and its analogues. Thalidomide, Lenalidomide and Pomalidomide are the three IMiDs approved by the FDA for the treatment of MM patients (Latif *et al.*, 2012).

Lenalidomide was proven to repair chronic lymphocytic leukemia T-cell defects in migration, restoring normal Rho GTPase activation signaling, particularly of RhoA, Rac1 and Cdc42, usually altered in this malignancy (Ramsay *et al.*, 2013). Also, its closely related compound Pomalidomide has been associated with an increase in RhoA and Rac1 activation, leading to enhanced F-actin formation, stabilized microtubules, and increased cell migration (Xu *et al.*, 2009).

To this moment nothing is known about the impact of these drugs on all other classical GTPases or on the expression of atypical GTPases like RhoU.

6. IL-6 AND STAT3 SIGNALING

The interaction between MM cells and the surrounding BM microenvironment leads to the expression and secretion of a set of chemokines and cytokines that provide essential support for the survival and expansion of MM cells. The best characterized MM growth factor is the cytokine IL-6 which is presumed to play an important role in its pathogenesis and malignant growth (Morgan, Walker and Davies, 2012).

IL-6 stimulus activates the IL-6 receptor (IL-6R) signaling and triggers the phosphorylation of STAT3 via Janus kinase 1 (JAK1), and for this reason it is of no surprise that in MM patients STAT3 was found to be constitutively activated (Bommert, Bargou and Stühmer, 2006).

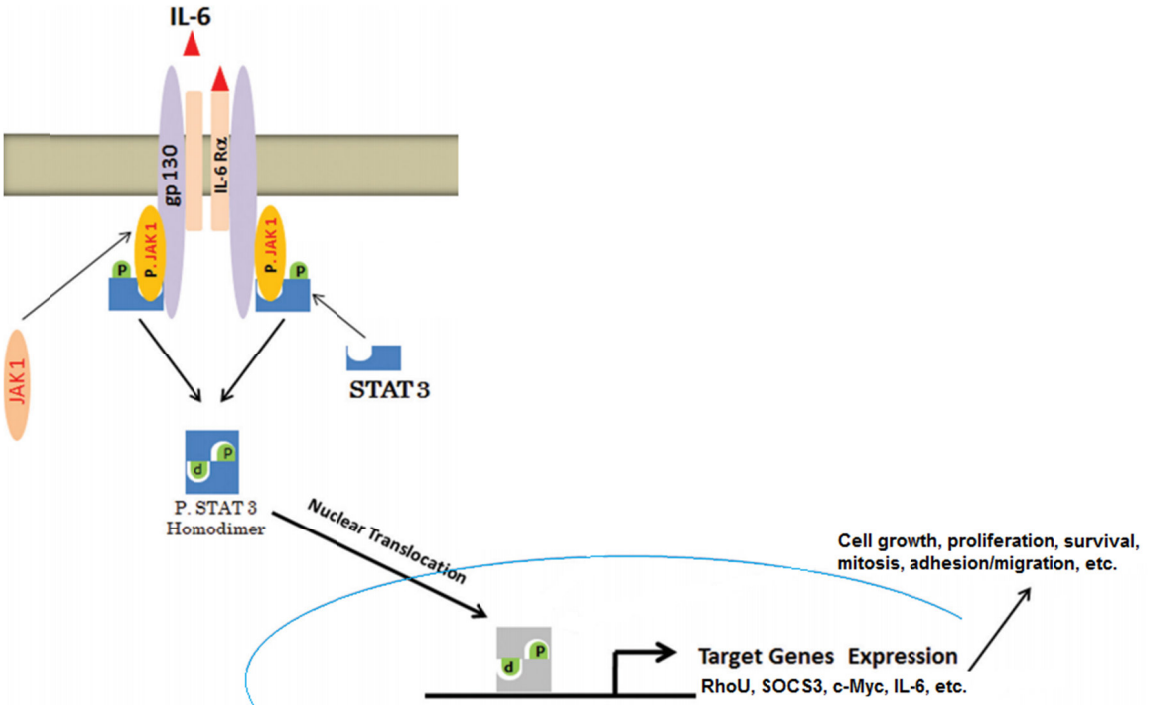

Figure 11: IL-6 signaling and activation of the JAK/STAT pathway. IL-6 cytokine binds to the IL-6R triggering the phosphorylation of STAT3 via JAK1. Phospho-STAT3 can dimerize and thus locate to the nucleus where it acts as a transcription factor of a large number of genes involved in a variety of cellular processes (edited from: Abroun *et al.*, 2015).

When phosphorylated, STAT3 can form homodimers that transit from the cytoplasm into the nucleus and regulate fundamental biological processes by activating the

expression of genes that control cell growth, proliferation, survival, mitosis, adhesion/migration, etc. (Figure 11) (Abroun *et al.*, 2015). RhoU is one of STAT3 target genes and could mediate its effects on changing cytoskeleton dynamics that enable cell migration or adhesion (Schiavone *et al.*, 2009).

Upon transient activation, STAT3 will work as a transcription factor of *IL-6* and of *STAT3* itself inducing the inflammatory response (Abroun *et al.*, 2015). On the other hand, a prolonged STAT3 activation will result in the transcription of 'suppressor of cytokine signaling 3' (SOCS3), which might either act directly by binding to JAK and inhibiting its activation or by facilitating the ubiquitination and subsequent proteasome degradation of essential proteins of this pathway, blocking in this way the propagation of the IL-6 signal (Carow and Rottenberg, 2014).

Moreover, other genes in this pathway might be of great importance in MM malignancy. For example, STAT3 can directly bind the transcription initiation site of the oncologic micro RNA 21 (miR21) or its upstream enhancer that contains two strictly conserved STAT3 binding sites, thereby promoting the expression of miR21 in MM cells (Löffler *et al.*, 2007; Iliopoulos *et al.*, 2010). A higher expression of miR21 promotes the survival of MM cells and blocks apoptosis by inhibiting the function of protein inhibitor of activated STAT3 (PIAS3), enhancing in this way the STAT3-dependent signaling pathway (Xiong *et al.*, 2012). These results clearly prove a positive feedback loop between miR21 and STAT3 that is probably essential for MM disease initiation and progression.

6.1. STATTIC: A STAT3 INHIBITOR

Since STAT3 is highly activated in a large number of cancers due to aberrant upstream signaling, it soon became an interesting target for cancer therapy. The Src Homology 2 (SH2) domain of STAT proteins is required for both tyrosine-phosphorylation and dimerization (Coleman *et al.*, 2005). A simple approach for the inhibition of STATs, in this case STAT3, would be to impair the functionality of its SH2 domain. Screening of chemical libraries resulted in the identification of a non-peptidic small molecule which was given the name Stattic (Figure 12), able to selectively inhibit STAT3 functions by binding to its SH2 domain regardless of the STAT3 activation state *in vitro* (Schust *et al.*,

2006). This mechanism of action enables Stattic to selectively inhibit STAT3 activation and dimerization, consequently abrogating its nuclear translocation, thus blocking the JAK/STAT signaling cascade.

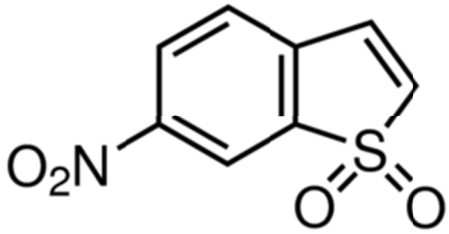

Figure 12: Stattic chemical structure. Stattic is a non-peptidic molecule that specifically binds to the SH2 domain of STAT3, directly inhibiting its functions as a transcriptional factor (Coleman *et al.*, 2005).

AIM OF THE STUDY

In MM, malignant PCs that resist chemotherapy and repopulate the BM are responsible for patients' relapse. Over the last few years, a lot of attention has been drawn to the BM microenvironment and to the interaction between MM cells and BMSCs. BMSC-produced soluble factors, like the IL-6 cytokine, are believed to impinge on MM intracellular signaling and cytoskeletal properties, protecting it from cytotoxic agents. The atypical Rho GTPase RhoU displays spontaneous activation and is expressed at low levels in most tissues and organs. This protein might mediate the effects of IL6R/STAT3 signaling in inducing filopodium formation and stress fiber dissolution, both critical steps in promoting cell motility. While typical Rho proteins (that share significant sequence homology with RhoU) as Cdc42 and Rac1 have an established role in cancer, very little is known about RhoU in tumorigenesis, in particular in hematologic malignancies.

Knowing that RhoU can alter cell adhesion, actin dynamics and cell motility, we hypothesize that this protein might mediate the adhesion of myeloma cells to the BM microenvironment, and that changes in its expression, and thus activity, might lead to a remodeling of MM associated BM niches.

This project aimed to investigate:

1) Rho GTPases expression in normal versus malignant PCs.
2) Rho GTPases expression in the different MM subgroups (TC groups).
3) The pathway(s) responsible for RhoU modulation in MM malignancy.
4) RhoU expression changes in MM and the impact it might have in adhesion, migration/motility and structural features (actin cytoskeleton dynamics) of malignant PCs.
5) The role of RhoU in malignant PC-BMSCs adhesion and in the creation of protective BM niches.
6) If immunomodulatory drugs like Lenalidomide, known to alter microenvironment signaling, have an effect on RhoU expression.

MATERIAL AND METHODS

PATIENT SAMPLES AND HEALTHY DONORS

Patient samples were collected in collaboration with Professor Antonino Neri's group (University of Milan, Italy). The study was performed in a cohort of 165 patients, representative of all the major forms of PC dyscrasia. This dataset, publicly available at the NCBI Gene Expression Omnibus repository (accession #GSE66293), includes 4 normal controls (Voden, Medical Instruments IT), 129 MM, 24 pPCL, and 12 sPCL patients. With the exception of sPCL, the cohort consists of newly-diagnosed patients. The proprietary 129 MM tumors employed for the study were representative of the major molecular characteristics of the disease. Samples were characterized for the presence of the most frequent chromosomal translocations and the ploidy status based on fluorescence in situ hybridization (FISH) evaluation criteria. Specifically, forty-eight showed an hypodiploid (HD) status; thirty-four were characterized by the t(11;14) or t(6;14) translocations; nineteen had the t(4;14) translocation; six had either the t(14;16) or t(14;20) translocations; and twenty-two did not fall into any of the other groups.

To better analyze RNA profile changes during disease progression, we have used the publicly available NCBI Gene Expression Omnibus repository accession # GSE47552, a dataset composed of 5 healthy controls, 20 MGUS, 33 SMM and 41 MM (López-Corral *et al.*, 2014).

PLASMA CELL SEPARATION

PCs were purified from BM samples using CD138 immunomagnetic microbeads (MidiMACS system, Miltenyi Biotec, Auburn, CA) according to manufacturer's protocol and the purity of the positively selected PCs, assessed by FACSCanto, was > 90% in all cases.

CELL LINES

INA-6 cell line was a kind gift from Professor Nicola Giuliani (University of Parma, Italy); U266, H929 and RPMI 8226 were purchased from ATCC (Milan, Italy). saMMi cell line was generated in our laboratory and is described in depth ahead.

INA-6 cell line was established from the pleural effusion of an 80-year-old PCL patient and is dependent either on exogenous human IL-6 or human BMSCs for its growth and survival, similarly to primary MM cells (Burger *et al.*, 2001).

U266 cell line was established from the peripheral blood of a 53-year-old patient with IgE-secreting PCL, these cells have been reported to produce human IL-6 (Nilsson *et al.*, 1970).

H929 cell line was established from the pleural effusion of an 62-year-old PCL patient, rearrangement of c-*MYC* proto-oncogene has been described in this cell line and it is able to grow independently of IL-6 growth factor (Gazdar *et al.*, 1986).

RPMI 8226 cell line was established from the peripheral blood of a 61-year-old patient with Igλ light chain-secreting PCL; these cells can survive without IL-6 stimulus (Matsuoka *et al.*, 1967).

HS5 BM stroma cell line was purchased from ATCC (Milan, Italy) and used in co-culture experiments to mimic the BM microenvironmental niche.

saMMi CELL LINE GENERATION

saMMi cell line was generated from a BM biopsy of a 82-year-old Caucasian woman with MM. The malignant PCs were purified using anti-CD138 magnetic beads and lised for RNA and protein studies. The remaining cells were put in culture for the purification of BMSCs. After 1 month of culturing, in the flask with BMSCs we found a population of malignant PCs that developed either from the $CD138^-$ fraction or most likely from the proliferation of few $CD138^+$ cells left from purification.

Cells were then separated from the BMSCs and various media with different IL-6 concentrations were tested. saMMi cell line was not able to survive without IL-6 or the support of BMSCs. The best growth culture condition for this cell line was found to be DMEM medium supplemented with 20% FCS and 2,5ng/mL of IL-6.

IMMUNOPHENOTYPE

To better understand the characteristics of this new cell line we have proceeded to determine its immunophenotype. We have marked the cells with the most common markers used in the characterization of MM cells: CD38, CD138, CD117, CD19, CD56, CD45, κ and λ light chains. Cells were positive for CD138, CD56, CD45 and λ light chains, and negative for all the other markers. Interestingly, $CD138^+$ cells from the patient

from whom this cell line derived were 95% $CD38^+$. This could mean that we have selected a $CD38^-$ clone or that these cells were initially $CD38^+$ cells that have suffered phenotypic changes in culture.

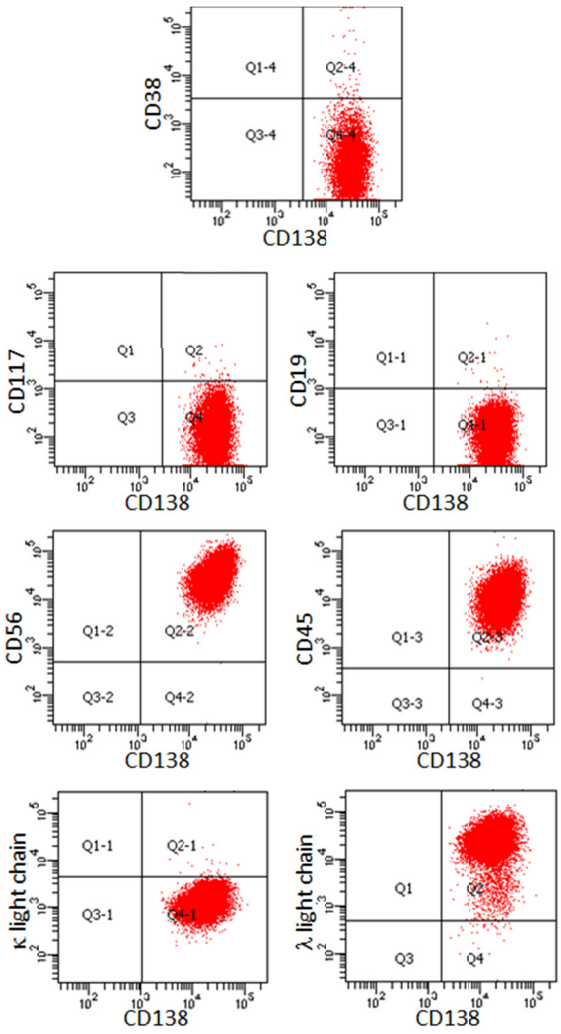

Figure 13: Surface markers of saMMi cell line. Dot plots showing the expression of surface markers assessed by flow cytometry.

KARYOTYPE AND FISH

To better evaluate the genetic alterations present in this cell line, and to confirm if these were the same present in the primary patient tumor, we have performed cytogenetic analysis.

The cell line's karyotype is as follows (chromosome count can be seen in Figure 14):

45,X,-X,idic(1)(p11), der(1)t(1;3)(q25;q21), del(4)(q25),t(4;12)(q26;q13), der(14)t(11;14)(q13;q32)t(8;14)(q23;q32),

der(9)del(9)(p21)t(1;18;9)(q12;p11;q34)[25].ish idic(1)(p11)(CDKN2C,CKS1B++), der(1)t(1;3)(CDK2C+,CKS1B+)del(17)(p13.1p13.1)(TP53-, 17p11.1-q11.1+), der(18)t(1;18;9)(CKS1B+)[4]

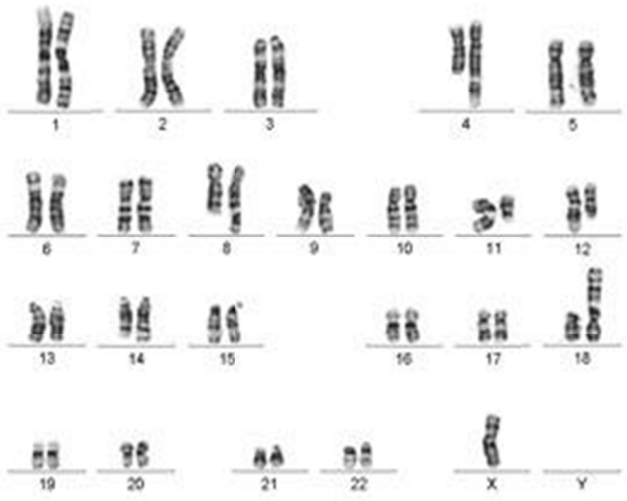

Figure 14: saMMi cell line karyotype. Karyogram showing number and appearance of chromosomes in saMMi cell line.

This karyotype is compatible with MM malignancy, and it is an evolution of the patient's karyotype. This cell line is a hypodiploid clone with 45 chromosomes (loss of 1 chromosome X), with a very complex karyotype with 1q gain confirmed also by FISH, and loss of TP53 observed only by FISH.

RNA PURIFICATION

RNA was purified using RNeasy mini kit (Qiagen). This procedure represents a well-established technology that combines the selective binding properties of a silica-based membrane with the speed of microspin technology. Briefly, cells were collected and washed, removing the medium; then the appropriate volume of RLT lysis buffer, that contains guanidine-thiocyanate, was added (350 µl for <5x106 cells, 600 µl for 5-9x106 cells). RLT was supplemented with β-mercaptoethanol 1:100 v/v, which inhibits RNases further. Samples were homogenized by vortexing and then 70% ethanol was added. After pipetting, lysed samples were transferred to RNeasy spin columns and centrifuged at 11000rpm for 1', discarding the flow-through. RNA bound to the silica membrane was washed with buffer RW1 to eliminate the contaminants and centrifuged at 1000rpm for

1'; a mix of DNase and buffer RDD (10µl and 70 µl respectively) were added directly on the membrane and kept in incubation for 15'-30', in order to degrade DNA. Afterwards a series of washes were performed to remove the contaminating DNA fragments, first of all with buffer RW1 (700µl) and then with ethanol containing buffer RPE (500µl). Samples were finally centrifuged at 12800rpm for 2', to ensure that the membrane was dry. At the end RNA was eluted by adding 30µl of RNase free water to the silica membrane and centrifuging it to a new collection tube at 11000rpm for 3'.

RNA was quantified by means of Nanodrop 1000 (Thermo Scientific).

REVERSE TRANSCRIPTION

Reverse transcription is the name given to the reaction exploited by a RNA-dependent DNA polymerase, also called reverse transcriptase, capable of synthesizing a complementary strand of DNA, called cDNA, using an RNA strand as template.

RNA was reversely transcribed to cDNA by means of Reverse Transcription System (Promega, USA). This system uses the AMV (namely avian myeloblastoma virus) reverse transcriptase enzyme, which synthesizes single-stranded cDNA from isolated mRNA; this enzyme shows polymerase activity from 5' to 3' versus, and RNase activity from 3' to 5', degrading the RNA strand when the hybrid cDNA/RNA is formed.

The reaction mix was done as follows:

- MgCl2 (25mM) 4µl
- Reverse transcription 10X buffer 2µl
- dNTPs mix (10mM) 2µl
- Oligo dT primer (0.5mg/ml) 1µl
- RNasin RNase inhibitor 0.5µl
- AMV Reverse Transcriptase 0.6µl
- 1 µg of RNA
- RNase free H_20 to a final volume of 20µl

Then samples underwent the following thermal protocol:

- 42°C for 15'
- 95°C for 5'
- 4°C maintenance

REAL-TIME PCR

The quantitative Real-Time PCR (qRT-PCR) is a method for the quantification of gene expression, characterized by high sensibility and specificity. It is called "Real-Time" because it allows the actual observation in real-time of the increase in the amount of DNA as it is amplified. This is possible because the qRT-PCR system combines a thermal cycler and an optical reaction module that detects and quantifies fluorophores. Molecules added to the PCR mix, as SYBR Green, bind the double-stranded DNA and emit a signal that increases in proportion to the rise of the amplified DNA products. An amplification curve is obtained where cycle numbers are found in the x axis and the normalized fluorescence in the y axis. At the beginning of the reaction there are only little changes in fluorescence and this is called the baseline region; an increase in fluorescence above this threshold underlines amplified product formation. From this point on, the reaction maintains an exponential course that degenerates in plateau when any of the reactants (dNTPs or primers) comes to an end.

The exponential amplification phase is the most important phase since the amount of amplified DNA is correlated with the amount of cDNA present at the beginning in the sample, being that this amount doubles at every cycle. In this linear region a threshold of fluorescence is chosen and from this value it is possible to obtain the Ct (threshold cycle), namely the number of cycles of amplification necessary for the sample to reach that threshold of emission. If the amount of cDNA present at the beginning in the sample is high, the curve will rise earlier and Ct values will be smaller.

As detector dye we used SYBR Green that emits low fluorescence if present in solution but has a strong signal when the dye binds to double-stranded DNA. However SYBR Green is not a selective dye and binds all double-stranded DNA, even primer dimers. For this reason it is recommended to introduce of a further step after amplification, called dissociation protocol. During this step, temperature rises gradually until all the double strands are denatured. This method allows the identification of contaminants or unspecific amplification products since they show different melting points. ROX is also present in the mix and works as an internal reference used by the instrument to normalize SYBR Green fluorescence.

For the evaluation of gene expression we chose a relative quantification method, using the ΔΔCt formula:

1) $\Delta Ct = Ct\ (target\ gene) - Ct\ (reference\ gene)$

2) $\Delta\Delta Ct = \Delta Ct$ (of sample) - ΔCt (of control sample)

3) $2^{\wedge -\Delta\Delta Ct}$

The thermal cycler used was the Sequence Detection System 7000 (Applied Biosystem) and the software was ABI PRISM 7000.

The reagents of the reaction mix were:

- Roche FastStart Universal SYBR Green Master (ROX) 7.5µl
- Forward primer (4pmol/µl) 1µl
- Reverse primer (4pmol/µl) 1µl
- H_2O 4.5µl
- cDNA 1µl

FastStart Universal SYBR Green Master (ROX) contains all reagents, including dNTPs and Taq polymerase, needed for running the qRT-PCR except for primers and template. FastStart Taq DNA Polymerase present in the mix is a hot start polymerase with the following amplification protocol:

- UDG activation 50°C 2’
- Polymerase activation 95°C 10’
- Denaturation 95°C 15’’ } for 40 cycles
- Annealing and amplification 60°C 1’

Dissociation protocol: increasing temperature from 60°C to 95°C.

In the table below are reported the sequences of the primers used for the qRT-PCR.

Table 2: Primers used for qRT-PCR. *GAPDH* was used to normalize the reaction.

GENE	FORWARD	REVERSE
RHOU	5’-AAA TGG GTG CCG GAG ATT CG -3’	5’-CCA ACT CAA TGA GGA CTT TGA CAT C -3’
IL-6	5’- GGC ACT GGC AGA AAA CAA CCT G -3’	5’- TCA CCA GGC AAG TCT CCT CAT TGA AT -3’
GAPDH	5’-AAT GGA AAT CCC ATC ACC ATC T-3’	5’-CGC CCC ACT TGA TTT TGG-3’

The sequences were found using Primer Express program (Applied Biosystem).

PROTEIN EXTRACTION AND QUANTIFICATION

WHOLE PROTEIN EXTRACTION

All steps were performed at 4°C. Cells (1-2x106) were collected, washed in PBS and centrifuged at 5000 rpm for 5'. Pellets were resuspended in 40-50µl of lysis buffer composed of: 150mM NaCl, 2 mM EDTA, 2mM EGTA supplemented with 0.5% Triton X-100 (Sigma, Germany), protease inhibitor cocktail (Sigma, Germany), phosphatase inhibitor cocktail (Thermo Scientific, USA), 1mM phenyl-methyl-sulfonyl fluoride (PMSF; Sigma, Germany), 1µM okadaic acid (Sigma, Germany), dithiothreitol (DTT; Sigma, Germany) in a buffer made up of Tris (pH7.5) 20mM, NaCl 150mM, EDTA 2mM, EGTA 2mM to final volume. Samples were incubated on ice for 30', vortexing every 10' and then centrifuged for 10' at 13000 rpm. Supernatants were collected and stored at -20°C or quantified immediately.

PROTEIN QUANTIFICATION

To measure the concentration of proteins after cell lysis we performed Bradford (Sigma,Germany) protein assay. It is based on an absorbance shift of the Comassie Brilliant Blue G-250 dye. Under acidic conditions, the red form of the dye is converted into its bluer form by binding to the protein being assayed. The bounded form of the dye has the maximum absorption spectrum at 595nm. The binding of the dye to the protein stabilizes the blue anionic form, increasing the absorbance at 595nm in proportion to the amount of bounded dye, and thus to the concentration of protein present in the sample can be extrapolated.

Bradford was diluted 1:2 in distilled water and 1mL of diluted reagent was added to each tube. Then, 1µl of cell lysate was added to the solution, mixed well and incubated 3' in the dark. Using 1.5 mL cuvettes, absorbance at 595nm was red using a spectrophotometer (Ultrospec 1100pro; Amersham).

Concentration values were obtained applying the Lambert-Beer formula:

$$A=\varepsilon \times c \qquad \varepsilon=\text{molar extinction coefficient}$$

Molar extinction coefficient was derived from a calibration curve, obtained using known concentrations of bovine serum albumin (BSA).

SDS-PAGE

Sodium dodecyl sulfate-polyacrylamide gel electrophoresis (SDS-PAGE) is a method that allows the separation of proteins according to their molecular weight and no other physical feature.

SDS is a detergent that can dissolve hydrophobic molecules and has a negative charge (sulfate) attached to it, so it can disrupt hydrophobic areas and coat proteins with many negative charges, which overpower any positive charges the protein might present. The resulting protein is denatured (reduced to its primary structure) and linearized. Moreover, proteins having now a large negative charge will migrate towards the positive pole when placed in an electric field.

When polyacrylamide, a polymer of acrylamide monomers, undergoes the process of polymerization, it turns into a gel that can be placed in an electric field to pull the proteins through it. The acrylamide concentration of the gel can vary, generally from 5% to 25%. Lower percentage gels form bigger pores and are thus better for separating high molecular weight proteins, while higher percentages are needed for separating smaller proteins. Small molecules can move through the polyacrylamide mesh faster than big molecules and so they will be at the frontline of migration.

The polyacrylamide gel is composed of two phases: the upper phase is the stacking gel (pH 6.8) and the lower phase is the separating gel (pH 8.8). The first one allows the protein to compact and enter the separating phase simultaneously. The second one allows the separation of proteins according to their molecular weight. We used fixed concentrations of acrylamide (8% or 10% for separating gel; 5% for stacking gel). Protein samples and a molecular weight reference (Seeblue Plus2 Prestained Standard 1X, Invitrogen) were loaded into different wells in the stacking gel and separated using Amersham electrophoretic chambers, a specific saline running buffer (pH 8.3) (25mM Tris, 192mM glycine, 0.1% SDS) and an applied electric field of 25mA.

15-30µg of protein lysates were mixed with sample buffer (1:4) composed by SDS 20%, Tris (pH 6.8) 1.5M, bromophenol blue 0.05%, DTT 6%, and β-mercaptoethanol 1:20. Samples were heated at 100°C for 4’ to favor denaturation.

WESTERN BLOTTING

After electrophoresis, proteins must be transferred from the electrophoresis gel to a membrane. The most commonly used transfer method is an electrophoretic transfer: this method involves placing a protein-containing polyacrylamide gel in contact with a membrane of polyvinylidene difluoride (PVDF) or other suitable material, and putting these together between two electrodes in a conducting solution. Since the PVDF is very hydrophobic, we previously incubated it in methanol for 1' to expose its full protein binding capacity. The blotting sandwich is composed inside a grid by the following components in this order: sponge, whatman paper, electrophoresis gel, PVDF membrane, whatman paper, sponge. When an electric field is applied, the proteins move out of the polyacrylamide gel onto the surface of the membrane, where they become tightly attached. The result is a membrane with a copy of the protein pattern that was originally in the gel. The transfer is performed in a specific saline buffer containing Tris 250mM, glycine 1.92M and methanol 20%. After the transfer the membrane is saturated to prevent unspecific binding of the detection antibodies during subsequent steps. Saturation is performed for 1 hour in a solution composed of non-fatty milk 5% (Ristora) and TBS (Tris buffered saline) supplemented with Tween-20 0.05% (Sigma). Saturation is followed by washing in TBS plus Tween-20 0.05% in order to remove unbound reagents and reduce the background signal. The membrane is then incubated overnight at 4°C with a primary antibody that recognizes a specific protein or epitope on a group of proteins. The primary antibody is not directly detectable. Therefore, tagged secondary antibodies that recognize the heavy chains of the primary antibodies are used to detect the target antigen (indirect detection). Secondary antibodies are enzymatically labelled with Horseradish peroxidase. After a final series of washes to remove unattached antibodies, the antibodies on the membranes are ready to be detected. An appropriate chemiluminescent substrate, which produces light when in contact with the enzymatically labeled secondary antibodies, is then added to the membrane. The light output was captured using ImageQuant LAS500 machine (GE Healthcare Life Sciences).

We used different chemiluminescent substrates:

- Pierce ECL western blotting substrate (Thermo Scientific);
- LiteAblot PLUS Enhanced Chemiluminescent Substrate (EuroClone);
- LiteAblot EXTEND Long Lasting Chemiluminescent Substrate (EuroClone);
- LiteAblot Turbo Extra Sensitive Chemiluminescent Substrate (EuroClone).

In order to detect more antibodies with the same specificity and similar molecular weight it is necessary to strip the membrane. Stripping buffer reagent (Thermo scientific) allows the efficient removal of primary and secondary antibodies from immunoblots without removing or damaging the immobilized proteins. This allows blots to be re-probed with new antibodies. For stripping, membranes were covered with this buffer and incubated for 20'-25' at 37°C and then washed with TBS, afterwards the membranes were washed and saturated again with milk.

ANTIBODIES

Primary antibodies: anti-GAPDH (Millipore, Germany); anti-cleaved PARP (Cell Signaling, USA); anti-RhoU (Abcam, UK); anti-phospho-JNK(Thr183/Tyr185) (Cell Signaling, USA); anti-phospho-STAT3(Tyr705) (Cell Signaling USA)

Secondary antibodies: anti-rabbit IgG HRP-linked antibody (Cell Signaling, USA); HRP labeled goat anti-mouse IgG (KPL, USA).

FLOW CYTOMETRY

Fluorescence Activated Cell Sorting (FACS) analysis was performed using FACSCanto Cytometer and FACSDiva 6.0 software (Becton-Dickinson, Italy).

ANNV/PI STAINING

After drug treatment with Stattic or Lenalidomide, and after RhoU silencing with siRNA, apoptosis was evaluated using the Apoptosis Detection Kit (Immunostep, Italy).

Annexin V (AnnV) is a member of a highly conserved protein family that binds acidic phospholipids in a calcium-dependent manner. The protein presents a high affinity for phosphatidylserine, which is translocated from the inner side of the plasma membrane to the outer layer when cells undergo death by apoptosis or necrosis. Exposed phosphatidylserine is one of several signals through which the cell, that is undergoing apoptosis, can be recognized by phagocytes. AnnV binding to the cell surface indicates that cell death is imminent. In order to differentiate apoptosis from necrosis, a dye exclusion test with propidium iodide (PI) is performed to establish if membrane integrity has been conserved or not. A combination test measuring AnnV binding and dye exclusion allows discrimination between live cells, apoptotic cells and necrotic cells.

$2x10^5$ cells were washed in PBS to remove medium and resuspended in 100µl of binding buffer. 1.7µl of AnnV-FITC were added and cells were incubated for 10' at room temperature in the dark. 100µl of binding buffer were further added to the cell suspension and DNA was stained with 5µl of PI immediately before proceeding with flow cytometric analysis.

CD38/CD138 STAINING

Identification of plasma is typically based on high expression of CD38 and CD138 surface markers, in conjunction with the scatter properties of the cell population. Unlike CD138 that is a specific marker of PCs; CD38 expression is also accessible in other cell populations but has a particularly high expression in PCs. However, in many abnormal PC populations the surface density of CD38 is decreased and these may have a staining intensity similar to that of normal B-cell precursors or activated T-cells. CD38/CD138 staining is still the best staining for identifying PCs. This staining was used to evaluate the initial plasmacytosis of fresh BM aspirates from MGUS, sMM, MM and PCL patients. This technique was also used to ensure a higher that 90% purity after PC separation protocol.

$2x10^5$ cells were washed in PBS to remove medium and resuspended in 100µl of PBS. 5µl of anti-CD138-FITC and anti-CD38-PE were added to the cells and incubated in the dark for 5'. Cells were again washed in PBS and resuspended in 200µl PBS before proceeding with the flow cytometric analysis.

GENE EXPRESSION PROFILING

For gene expression analysis, samples were profiled on the GeneChip Human Gene 1.0 ST array (Affymetrix, Santa Clara, CA, USA) as previously described (Todoerti *et al.*, 2013). The raw intensity expression values were processed by Robust Multi-array Average (RMA) procedure (Irizarry *et al.*, 2003), with the re-annotated Chip Definition Files from BrainArray libraries version 19.0.0, available at: http://brainarray.mbni.med.umich.edu.

Supervised analyses were carried out using the Significant Analysis of Microarrays software version 5.00 (Tusher, Tibshirani and Chu, 2001) using the web application provided in the shiny package for R software (https://github.com/MikeJSeo/SAM). The

cutoff point for statistical significance (at a q-value = 0) was determined by tuning the Δ parameter on the false discovery rate (FDR) and controlling the q-value of the selected gene lists. A higher stringency level (90^{th} percentile FDR = 0) was also applied to the differentially expressed gene lists at q-value 0. The list of differentially expressed genes was functionally analyzed by means of NetAffx (Affymetrix at https://www.affymetrix.com/analysis/netaffx/), the Database for Annotation, Visualization and Integrated Discovery (DAVID) Tool 6.7 (http://david.abcc.ncifcrf.gov/) (Huang, Lempicki and Sherman, 2009). The Gene Ontology Biological Process and Molecular Function terms were selected as annotation categories in DAVID, and highly stringent classification was used for analysis in the Functional Annotation Clustering option. The annotation clusters with an enrichment score (ES) of >1.3 (Pvalue <0.05) were considered significant.

SIRNA TRANSFECTION BY ELECTROPORATION

Electroporation is a transfection technology based on the momentary creation of small pores in cell membranes by applying an electrical pulse. For siRNA transfection we have used Lonza's Amaxa Nucleofector™ Technology (USA).

A mix of transfection solution was done by adding 100pmol of RhoU siRNA (SMARTpool: ON-TARGETplus RHOU siRNA, Dharmacon, Italy) or 100pmol of Scrambled (ON-TARGETplus Non-targeting siRNA, Dharmacon, Italy) together with 100pmol of siGLO Green (Dharmacon, Italy) for transfection control to 90µL of Amaxa Nucleofector® Kit C (Lonza, USA).

$2x10^6$ cells per condition were washed with PBS and centrifuged at 90g for 10 minutes at room temperature. Supernatant was discharged and 3 conditions of transfection medium were added to different tubes: RhoU siRNA + siGLO Green; Scrambled + siGLO Green; Amaxa only.

Each mix was transferred into supplied certified cuvettes, and transfected using the program X-005 in Amaxa Nucleofector® I device. Cells were then collected from the cuvettes, resuspended into their favorite medium and incubated for 48hours before further analysis were done.

Transfection control was done by siGLO Green reads in FACSCanto Cytometer after 24hours to ensure that transfection was efficient. Transfections with efficiency lower than 80% were discarded.

IMMUNOFLUORESCENCE (IF)

Cells (5 x 10^4) were seeded on polylysine-coated glass slides and incubated at 37°C for 1 hour to let them adhere to the polylysine. Afterwards, cells were washed with PBS, fixed with shilled formaldehyde 3.7% for 20' and permeabilized with Triton 0.1% in PBS for 5' at room temperature. After three washes with PBS, cells were blocked with BSA 3% for 30'. Samples were then stained with Phalloidin Alexa Fluor 594 (Invitrogen, USA) for 30'. After washing with PBS, specimens were mounted in Vectashield mounting medium with DAPI (4′,6-diamidino-2-phenylindole) (Vector Laboratories, USA), in order to distinguish the nuclei and analyzed using ZEISS LSM700 confocal microscope with 63x magnification objective. Images were analyzed with ImageJ software.

IMMUNOHISTOCHEMISTRY (IHC)

IHC was performed on 4 μm-thick formalin-fixed, paraffin-embedded sections of BM biopsies of 1 healthy, 8 MGUS and 15 MM biopsies, using anti-RhoU (HPA049592, Sigma-Aldrich, USA) and anti-IRF4 (HPA002038, Sigma-Aldrich, USA) monoclonal primary antibodies. Heat/EDTA-based Ag retrieval methods were applied, as previously described. All sections were processed using the sensitive Bond Polymer Refine Detection kit, a biotin-free, polymeric horseradish peroxidase–linker antibody conjugate system, in an automated immunostainer (Bond maX, Menarini, Italy). Appropriate positive and negative controls were run concurrently. RhoU immunostain was semiquantitatively scored in a four-tiered scale, as follows: score 0 = negative staining; score 1 = weak positivity staining; score 2 = moderate positivity staining; score 3 = strong positive staining. Immunohistochemical reactions were independently scored by two investigators (agreement k>0.8). In case of discrepancies, a consensus opinion was rendered

TRANSWELL MIGRATION ASSAY

For migration assays 5µmTranswell® Permeable Supports on 24 well plates (Corning, USA) were used. 600µL of non-supplemented standard medium (RPMI or DMEM depending of cell line used) + 0.1%BSA were added to the bottom of the multi well plate, and 50µL of the same mix were added on top of the transwell insert. Plates were incubated over night to ensure that the filter was properly wet before performing the experiment.

Cells were washed four times with HBSS buffer to free the receptors on the cell membrane from previous binding partners. $4x10^5$ cells were then resuspended in 50µL of recommended medium + 0.1%BSA and added to the top well insert. Plates were returned to the incubator for 20 minutes to allow cell to precipitate.

Afterwards, IL-6 stimulus (10ng) was carefully added to the bottom well, without moving the insert. IL-6 was not added to control wells. The plates were left in the incubator for 6 hours.

Lastly, cells in the bottom well were mixed well by pipetting and two 200µL samples were transferred to two cytofluorimetry tubes. The amount of cells in the tube was assessed by 1 minute reads in FACSCanto at high speed.

The number of cells that have responded to the stimulus was given by the total number of cells that migrated to the well with the stimulus minus the number of cells that migrated to the control well (without stimulus).

OTHER CHEMICALS

Cells were stained with Trypan Blue (Sigma, Germany) and counted in a Neubauer chamber. An appropriate number of cells was then centrifuged and plated with fresh medium at a concentration of $1x10^6$ cells/ml.

The following treatments were employed:

- Stattic (Selleckchem, USA), STAT3 inhibitor;
- IL-6 (ImmunoTools, Germany), Recombinant Human Interleukin 6;
- Lenalidomide (Cellgene, USA), IMiD used in MM treatment.

STATISTICAL ANALYSIS

Data were evaluated for their statistical significance with appropriate tests: Student's *t* test was used to assess if a mean value of a certain distribution was significantly different from a reference value; differences between groups were tested by applying the Analysis of Variance (ANOVA) or Fisher's exact test; Student's t test for trend was applied when a trend needed to be verified. P values below 0.05 were considered statistically significant.

To evaluate the correlation between the expressions of two genes "Pearson product-moment correlation coefficient" was used. Pearson's *r* values are comprised between -1 and 1. If $r < 0$ there is a negative correlation; if $r = 0$ there is no correlation; if $r > 0$ there is a positive correlation. The strength of the correlation also depends on the *r* value the closer the value is to 1, the stronger the linear correlation.

All analyses were performed using GraphPad Prism 6, Microsoft Excel or R software.

RESULTS

RHO GTPASES' EXPRESSION IS ALTERED IN MM PCS

To assess the expression of the Rho GTPase family members in PCs from BM biopsies of MM patients and in normal PCs from healthy BM donors, we have used the gene expression profiling data of 129 MM patient samples at diagnosis and 4 healthy controls. The members of the Rho GTPase family have been found variably expressed in MM PCs when compared to healthy PCs (Figure 15). More precisely, 13 out of the 21 GTPases analyzed are expressed at significantly lower levels in MM when compared to healthy controls (*CDC42*, *RAC1*, *RAC2*, *RHOA*, *RHOBTB1*, *RHOD*, *RHOF*, *RHOG*, *RHOH*, *RHOJ*, *RHOU*, *RHOV* and *RND1* ($p < 0.05$)).

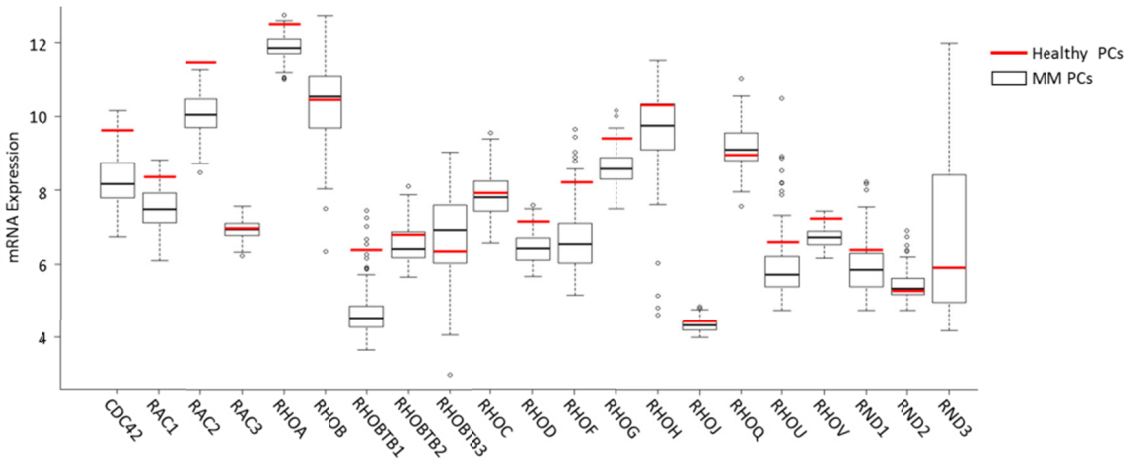

Figure 15: Rho GTPase family members' expression in healthy and MM PCs. Box plot showing mean expression in healthy PCs purified from 4 donors' BM (red) and expression ±Standard deviation in MM PCs purified from BM biopsies of 129 patients at diagnosis (black). In the x axis are all the members of the Rho GTPase family in alphabetical order.

ATYPICAL RHO GTPASES' EXPRESSION IS SIGNIFICANTLY MODULATED IN DIFFERENT MM SUBGROUPS

The fact that typical GTPases are less expressed in MM does not mean that they are less active since there is the need to further evaluate their activation (GTP-bound) status. Instead, atypical Rho GTPases are constitutively active whenever expressed and most of them are actually regulated at the RNA level.

We have subsequently looked at the expression of atypical Rho GTPases in PCs of MM patients from different TC groups and found a significant modulation of 7 out of the 9 proteins (Figure 16). This means that even the atypical Rho GTPases that were not differently expressed when compared to healthy controls have actually a diverse modulation in the different TC groups and this could correlate with disease progression and prognosis.

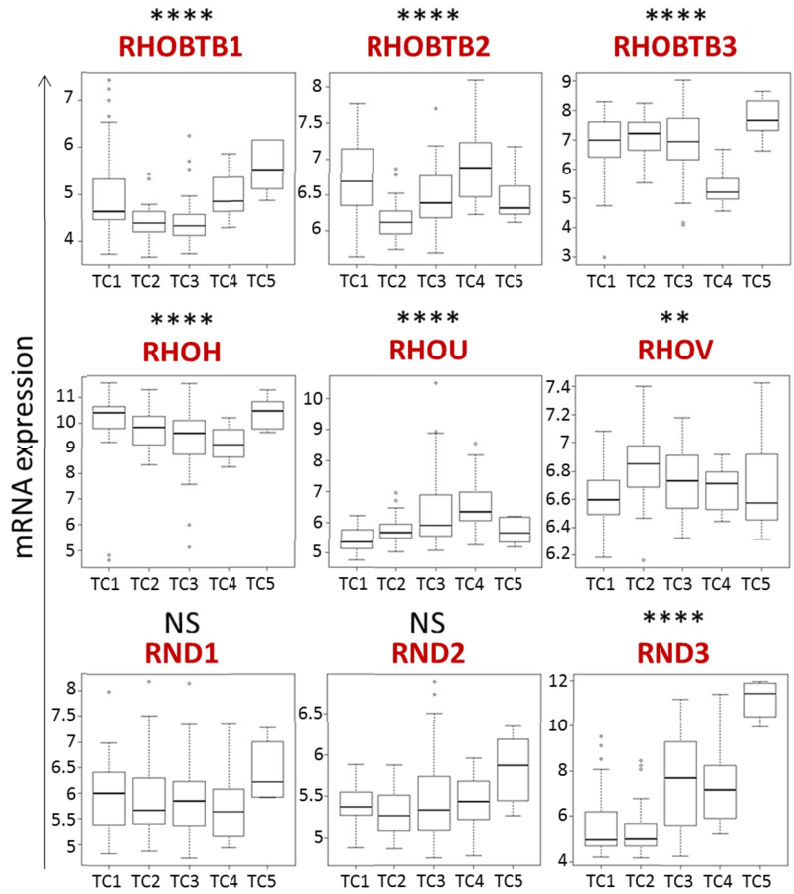

Figure 16: Expression of atypical Rho GTPases in MM patients in the different TC groups. Box plots showing mean expression and standard deviation in PCs from MM patients of different TC groups (TC1 n=34; TC2 n=30; TC3 n=40; TC4 n=19; TC5 n=6). ANOVA: NS = no significant changes; ** $p < 0.01$; **** $p < 0.0001$

RHOU IS HETEROGENEOUSLY EXPRESSED IN DIFFERENT STEPS OF MM PROGRESSION

Of all the atypical GTPases, the RhoU/V family is particularly interesting due to its domain organization, different from all the other known GTPases.

For this reason we focused our attention on the RhoU/V family and found out that *RHOU* expression is not only significantly different in diverse TC groups but also that this protein is significantly modulated with disease progression. Indeed, it is up-regulated in BM PCs from MGUS patients and down-modulated in the majority of BM PCs from both MM and PCL patients (Figure 17).

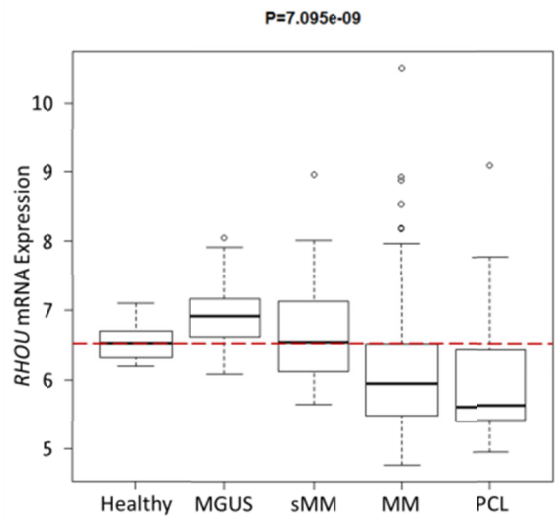

Figure 17: *RHOU* expression in the different steps of MM progression. Box plot showing mean expression and standard deviation in healthy PCs purified from 9 donors' BM, MGUS PCs purified from BM biopsies of 20 patients, sMM PCs purified from BM biopsies of 33 patients; MM PCs purified from BM biopsies of 170 patients at diagnosis, and PCL PCs purified from BM biopsies of 36 patients. P value was calculated by ANOVA.

Seeing the high deviation in *RHOU* expression especially at later stages of the disease we have divided the patients in 3 groups with low (< Mean - 2SD of healthy controls), intermediate, and high (> Mean + 2SD of healthy controls) expression. There is an evident decrease in the percentage of patients that fall in the intermediate groups (with

normal *RHOU* expression) with disease progression (Figure 18). However, there is also an increase in the heterogeneity of *RHOU* expression. In MM in particular, there are 3 distinct groups of patients: 42% with low, 47% with intermediate and 11% with high *RHOU* expression. Indeed, there seems to be a gradual increase in the percentage of patients with low *RHOU* levels in their BM PCs: 0% in MGUS, 3% in sMM, 42% in MM and 64% in PCL.

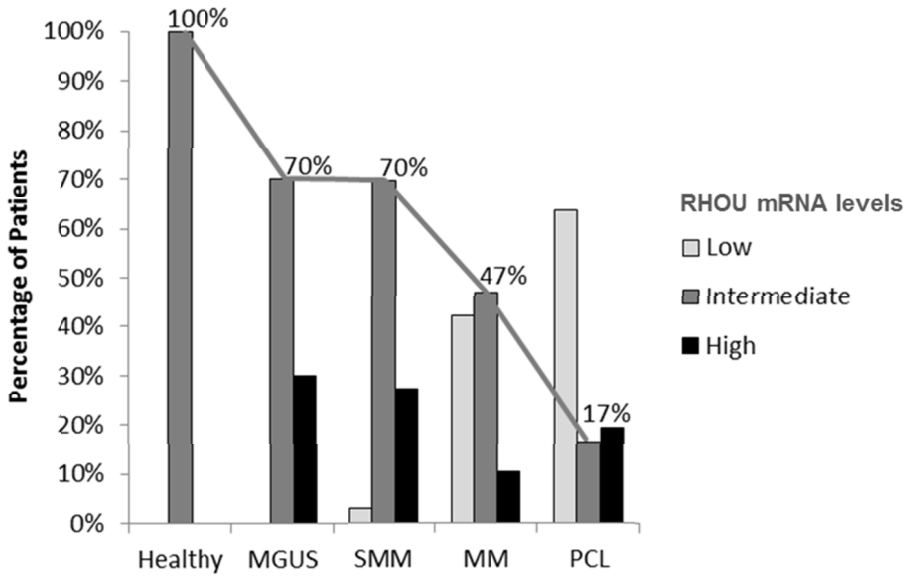

Figure 18: Percentage of patients for each step of the disease that fall in the diverse groups of *RHOU* expression. Patients were divided in 3 groups with low (< Mean - 2SD of healthy controls), intermediate, and high (> Mean + 2SD of healthy controls) *RHOU* expression. The distribution of patients at each step of the disease was then represented in a bar chart.

To confirm the expression results obtained from the gene expression profiling studies we have also performed immunohistochemistry (IHC) in formalin-fixed, paraffin-embedded sections of BM biopsies of a healthy donor, MGUS and MM patients. BM sections from healthy donor or MGUS patients were stained with anti-RhoU (brown) and anti-IRF4 (red), a marker of PCs. Healthy PCs have a low intensity of RhoU staining while all MGUS patients' PCs assessed showed a high intensity cytoplasmic staining for RhoU (Figure 19).

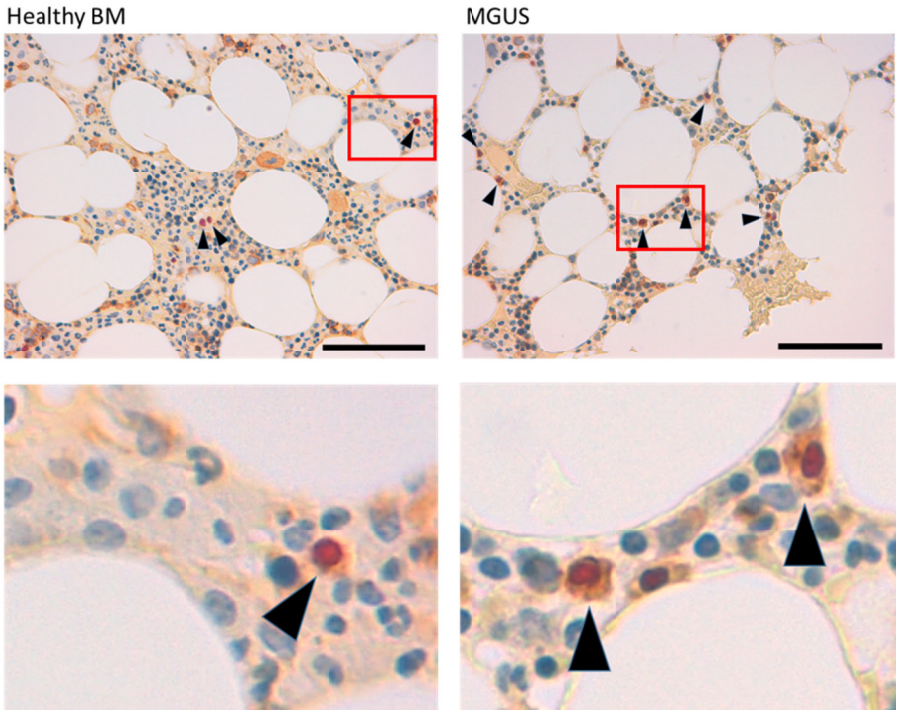

Figure 19: RhoU expression in BM biopsies of a healthy donor and a representative MGUS patient. PCs in the samples are indicated with black arrows. IHC staining shows low positivity of RhoU in PCs from healthy donors and a strong cytoplasmic positivity in MGUS patients. Nucleuses of PCs are positive for IRF4 staining and are therefore red. Original magnification x60; inset with x5 digital zoom; scale bar = 100µm.

Biopsy sections from MM patients were stained only with anti-RhoU (brown) because anti-IRF4 signal was too strong in these patients and smeared RhoU staining.

Zones with a clearly abundant plasmacytosis were used in evaluating RhoU positivity.

MM patients' PCs were given a score based on the intensity of the staining: score 0 = negative; score 1 = weak; score 2 = moderate; score 3 = high (Table 3). All patients showed positivity for RhoU staining. More precisely 20% showed weak, 40% moderate and 40% high RhoU expression, consistent with the heterogeneous levels of *RHOU* mRNA observed previously in MM patients.

Table 3: RhoU expression has variable intensity scores in BM biopsies of MM patients.

RhoU score	0	1	2	3
MM patients	0%	20%	40%	40%

Cells with different scores seem to also have a diverse localization of RhoU (Figure 20). In MM cells with score 1 RhoU had a dot-like localization in proximity of the nucleus, in what could be the actin microtubule-organizing center. On the other hand, in cells that scored 2 or 3, RhoU had a granular cytoplasmic and membrane localization.

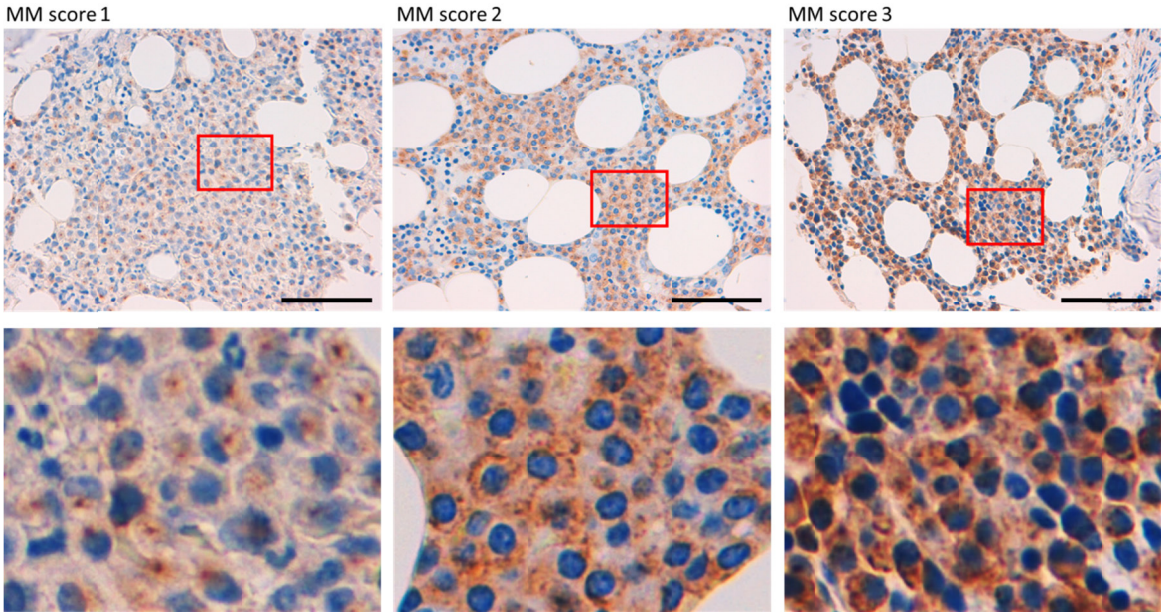

Figure 20: RhoU expression heterogeneity in MM patients. In PCs from representative MM patients, IHC staining shows low (MM score 1), intermediate (MM score 2) and high (MM score 3) positivity for RhoU. RhoU staining showed dot-like, granular cytoplasmic and membrane localization. Original magnification x60; inset with x5 digital zoom; scale bar = 100μm

RHOU EXPRESSION CORRELATES WITH POOR PROGNOSIS

Understanding now that RhoU expression is clearly modulated with disease progression we wondered if the expression of this GTPase somehow correlated with a better or worse prognosis in MM patients. For this analysis we did not consider MGUS, sMM and PCL patients since these are not divided into TC groups and we did not have enough information about the cyclin levels nor the translocations present in these patients.

Patients were divided in 2 groups: standard risk patients that fall into TC1 and TC2 groups (n=64), and high risk patients that comprise TC3, TC4 and TC5 groups (n=65).

Patients in the high risk group have significantly higher levels of *RHOU* expression (Figure 21).

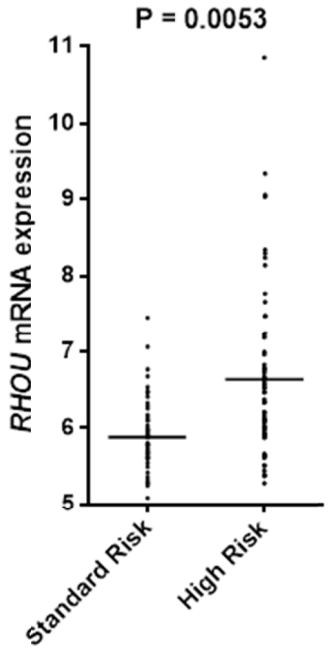

Figure 21: *RHOU* expression changes in standard or high risk MM patients. Aligned dot plot with *RHOU* expression in patients that fall in the standard risk (TC1 and TC2) and high risk (TC3, TC4 and TC5) groups. The mean expression in each group is marked with a bar. P value was calculated by Student's t test.

We have then decided to also compare the levels of *RHOU* expression with the mutations assessed at diagnosis in the whole cohort of MM patients, independently of the TC group where they fall (Figure 22). The patients for which we did not have all the genetic background information were excluded, leaving a total of 119 samples used in this analysis. Patients with high *RHOU* expression have a higher frequency of genetic alterations that correlate with a bad prognosis: t(4;14), del(13) and q1 gain. On the other hand, high *RHOU* expression patients never showed the t(11,14) translocation that correlates with a better prognosis.

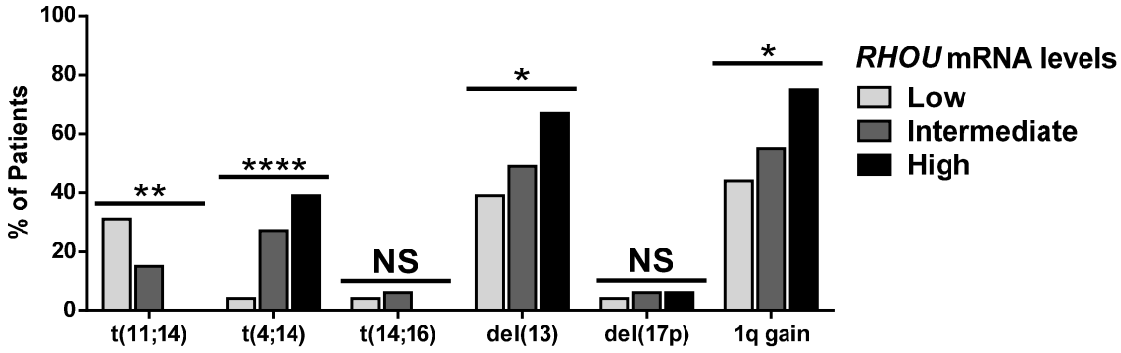

Chi square test for trend

t(11;14)	0.0023
t(4;14)	<0.0001
t(14;16)	0.1793
del(13)	0.0251
del(17p)	0.6825
1q gain	0.0265

Figure 22: Correlation between *RHOU* levels and specific MM mutations. Patients were divided in 3 groups with low (< Mean - 2SD of healthy controls), intermediate, and high (> Mean + 2SD of healthy controls) *RHOU* expression. The distribution of patients with each studied genetic change was then represented in a bar chart. Student's t test for trend * $p < 0.05$; ** $p < 0.01$; **** $p < 0.0001$.

PATIENTS WITH HIGH AND LOW *RHOU* EXPRESSION HAVE A DIFFERENT EXPRESSION PROFILE FOR 557 GENES

By interrogating the tumor genome we have discovered that patients with high and low *RHOU* mRNA levels display different gene expression profiles. For this study since we needed an equal number of patients in each group, we have divided the cohort of MM patients in quartiles and we have compared the genetic profiles of the first (lowest *RHOU* expression) and fourth (highest *RHOU* expression) quartiles. More precisely, 557 genes are distinctively expressed between MM patients with high and low *RHOU* and this could give us some hints on the prognosis value of this GTPase. To better understand the differences in the gene expression profiles between the two groups, we have created a heat map of *RHOU* expression together with these 557 genes (Figure 23). Of these, 101 had the same trend of expression as *RHOU* while 456 had an opposite expression profile and were up-regulated when *RHOU* mRNA levels were low.

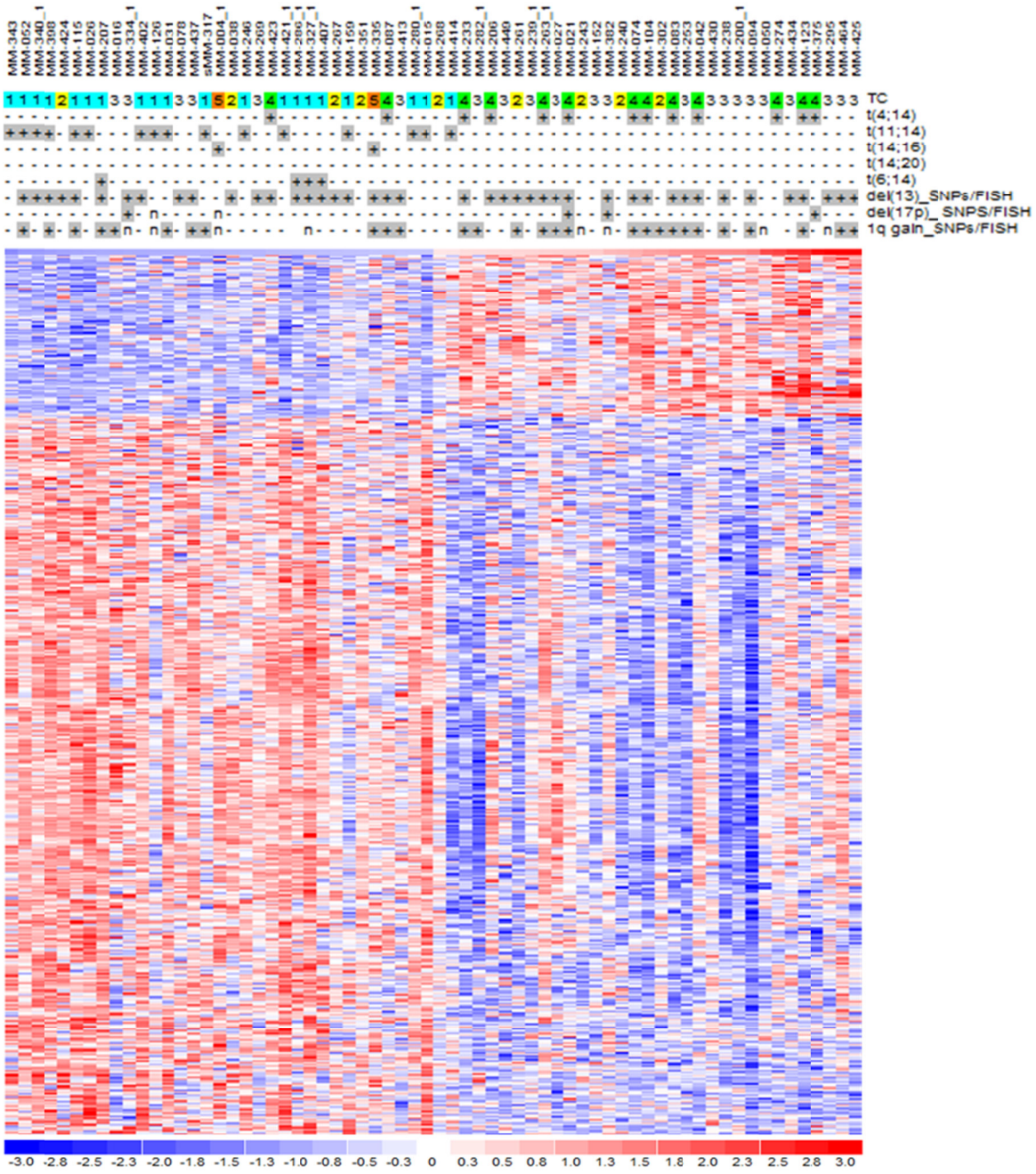

Figure 23: Heat map showing the expression profiles of patients with low and high *RHOU*. In the first row is depicted *RHOU* expression in each of these patients' samples. Genes in the first block have the same expression profile as *RHOU* while genes in the second block are inversely expressed.

RHOU CLUSTERS WITH GENES ASSOCIATED WITH CELL CYCLE AND MITOSIS

To better understand the significance of the different gene expression profiles we have taken to REACTOME data analysis tool (http://www.reactome.org/) and looked for gene clusters that associated with *RHOU*.

We have found out that *RHOU* expression clusters with the expression of genes that regulate the cell cycle and mitotic process (Table 4).

Table 4: REACTOME "cell cycle, mitotic" genes that significantly cluster with RhoU.

Category	Term	Count	%	P value	Genes
REACTOME_PATHWAY	REACT_152: Cell Cycle, Mitotic	14	2.7559	0.05	*ITGB3BP, NUP160, BTRC, POLE, ANAPC4, KIF18A, POLA2, MCM8, APITD1, CCND2, PSMA3, CEP290, ANAPC7, NUP43*

We have created a heat map of the genes that arose from this analysis to evaluate which of these positively or negatively correlated with *RHOU* expression (Figure 24). *CCND2* was the only gene in the list that positively correlated with *RHOU* (Pearson's r = 0.402), and this could mean that cells with high *RHOU* expression have increased levels of cyclin D2 and a higher replication rate. All the other genes responsible for cell cycle control and DNA damage response had a negative correlation with *RHOU* expression. Extensively, *ITGB3BP* which overexpression induced apoptosis in cancer cells (Li *et al.*, 2004); *NUP160*, *NUP43*, *KIF18A*, *BTRC*, *APITD1* and *CEP290* that are required for correct mitosis, centrosome dynamics and chromosome alignment (Orjalo *et al.*, 2006; Platani *et al.*, 2009; Thomas, Coux and Baldin, 2010; Osman and Whitby, 2013; Kim, Fonseca and Stumpff, 2014; Song, Park and Jang, 2015); *POLE, POLA2* and *MCM8* which have extremely important roles in DNA replication and genome stability (Gozuacik *et al.*, 2003; Pollok *et al.*, 2003; Henninger and Pursell, 2014); *ANAPC4* and *ANAPC7* that have emerging roles in differentiation control, genomic stability and tumor suppression (Wäsch, Robbins and Cross, 2010); and *PSMA3* which is part of the

proteasome complex and essential for protein degradation during cell cycle progression (Boncela *et al.*, 2011).

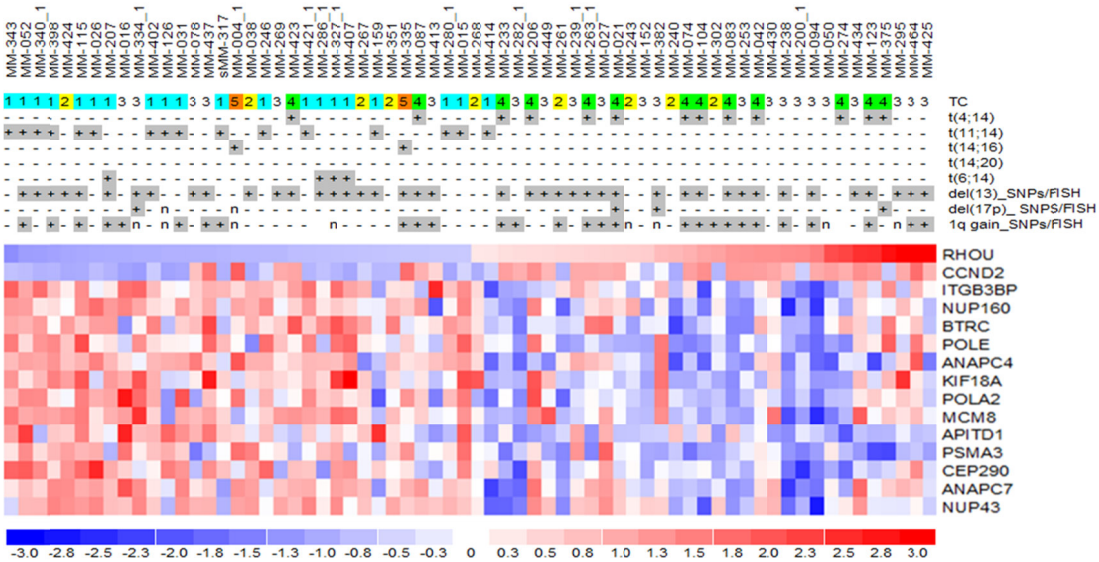

Figure 24: Heat map showing the expression of cell cycle and mitotic process genes that cluster with *RHOU* expression. In the first row is depicted *RHOU* expression in each of these patients' samples, followed by all the genes that resulted from the cell cycle, mitotic cluster on REACTOME.

RHOU CLUSTERS WITH DNA DAMAGE ASSOCIATED GENES

To further investigate *RHOU* association with DNA damage repair genes we have explored the "DNA Repair" pathway with REACTOME and found that 10 genes in this pathway significantly cluster with *RHOU* expression (Table 5). These genes are extremely important since they encode for proteins essential in a number of cellular pathways that maintain genomic stability, including DNA damage-induced cell cycle checkpoint activation, DNA damage repair, protein ubiquitination, chromatin remodeling, as well as transcriptional regulation and apoptosis (Bakkenist and Kastan, 2003; Jeong *et al.*, 2005; Klungland and Bjelland, 2007; Wu, Lu and Yu, 2010; Roy, Bagchi and Raychaudhuri, 2012; Eddy *et al.*, 2014; Roset *et al.*, 2014; Abdou *et al.*, 2015; Saito and Komatsu, 2015).

Table 5: REACTOME "DNA Repair" genes that significantly cluster with RhoU.

Category	Term	Count	%	P value	Genes
REACTOME_PATHWAY	REACT_216: DNA Repair	10	1.9685	0.001	*NBN, REV1, POLR2K, POLE, DDB2, LIG3, OGG1, ATM, RAD50, BRCA1*

A heat map was also created for the genes that arose from this analysis to evaluate which of these positively or negatively correlated with *RHOU* expression (Figure 25). All the 10 genes in the list negatively correlate with *RHOU* expression. This could suggest a deeper impairment in DNA damage response in PCs where *RHOU* is over-expressed.

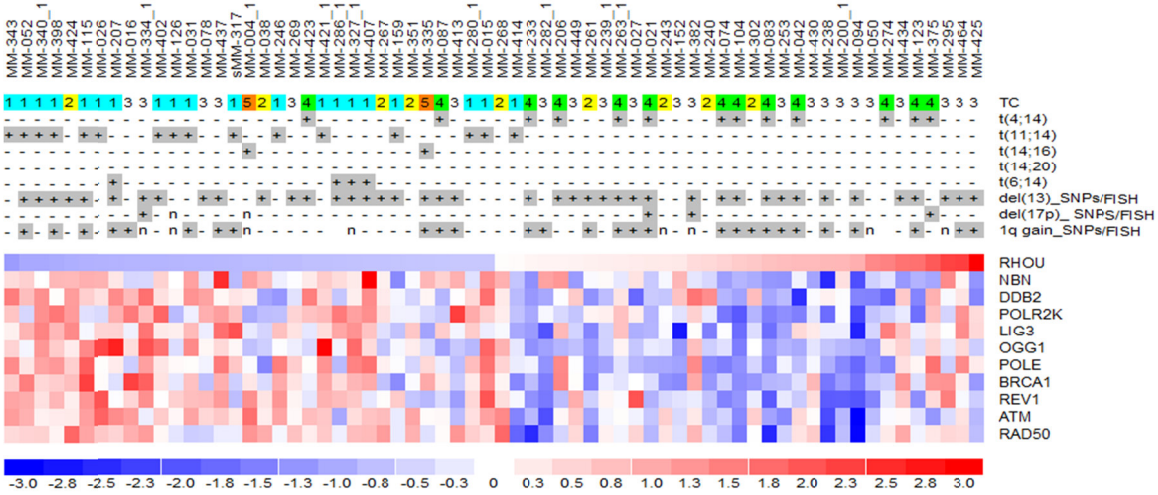

Figure 25: Heat map showing the expression of DNA repair genes that cluster with *RHOU* expression. In the first row is depicted *RHOU* expression in each of these patients' samples, followed by all the genes that resulted from DNA repair cluster on REACTOME.

RHOU EXPRESSION IN MM CELL LINES CORRELATES WITH IL-6 DEPENDENCE

To better understand *RHOU* regulation in MM malignancy we have studied the 5 MM cell lines available in our laboratory. Firstly, we have measured *RHOU* expression by qRT-PCR and compared it to the expression in healthy PCs (Figure 26). Two cell lines

expressed RHOU at very low levels (RPMI-8826 and H929) while three others over-expressed it (saMMi, INA-6 and U266).

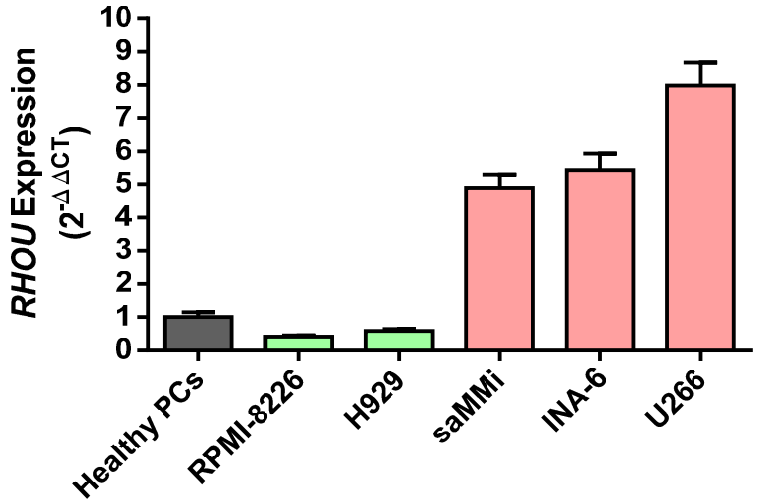

Figure 26: *RHOU* expression in MM cell lines as compared to healthy PCs. Bar chart with mean expression of RHOU from three independent samples of each cell line as compared to R*HOU* expression in 4 healthy controls. Mean and SD of all cell lines normalized over the mean expression in healthy PCs.

We have then looked at some important characteristics of each MM cell line: year of creation, tissue of provenience and IL-6 dependence status (Table 6). In some cases the time these cells have been in culture can determine the accumulation of mutations that lead to changes in gene expression; in this case there were no evident correlations. There was also no correlation between the expression of *RHOU* and the tissue from where these cells were extracted. However, looking at the IL-6 dependence status, cells that are dependent on IL-6 stimulus for survival have up-regulated *RHOU* while those that are independent from this stimulus down-modulated it.

Table 6: Main characteristics of MM cell lines and *RHOU* expression.

Name	Year	Tissue	IL-6	*RHOU* mRNA
RPMI-8226	1967	Peripheral Blood	Independent	0.40
H929	1986	Pleural Effusion	Independent	0.57
saMMi	2015	Bone Marrow	Dependent	4.89
INA-6	2001	Pleural Effusion	Dependent	5.43
U266	1970	Peripheral Blood	Dependent Autocrine	7.98

IL-6 STIMULUS UP-REGULATES *RHOU* EXPRESSION

To determine whether IL-6 stimulus could lead to an up-regulation of *RHOU* expression we have stimulated cells with IL-6 (10ng) and collected samples at 1, 4, 8, 12 and 24 hours (Figure 27). Cell lines that are usually cultured in medium supplemented with IL-6 (saMMi and INA-6) were starved from this cytokine for 12 hours previous to stimulus. All three cell lines up-regulated *RHOU* expression as early as 1 hour after stimulus. In detail, 1 hours after the addition of IL-6, there was an increase in *RHOU* expression equal to 1.7 times-fold in saMMi, 2.4 times-fold in INA-6 and 1.2 times-fold in U266. U266 might have displayed the lowest changes due to the fact that this cell line cannot be starved from IL-6 since it autocrinally produces it.

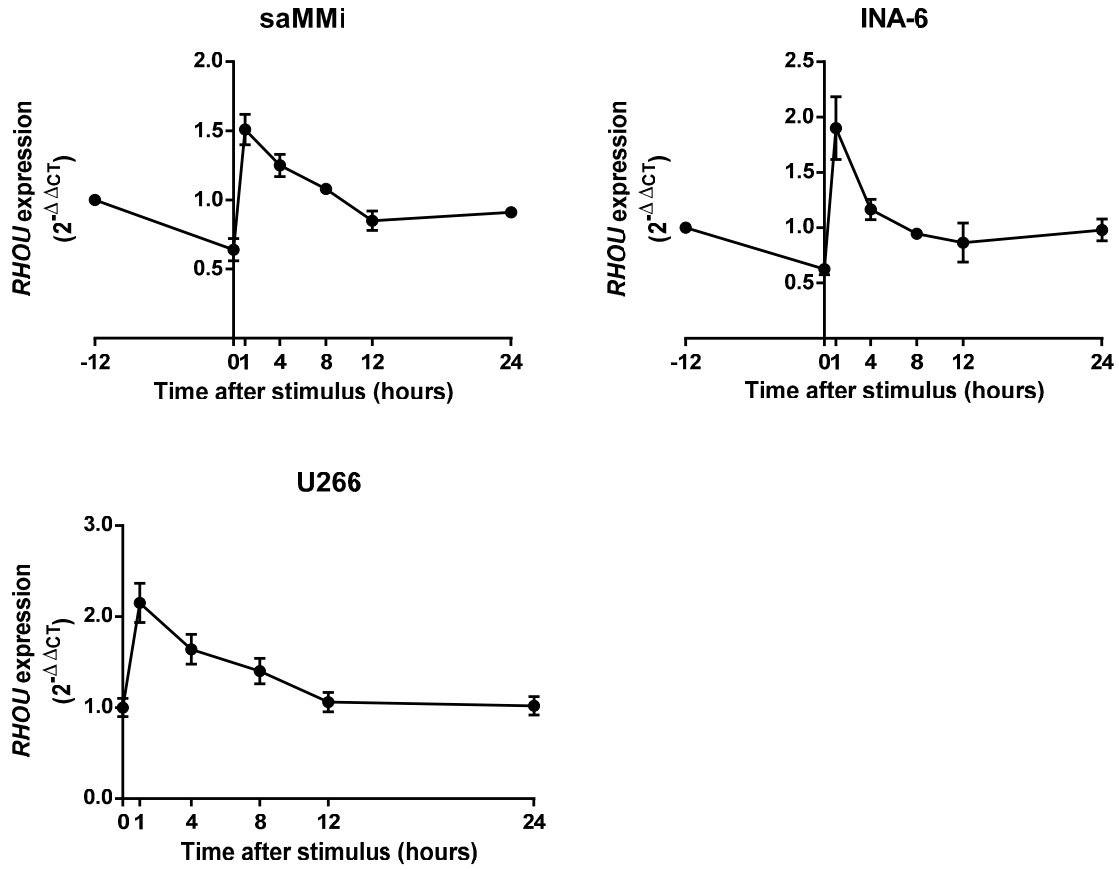

Figure 27: *RHOU* expression is significantly up-regulated after IL-6 stimulus. Time-course of *RHOU* expression after IL-6 stimulus showing a significant increase in *RHOU* expression as early as one hour after stimulus. Mean and SD of all cell lines normalized over time zero.

To verify if this effect was due to the specific activation of the IL6R/STAT3 pathway rather than an unspecific effect of growth factors, we have stimulated INA-6 cell line with TNF-α, another MM growth factor that activates the ERK and NF-κB pathways, rather than the STAT3 cascade (Figure 28, orange). Another condition that we compared to IL-6 stimulus was the addition of conditioned medium from BMSCs' culture (Figure 28, green) since this should contain all growth factors produced by BMSCs including IL-6 and TNF-α. BMSCs' from patients were cultured in unsupplemented RPMI medium for 24 hours, culture supernatant was collected, centrifuged and filtered to remove any remaining cells or debris. INA-6 cells were then resuspended in this medium containing all the cytokines released by BMSCs. Unsupplemented fresh medium was used as a negative control of stimulation (Figure 28, black). RHOU expression dynamics after the addition of BMSCs' conditioned medium were similar to the ones observed after IL-6 stimulus, while adding TNF-α did not cause any significant changes.

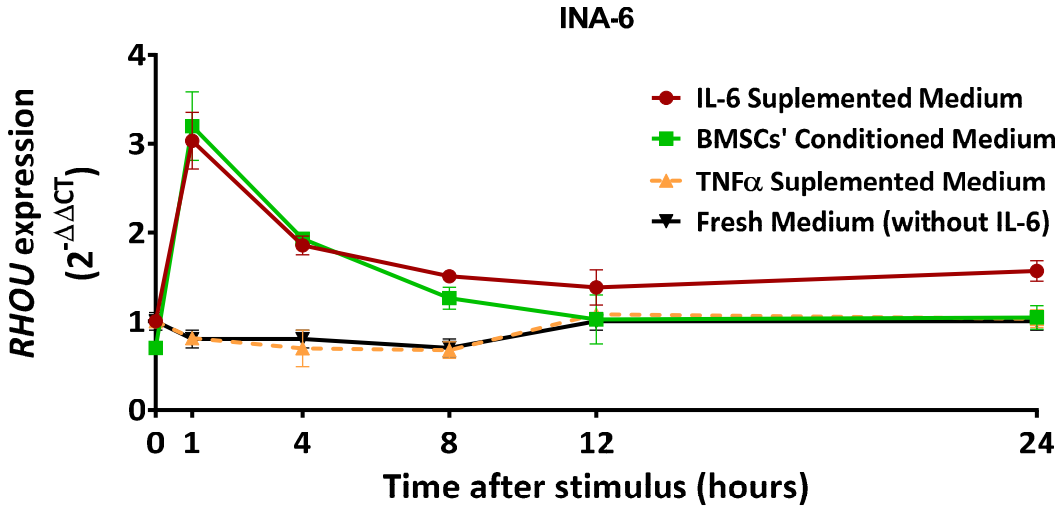

Figure 28: *RHOU* expression is significantly up-regulated to the same levels after IL-6 stimulus or addition of BMSCs' conditioned medium. Time-course showing the changes in *RHOU* expression after the addition of different stimulus to INA-6 cell line. Mean and SD of all conditions were normalized over time zero of cells in unsupplemented fresh medium.

CO-CULTURE OF MM CELL LINES WITH STROMA CELL LINE HS5 HAS A SIGNIFICANT IMPACT IN *RHOU* EXPRESSION

To deep our knowledge on *RHOU* modulation in the context of MM microenvironment, we have then co-cultured MM cell lines with HS5 stromal cell line (Figure 29). Two co-culture conditions were created: one where cells were cultured directly from their "normal" growth conditions and another one where cells were starved from IL-6 for 12 hours previous to co-culture. Again, starvation could not be performed for U266 cell line since these cells autocrinally produce IL-6. As a control of the ability of HS5 soluble factor ability to stimulate *RHOU* expression, starved cells were resuspended in medium containing all the cytokines released by HS5 (24 hours culture) as done previously with BMSCs. It is important to say that the medium was removed from HS5 cells before co-culture and fresh unsupplemented medium where MM cell lines were resuspended was added at time zero.

As expected, HS5 conditioned medium led to an upregulation of RHOU expression as early as 1 hour after addition, that resulted normalized after 24 hours.

Interestingly, in the co-culture condition we observed opposite results for the same cell lines with or without starvation. In starved cells, *RHOU* expression was up-regulated overtime on the following 72 hours after co-culture that could result from a slower/gradual stimulus production by HS5. On the other hand, in non-starved cells that had high *RHOU* levels at time zero, we unexpectedly observed a down-modulation of its expression over the next 72 hours that might be contact dependent.

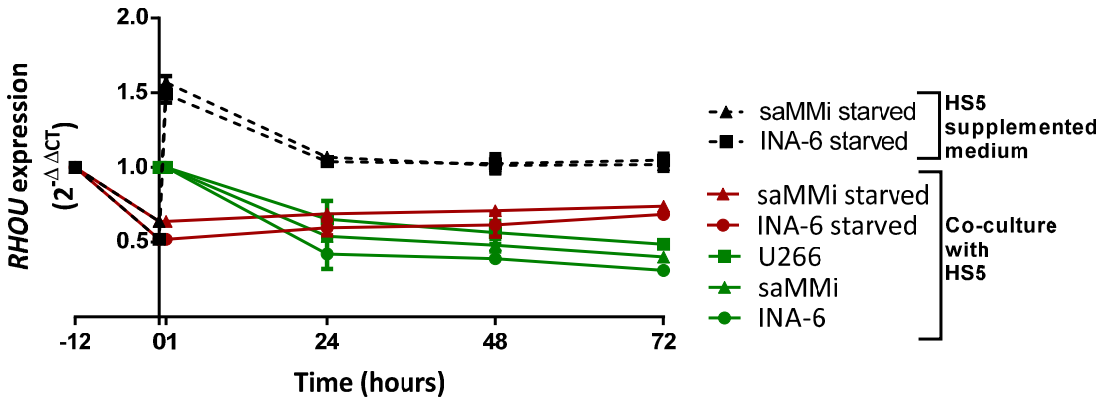

Figure 29: *RHOU* expression is significantly modulated after co-culture with stromal cell line HS5. Time-course showing the changes in *RHOU* expression after the addition of HS5 supplemented medium or after co-culture with HS5. Mean and SD of all conditions were normalized over time zero of each cell line.

RHOU EXPRESSION CORRELATES WITH STAT3 PATHWAY GENES' EXPRESSION

We took back to the gene expression profile data of MM patients to evaluate our hypothesis that in this disease, *RHOU* expression was highly dependent on the activation of the STAT3 pathway. We found a weak correlation with *STAT3* expression, which is important to remember, is not parallel to STAT3 protein activation (Figure 30). On the other hand, we have found a quite strong correlation with the expression of STAT3 pathway enhancer miR21 and with STAT3 target *SOCS3* (Figure 30).

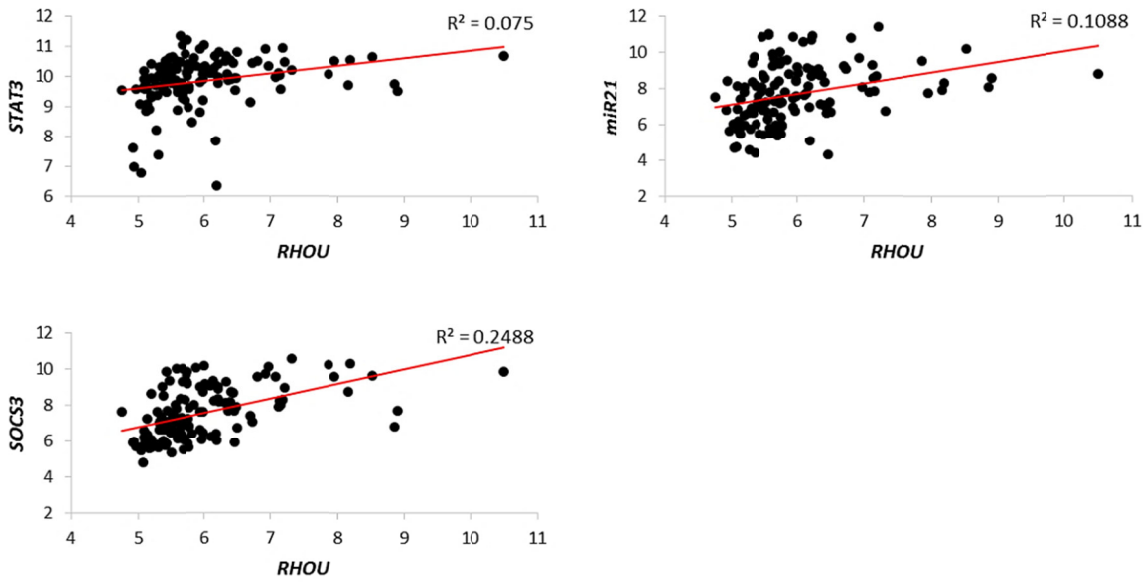

Figure 30: *RHOU* expression positively correlates with STAT3 pathway genes. *RHOU* expression showed a weak correlation with *STAT3* expression (Pearson's r = 0.274). However, it exhibbited a quite strong correlation with the expression of *miR21* (Pearson's r = 0.330), an enhancer of the STAT3-dependent signaling pathway and of *SOCS3* (Pearson's r = 0.499), a transcritional target of STAT3.

STAT3 INHIBITION AFFECTS *RHOU* EXPRESSION

To verify that STAT3 was the only target downstream of the IL-6R that could work as a transcription factor of *RHOU*, we have inhibited STAT3 with Stattic, a chemical inhibitor that by binding to the SH2 domain of STAT3 blocks its phosphorylation,

dimerization and nuclear transition. In this way STAT3 cannot activate the transcription of its target genes. Stattic was employed for 5 hours and then IL-6 was added or not to the cells for 1 hour to evaluate the ability of cells to up-regulate *RHOU* mRNA expression in response to this stimulus (Figure 31). Cells were starved of IL-6 only during the 6 hours of treatment since 12 hours starvation previous to treatment resulted in extensive cell death. Untreated (UN) cells were still able to up-regulate *RHOU* expression in response to IL-6 stimulus. After Stattic treatment U266 were less able to up-regulate *RHOU* mRNA. The same thing happened for saMMi at the lowest drug concentration, while at higher concentration this cell line was not able to up-regulate *RHOU*. INA-6 cells were not able to up-regulate it at any concentration of Stattic, with the highest concentration leading to extreme cell death.

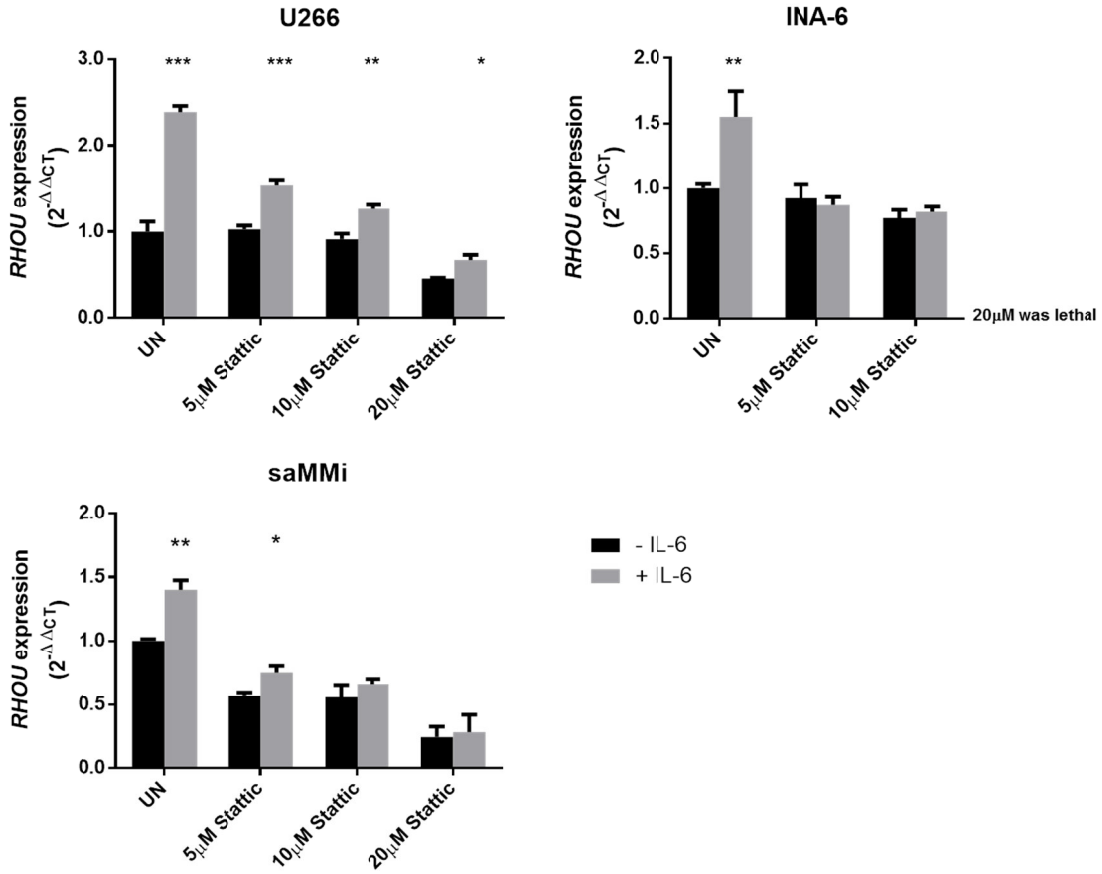

Figure 31: *RHOU* expression after STAT3 inhibition before and after IL-6 stimulus. Bar charts exhibit mean expression of RHOU from three independent samples, after treatment with increasing concentrations of Stattic. Black bars represent *RHOU* expression after 6 hours of culture with different concentrations of Stattic. Grey bars show *RHOU* expression after 5 hours of Stattic treatment + 1 hour of IL-6 stimulus. * $p<0.05$; ** $p<0.01$; *** $p<0.001$ when compared with the same treatment conditions without IL-6 stimulus.

MIGRATION CAPABILITY DECREASES AFTER STAT3 INHIBITION

Since RhoU an important controller of proteins involved in the regulation of the cytoskeleton, we aimed at validating if STAT3 inhibition had an effect in the migration capability of MM cell lines. We have created a transwell migration assay and evaluated by FACSCanto 1 minute reads the number of cells that were able to migrate through a 5µm filter. Stattic treatment led to a dose dependent decrease in cell migration that could be dependent on *RHOU* expression (Figure 32). Untreated (UN) cells were able to migrate as expected through the 5µm filter. Cells treated with increasing doses of Stattic were significantly less able to migrate.

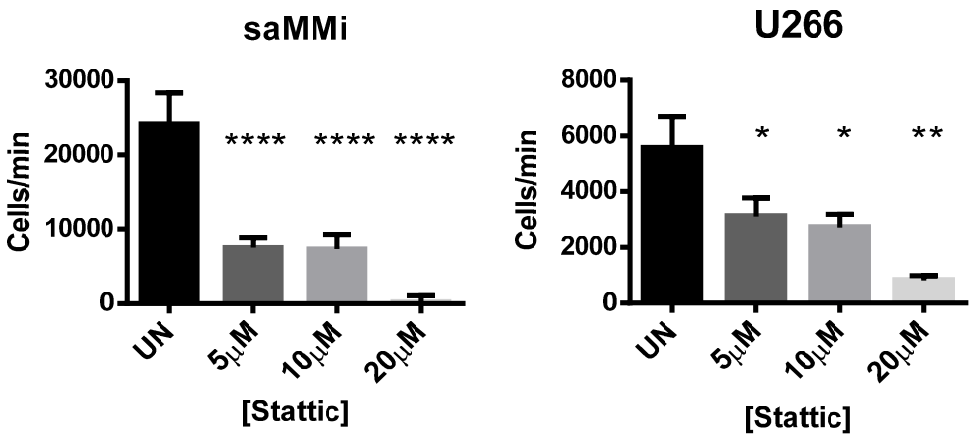

Figure 32: STAT3 inhibition led to a dose dependent decrease in MM cell migration. Bar charts exhibit mean cell count from three independent samples, after treatment with increasing concentrations of Stattic. Students t test * $p<0.05$; ** $p<0.01$; **** $p<0.0001$

RHOU SILENCING BY SIRNA AFFETCS JNK ACTIVATION

Next, we wanted to assess the effects of RhoU inhibition alone. With this purpose, we have silenced RhoU by transfecting cells with siRNA directed against *RHOU* mRNA and that prevents its translation into protein. Scrambled non-targeting siRNA (SCR) was used as control.

RhoU silencing led to a clear decrease in JNK activating phosphorylation, but does not seem to have an effect on cell death nor on STAT3 activation (Figure 33). JNK1 is a

target of RhoU important in the development of filopodia, a decrease in its activation could translate in a decreased migration capability.

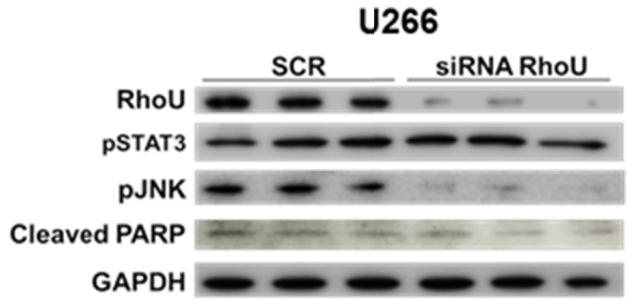

Figure 33: Immunoblot of U266 proteins after 24 hours of transfection with RhoU or SCR siRNA. Protein expression is showed in the following order: RhoU, phospho-STAT3 (Tyr705), phospho-JNK (Thr183/Tyr185), Cleaved PARP and GAPDH.

SILENCING OF *RHOU* LEADS TO A COMPLETE LOSS OF MIGRATION CAPABILITY

In studying the changes in cell migration after RhoU silencing, we have again performed a transwell migration assay. Cells where RhoU expression was inhibited and that consequently have lower levels of active JNK were no longer able to migrate when compared to SCR transfected cells (Figure 34).

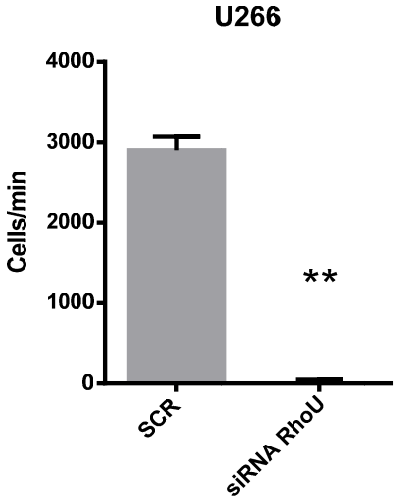

Figure 34: RhoU silencing led to a blockade in MM cell migration. Bar charts exhibit mean cell count from three independent samples, 24 hours after transfection with SCR or RhoU siRNA. Students t test ** $p<0.01$

LENALIDOMIDE AFFECTS IL-6 SIGNALING AND *RHOU* EXPRESSION

Lastly, since IMIDs were shown to be able to regulate the activation of classical Rho proteins, we aimed at studying the effects Lenalidomide could have in RhoU expression.

We have found an almost linear increase of *RHOU* expression over 24 hours after Lenalidomide treatment, independently of the dose used (2, 5 or 10 µM) (Figure 35).

Since this cell line is able to autocrinally produce IL-6, we have looked at *IL-6* expression and found it also over-expressed after Lenalidomide treatment, independently of the dose used (Figure 36)

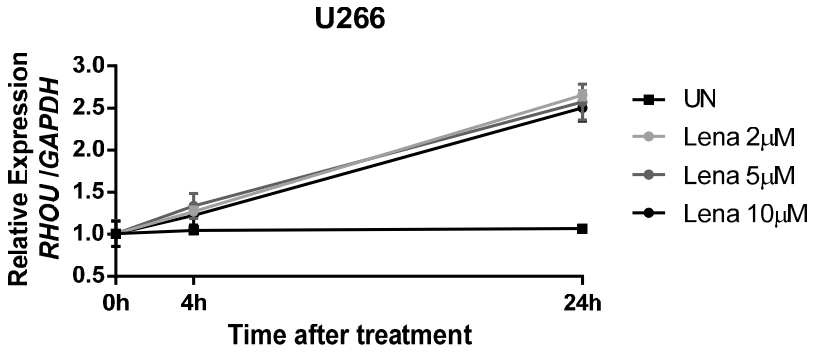

Figure 35: *RHOU* expression changed overtime after treatment with Lenalidomide. Time-course of *RHOU* expression in U266 cell line after treatment with increasing doses of Lenalidomide. Mean and SD normalized over time zero.

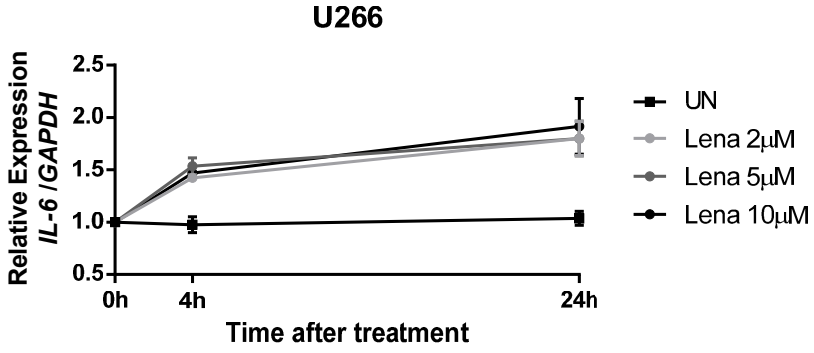

Figure 36: IL-6 expression changed overtime after treatment with Lenalidomide. Time-course of *IL-6* expression in U266 cell line after treatment with increasing doses of Lenalidomide Mean and SD normalized overtime zero.

Immunoblot showed indeed an increase in STAT3 activation after treatment with Lenalidomide, coherent with an increase in *IL-6* cytokine (Figure 37). We also observed

an increase in RhoU expression and in JNK activating phosphorylation (Figure 37) that could result in increased cell mobility. An increase in apoptosis at the highest doses can also be appreciated by the augmented PARP cleavage (Figure 37).

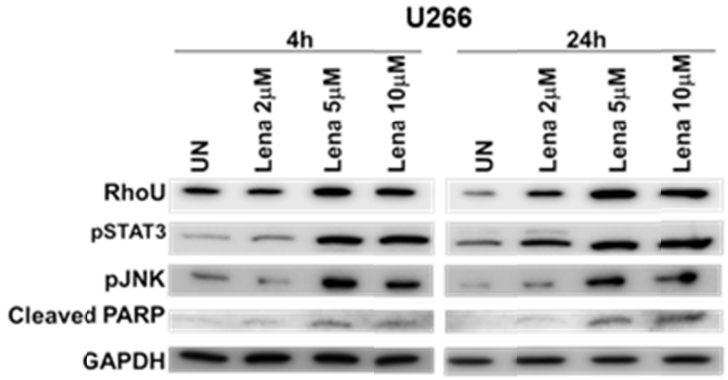

Figure 37: Immunoblots of U266 proteins after 4 and 24 hours of treatment with Lenalidomide. Protein expression is showed in the following order: RhoU, phospho-STAT3(Tyr705), phospho-JNK(Thr183/Tyr185), Cleaved PARP and GAPDH.

LENALIDOMIDE TREATMENT INCRESES MIGRATION ABILITY

We have then evaluated the changes in cell migration after Lenalidomide treatment by performing a transwell migration assay. Cells treated with Lenalidomide and that consequently have higher levels of RhoU and active JNK had a much higher migration rate when compared to untreated cells (UN) (Figure 38).

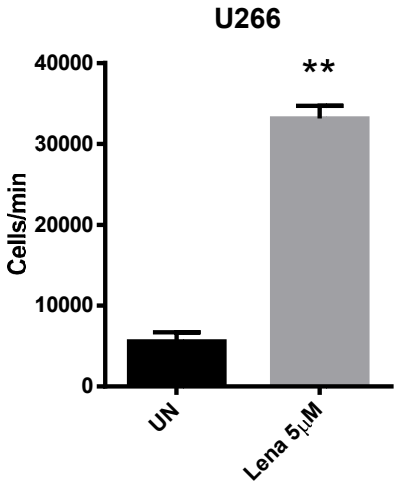

Figure 38: Lenalidomide treatment led to an increase in MM migration of around 6 times. Bar charts exhibit mean cell count from three independent samples, 4 hours after treatment with 5μM of Lenalidomide Students t test ** $p<0.01$

CHANGES IN *RHOU* EXPRESSION LEAD TO ACTIN CYTOSKELETON ALTERATIONS

To better study the cytoskeleton changes and possible alterations in cell adhesion after treatments we have employed immunofluorescence techniques.

Although all cells were able to adhere to polylysine coated glass, the changes in cell morphology were evident.

Untreated cells (UN) displayed round-up morphology (3D view) with smooth lamellipodia-like edges and some spiky protrusions that resembled filopodia (bottom layer view); siRNA RhoU cells had bigger lamellipodia-like edges with an accumulation of stress fibers and focal adhesions; lastly, Lenalidomide treated cells were flattened (3D view) and with multiple filopodial protrusion (bottom layer view), typical of migrating cells (Figure 39).

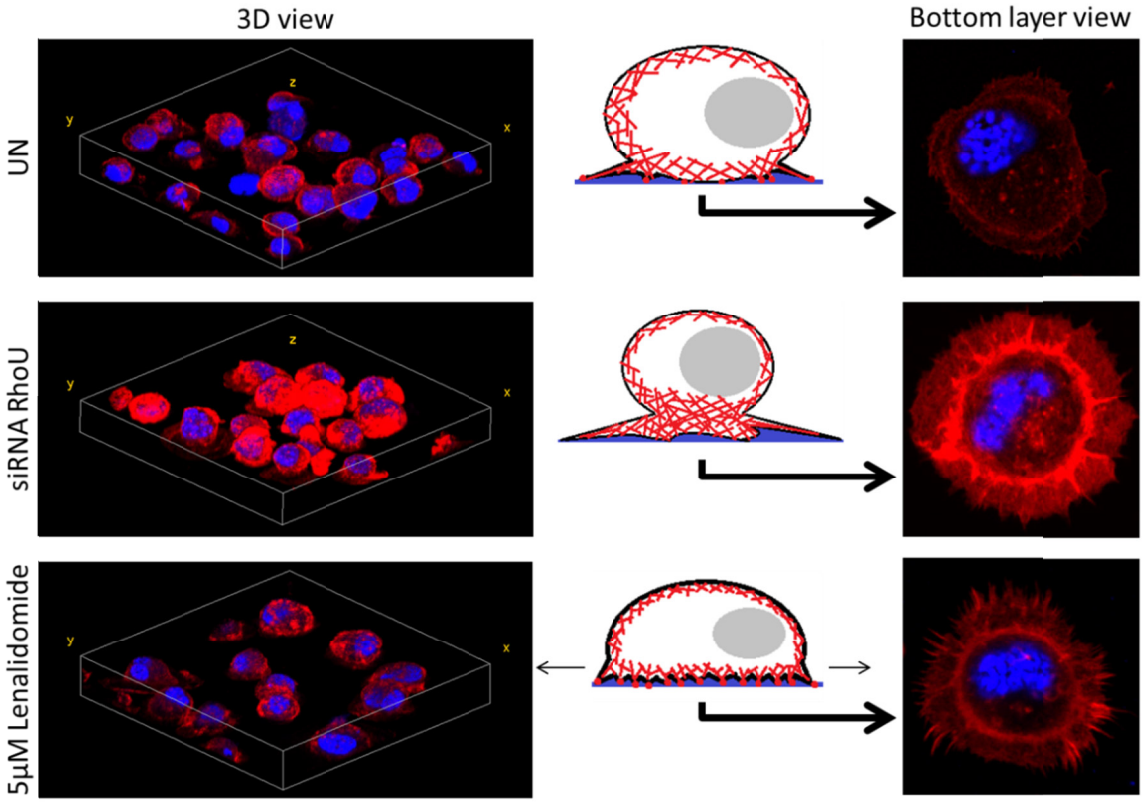

Figure 39: Changes in the actin cytoskeleton after RhoU silencing or treatment with Lenalidomide. DAPI staining shows the nucleus in blue, phalloidin staining in red shows F-actin filaments. Cells were fixed after 48h siRNA transfection or 24h of 5µM Lenalidomide treatment. All cells were plated at the same concentration in a 6 well plate for 48 hours to maintain the same growth conditions.

RHOU CORRELATES WITH GENES IMPORTANT FOR ADHESION, MIGRATION AND CYTOSKELETON DYNAMICS

We went back to our patients' gene expression profiling to look for possible correlations that could explain the changes in adhesion, migration and cytoskeleton dynamics in these cells.

Cdc42 small effector 1 (*CDC42SE1*) that regulates F-actin in T cells (Ching, Kisailus and Burbelo, 2005) was found to be correlated to *RHOU* expression in MM patients (Figure 40). RhoU and Cdc42 proteins are homologous Rho GTPases, so it is plausible that they can in some cases activate the same effectors.

Also, *MARK1* and neural cell adhesion molecule 1 (*NCAM1)*, both important in the regulation of neuron cells' migration and adhesion (Kaiser, Auerbach and Oldenburg, 1996; McDonald, 2014), and unexpectedly expressed in MM, were found to also correlate with *RHOU* expression (Figure 41 and 42).

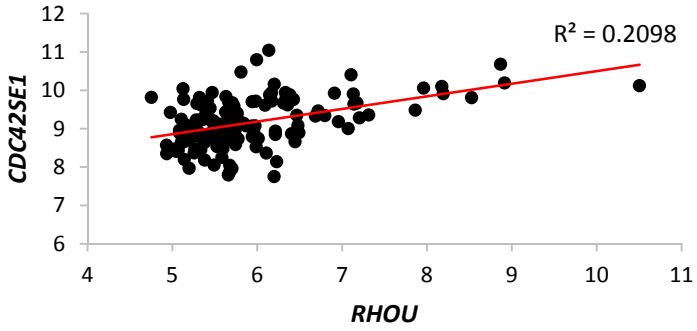

Figure 40: Correlation of *RHOU* expression with *CDC42SE1* expression in MM patients' cells. In MM patients, *RHOU* expression exhibits a quite strong correlation with the expression of *CDC42SE1* (Pearson's $r = 0.458$).

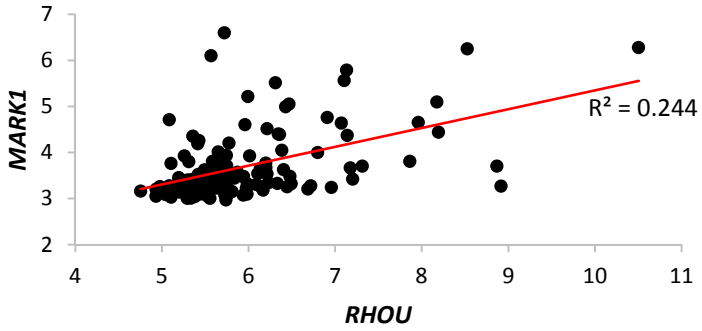

Figure 41: Correlation of *RHOU* expression with *MARK1* expression in MM patients' cells. In MM patients, *RHOU* expression exhibits a quite strong correlation with the expression of *MARK1* (Pearson's $r = 0.494$).

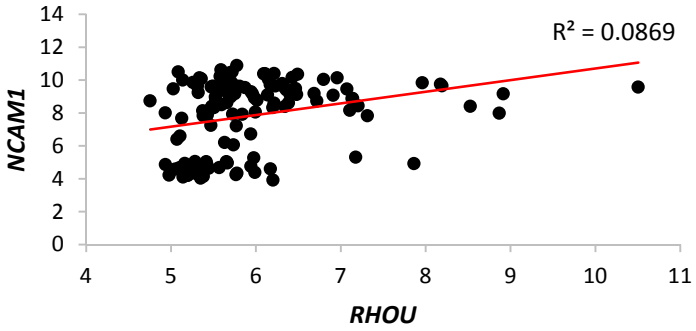

Figure 42: Correlation of *RHOU* expression with *NCAM1* expression in MM patients' cells. In MM patients, *RHOU* expression exhibits a quite strong correlation with the expression of *NCAM1* (Pearson's *r* = 0.295).

DISCUSSION

Rho GTPases are potent regulators of cytoskeleton dynamics and of the actin filament system, thereby affecting the morphologic and migratory properties of cells (Raftopoulou and Hall, 2004). Very little is known on the role of these proteins in the establishment and progression of MM malignancy.

We report for the first time a clear unbalance on the expression of multiple members of the Rho GTPase family in MM PCs when compared to normal PCs. Interestingly, opposite to what was seen in other tumors where there is an over-expression of some of the members of this family, in MM PCs we have found that more than 60% of Rho GTPases are actually down-modulated when compared to healthy PCs.

Looking at the different TC groups in which MM patients might fall depending on the translocations they present and on the expression of cyclin proteins, we have also unraveled a modulation of the majority of the atypical Rho proteins.

The RhoU/V family is particularly interesting to study due to its unique domain organization (Vega and Ridley, 2008). Besides being always in a GTP-bound conformation and therefore always active, both members of this family, RhoU and RhoV, have an N-terminal proline-rich domain that is not present in any other Rho GTPase and that enables them to permanently bind to their effectors (Risse *et al.*, 2013).

Focusing our attention on this family, we have found that *RHOU* expression is significantly modulated during the different steps of MM progression. Here we proved that MGUS patients have higher *RHOU* expression levels when compared to normal controls, raising the hypothesis that this protein might be important in the early stages of MM malignancy. With disease progression and accumulation of malignant PCs in the BM, we observed a decrease in *RHOU* (when compared to MGUS patients). With the progression to PCL we unexpectedly attested a further decrease in the levels of *RHOU* mRNA. It is important to remember that all the cells in this study are from BM biopsies, even the ones from PCL patients. This could explain the low levels of *RHOU* mRNA found in these samples since cells with high levels of this protein and thus more motile could be the ones to have left the patients' BM. We still need to verify this hypothesis by studying PCL cells extracted from the peripheral blood or pleural effusion of patients but unfortunately at this moment we do not have enough samples to perform this kind of analyses.

Basing on the fact that high RhoU levels have been described to lead to higher cell motility, while low RhoU levels are essential for adhesion (Faure and Fort, 2011), it makes sense that in the initial steps of the disease *RHOU* is expressed at high levels. In fact, in the early stages, PCs are competing for BM niches and are thought to be more motile (Podar, Chauhan and Anderson, 2009). With disease progression inside the BM, cells adhere, become more and more niche-dependent, and rely on this microenvironment for their survival, which seems to translate in lower *RHOU* levels.

Once we have divided patients in 3 groups with low (< Mean - 2SD of healthy controls), intermediate, and high (> Mean + 2SD of healthy controls) expression levels of *RHOU*, we have found a clear decrease in the number of patients with normal *RHOU* expression levels in all the steps of this malignancy. Around 30% of MGUS patients over-express *RHOU* while many MM and PLC patients actually down-modulate it, 42% and 64% respectively. It remains to be determined if these numbers correlate with how the patients' disease will progress.

Centering our attention on MM patients we have found that its expression is positively correlated with the presence of bad prognosis mutations t(4,14) (p value < 0.0001), del(13) (p value = 0.025), and 1q gain (p value = 0.027). We also established that *RHOU* expression is negatively correlated with the presence of the good prognosis mutation t(11,14) (p value = 0.002). Also, once we have divided MM samples into standard and high risk patients, we confirmed that patients in the high risk group have significantly higher levels of *RHOU* mRNA. Put together, these results prove that even though most MM patients actually down-modulate *RHOU*, a high expression of this GTPase actually correlates with a worse prognosis.

Furthermore, in MM patients *RHOU* clusters with genes of "cell cycle and mitosis" and "DNA damage". Its expression is indeed positively correlated with *CCND2* expression (Pearson's r = 0.402), while all the other genes responsible for cell cycle control and DNA damage response showed a negative correlation. This could be a possible explanation for the high frequency of bad prognosis mutations in MM patients with high *RHOU* levels.

To understand the dynamics of *RHOU* expression in MM PCs we have switched our study to MM cell lines. By analyzing the basal levels of *RHOU* in these cells, we have noticed that its mRNA expression was higher in IL-6 dependent cell lines (saMMi, INA-6 and U266) than in cell lines that were not dependent on IL-6 stimulus for their survival (RPMI-8226 and H929).

Stimulating MM cell lines with IL-6 resulted in a STAT3 dependent increase in *RHOU* expression. Indeed the inhibition of STAT3 resulted in a dose dependent decrease in *RHOU* expression and in a failure to up-regulate it in response to IL-6 stimulus. MM cell lines also up-regulated *RHOU* expression to a similar extent after the addition of BMSCs/HS5 conditioned medium, confirming that a high expression of *RHOU* might be important during the time when cells are in search of a growth niche. However the co-culture of MM cell lines (with high RhoU levels) with HS5 stroma cell line resulted in an actual decrease in *RHOU* expression, supporting the hypothesis of a contact dependent down-modulation of *RHOU* needed for cell adhesion, as previously observed in neural crest cells (Faure and Fort, 2011).

To note, in MM patients *RHOU* expression correlated with the expression of *STAT3* itself, of *miR21* (an enhancer of the STAT3 pathway) and of *SOCS3* (a STAT3 target gene), confirming that the expression of this GTPase in MM patients might be highly dependent on the activation of the STAT3 pathway, as observed in MM cell lines.

Moreover, the inhibition of STAT3 with Stattic led to a dose dependent decrease of the cells' migration capability, measured by transwell migration assay that might be RhoU dependent.

To verify if the effects on migration could be dependent on RhoU, we have directly blocked RhoU expression with siRNA particles. RhoU silencing did not impair STAT3 phosphorylation but it led to a clear depletion of JNK activating phosphorylation. Schiavone *et al.* (2009) had showed that RhoU is transcriptionally induced by both MAPK/JNK and JAK/STAT3 pathways. Even though this work only made clear that the phosphorylation of JNK or STAT3 and their translocation into the nucleus are essential for *RHOU* mRNA production, other studies suggested that the constitutively active RhoU mutant was able to increase JNK activation (Tao *et al.*, 2001) and that RhoU depletion inhibited JNK activating phosphorylation after induction by wound healing (Chuang *et al.*, 2007).

Accordingly, RhoU silencing led to the complete loss of migration capability that could be dependent on the decrease in JNK activation observed. The inhibition of JNK activation has as a consequence the impairment of filopodium formation, a type of cell protrusion essential for cell migration (Chuang *et al.*, 2007).

On the last part of this project we aimed at studying the effects of IMIDs on the IL-6/STAT3/RhoU/JNK branch. IMIDs are new generation drugs for MM treatment that have been shown to reorganize the cells cytoskeleton by modulating Rho GTPases (Xu *et*

al., 2009). However, only a few classical proteins (Cdc42, Rac1, RhoA) have been deeply studied. For these reasons we decided to investigate the effects of Lenalidomide on the modulation RhoU GTPase and on MM cytoskeleton dynamics.

Lenalidomide treatment led to a dose independent escalation in IL-6 production by MM cell line U266 that resulted in increased activation of STAT3, augmented RhoU expression and amplified activation of JNK. Consistently and opposite to what was observed with Stattic or RhoU silencing, Lenalidomide treatment led to a high increase in cell motility assessed by transwell migration assay. These results give new insights to a mechanism never described before for Lenalidomide and prove that this drug can somehow stimulate the activation of STAT3 transcription factor enhancing the expression of its target genes including *RHOU*, leading to cytoskeletal changes in MM PCs.

To better understand the cytoskeleton dynamics involved in MM adhesion, we have used polylysine coated cover-slips to which we added MM cells untreated, after RhoU silencing or treated with Lenalidomide. Although all cells were able to stick to polylysine coated glass, the cells where RhoU was inhibited were clearly more adherent, with a complex F-actin net that extended from the cell membrane, and a clear accumulation of stress fibers. On the other hand, cells where Lenalidomide treatment was employed had a less complex cytoskeleton but presented multiple filopodia-like protrusions, typical of migrating cells.

Given the clear changes in adhesion, migration and cytoskeleton dynamics after RhoU silencing or up-modulation, we went back to the gene expression studies done in the cohort of 129 MM patients to look for possible correlations that might help explain these observations. Interestingly, *RHOU* expression correlated with the expression of *CDC42SE1*, a protein that was found to mediate F-actin regulation in T cells after T cell receptor activation (Ching, Kisailus and Burbelo, 2005). CDC42SE1 is a known effector of the classical GTPase Cdc42. However, the fact that Cdc42 and RhoU share 57% of their amino acid sequence and have a 70% structure similarity opens the possibility of the existence of common effectors for these two GTPases (Tao *et al.*, 2001).

RHOU expression was also correlated, in MM patients, with the expression of proteins involved in neuron migration and adhesion processes: *NCAM1* and *MARK1*. Some neuronal genes have already been described to be expressed on MM cells but their functions and regulation remain to be fully understood (Kaiser, Auerbach and Oldenburg, 1996; Iqbal *et al.*, 2010). MARK1 is involved in the regulation of neuronal migration through the regulation of cellular polarity and microtubule dynamics, and is required for

the migration of multiple cell types (McDonald, 2014) however, it was never described to have a function in MM malignancy. NCAM1 also called CD56, on the other hand, is an adhesion molecule of neuron cells that in MM is expressed in 70-80% of patients and its serum levels seem to correlate with loss of adhesive function (Kaiser, Auerbach and Oldenburg, 1996; Chang S.; Yi, Q. L., 2006). It would be interesting to study if NCAM serum levels also correlate with *RHOU* expression since an increase in any of these two seems to lead to the same outcome of loss of adhesion.

CONCLUSIONS

This study demonstrates for the first time a deregulation on the expression of a large number of GTPases from the Rho family in MM malignancy. RhoU is a singular protein that besides being always in an active GTP-bound state like all the other atypical GTPases has a unique domain organization that renders it different from all the proteins in this family. We have found that it is significantly modulated during disease progression. Indeed, when compared to healthy controls MGUS patients have higher *RHOU* mRNA levels that decrease with disease progression and accumulation of malignant PCs in the BM, raising the premise that this protein could be important in the early stages of MM malignancy.

However, even if the median levels of *RHOU* expression decrease with disease progression, high levels of *RHOU* mRNA in MM patients actually positively correlate with the expression of *CCND2*, which might determine a higher proliferation rate in this cells. Besides this, it negatively correlates with the expression of cell cycle control and DNA damage response genes. We have also found a higher rate of t(4;14), del(13) and q1 gain mutations in patients that have high *RHOU* expression levels, coherent with high proliferation rate and low DNA damage response in these cells.

We have confirmed that *RHOU* expression lays downstream of STAT3 activation and that silencing of this GTPase causes impairment in MM cells' migration. Interestingly, *RHOU* expression correlated with the expression of *CDC42SE1*, an effector protein that was found to mediate F-actin regulation, and with the expression of *NCAM1* and *MARK1* that are involved in neuron migration and adhesion processes. These correlations might explain how different levels of this protein can actually affect many branches of the actin polymerization and organization system, impacting cells' cytoskeleton dynamic, migration and adhesion.

Put together, these results seem to confirm that also in the context of MM malignancy high RhoU levels are needed for migration and search of a growth niche, while its down-modulation increases cell adhesion probably empowering a niche mediated protection.

Lastly, the treatment with Lenalidomide, an IMiD used in MM therapy, led to an increase in IL-6 production by MM cell line U266, amplified activation of the STAT3 pathway and augmented RhoU levels. This increase in STAT3 activation and RhoU expression translated in increased cell migration rates that could actually be very

important since this renders cells less adherent and more easily struck through parallel mechanisms.

The fact that a decrease in RhoU expression actually boosts cell adhesion opens-up new debate on whether or not we should actually inhibit the IL-6 pathway in MM treatment, since this could lead to higher adhesion and consequently augmented protection from the microenvironmental niche.

REFERENCES

Abdou, I., Poirier, G. G., Hendzel, M. J. and Weinfeld, M. (2015) 'DNA ligase III acts as a DNA strand break sensor in the cellular orchestration of DNA strand break repair', *Nucleic Acids Research*, 43(2), pp. 875–892. doi: 10.1093/nar/gku1307.

Abroun, S., Saki, N., Ahmadvand, M., Asghari, F., Salari, F. and Rahim, F. (2015) 'STATs: An old story, yet mesmerizing', *Cell Journal*, 17(3), pp. 395–411.

Agnelli, L., Bicciato, S., Mattioli, M., Fabris, S., Intini, D., Verdelli, D., Baldini, L., Morabito, F., Callea, V., Lombardi, L. and Neri, A. (2005) 'Molecular Classification of Multiple Myeloma : A Distinct Transcriptional Profile Characterizes Patients Expressing CCND1 and Negative for 14q32 Translocations', *Journal of Clinical Oncology*, 23(29), pp. 7296–7306. doi: 10.1200/JCO.2005.01.3870.

Anderson, K. C. (2005) 'Lenalidomide and thalidomide: mechanisms of action--similarities and differences.', *Seminars in hematology*, 42(4 Suppl 4), pp. S3-8. doi: 10.1053/j.seminhematol.2005.10.001.

Anderson, K. C. and Carrasco, R. D. (2011) 'Pathogenesis of myeloma.', *Annual review of pathology*, 6, pp. 249–74. doi: 10.1146/annurev-pathol-011110-130249.

Aspenström, P., Ruusala, A. and Pacholsky, D. (2007) 'Taking Rho GTPases to the next level: The cellular functions of atypical Rho GTPases', *Experimental Cell Research*, 313(17), pp. 3673–3679. doi: 10.1016/j.yexcr.2007.07.022.

Bakkenist, C. J. and Kastan, M. B. (2003) 'DNA damage activates ATM through intermolecular autophosphorylation and dimer dissociation.', *Nature*, 421(6922), pp. 499–506. doi: 10.1038/nature01368.

Bayer-Garner, I. B., Sanderson, R. D., Dhodapkar, M. V, Owens, R. B. and Wilson, C. S. (2001) 'Syndecan-1 (CD138) immunoreactivity in bone marrow biopsies of multiple myeloma: shed syndecan-1 accumulates in fibrotic regions.', *Modern pathology : an official journal of the United States and Canadian Academy of Pathology, Inc*, 14(10), pp. 1052–8. doi: 10.1038/modpathol.3880435.

Bergsagel, P. L., Kuehl, W. M., Zhan, F., Sawyer, J., Barlogie, B. and Shaughnessy, J. (2005) 'Cyclin D dysregulation: An early and unifying pathogenic event in multiple myeloma', *Blood*, 106(1), pp. 296–303. doi: 10.1182/blood-2005-01-0034.

Berzat, A. C., Buss, J. E., Chenette, E. J., Weinbaum, C. A., Shutes, A., Der, C. J., Minden, A. and Cox, A. D. (2005) 'Transforming activity of the Rho family GTPase, Wrch-1, a Wnt-regulated Cdc42 homolog, is dependent on a novel carboxyl-terminal palmitoylation motif', *Journal of Biological Chemistry*, 280(38), pp. 33055–33065. doi: 10.1074/jbc.M507362200.

Bhavsar, P. J., Infante, E., Khwaja, a and Ridley, a J. (2013) 'Analysis of Rho GTPase expression in T-ALL identifies RhoU as a target for Notch involved in T-ALL cell migration.', *Oncogene*, 32(2), pp. 198–208. doi: 10.1038/onc.2012.42.

Bladé, J., Rosiñol, L., Cibeira, M. T. and de Larrea, C. F. (2008) 'Pathogenesis and progression of monoclonal gammopathy of undetermined significance.', *Leukemia : official journal of the Leukemia Society of America, Leukemia Research Fund, U.K*, 22(9), pp. 1651–1657. doi: 10.1038/leu.2008.203.

Bommert, K., Bargou, R. C. and Stühmer, T. (2006) 'Signalling and survival pathways in multiple myeloma', *European Journal of Cancer*, 42(11), pp. 1574–1580. doi: 10.1016/j.ejca.2005.12.026.

Boncela, J., Przygodzka, P., Papiewska-Pajak, I., Wyroba, E., Osinska, M. and Cierniewski, C. S. (2011) 'Plasminogen activator inhibitor type 1 interacts with alpha3 subunit of proteasome and modulates its activity.', *The Journal of biological chemistry*, 286(8), pp. 6820–31. doi: 10.1074/jbc.M110.173781.

Boureux, A., Vignal, E., Faure, S. and Fort, P. (2007) 'Evolution of the Rho family of Ras-like GTPases in eukaryotes', *Molecular Biology and Evolution*, 24(1), pp. 203–216. doi: 10.1093/molbev/msl145.

Boyd, S. D., Natkunam, Y., Allen, J. R. and Warnke, R. a. (2013) 'Selective Immunophenotyping for Diagnosis of B-cell Neoplasms: Immunohistochemistry and Flow Cytometry Strategies and Results', *Applied Immunohistochemistry & Molecular Morphology*, 21(2), pp. 116–131. doi: 10.1097/PAI.0b013e31825d550a.

Brazier, H., Stephens, S., Ory, S., Fort, P., Morrison, N. and Blangy, A. (2006) 'Expression profile of RhoGTPases and RhoGEFs during RANKL-stimulated osteoclastogenesis: identification of essential genes in osteoclasts.', *Journal of bone and mineral research : the official journal of the American Society for Bone and Mineral Research*, 21(9), pp. 1387–1398. doi: 10.1359/jbmr.060613.

Burger, R., Guenther, a, Bakker, F., Schmalzing, M., Bernand, S., Baum, W., Duerr, B., Hocke, G. M., Steininger, H., Gebhart, E. and Gramatzki, M. (2001) 'Gp130 and ras mediated signaling in human plasma cell line INA-6: a cytokine-regulated tumor model for plasmacytoma.', *The hematology journal : the official journal of the European Haematology Association / EHA*, 2(1), pp. 42–53. doi: 10.1038/sj.thj.6200075.

Carow, B. and Rottenberg, M. E. (2014) 'SOCS3, a major regulator of infection and inflammation', *Frontiers in Immunology*. doi: 10.3389/fimmu.2014.00058.

Chang S.; Yi, Q. L., H. . S. (2006) 'Prognostic relevance of CD56 expression in multiple myeloma: a study including 107 cases treated with high-dose melphalan-based chemotherapy and autologous stem cell transplant', *Leuk Lymphoma*, 47(1), pp. 43–47. doi: M550664643878LG2 [pii]; 10.1080/10428190500272549 [doi].

Chardin, P. (2006) 'Function and regulation of Rnd proteins.', *Nature reviews. Molecular cell biology*, 7(1), pp. 54–62. doi: 10.1038/nrm1788.

Ching, K. H., Kisailus, A. E. and Burbelo, P. D. (2005) 'The role of SPECs, small Cdc42-binding proteins, in F-actin accumulation at the immunological synapse', *Journal of Biological Chemistry*, 280(25), pp. 23660–23667. doi: 10.1074/jbc.M500128200.

Chuang, Y., Valster, A., Coniglio, S. J., Backer, J. M. and Symons, M. (2007) 'The atypical Rho family GTPase Wrch-1 regulates focal adhesion formation and cell migration.', *Journal of cell science*, 120, pp. 1927–1934. doi: 10.1242/jcs.03456.

Coleman, D. R., Ren, Z., Mandal, P. K., Cameron, A. G., Dyer, G. A., Muranjan, S., Campbell, M., Chen, X. and McMurray, J. S. (2005) 'Investigation of the binding determinants of phosphopeptides targeted to the Src homology 2 domain of the signal transducer and activator of transcription 3. Development of a high-affinity peptide inhibitor', *Journal of Medicinal Chemistry*, 48(21), pp. 6661–6670. doi: 10.1021/jm050513m.

Corre, J., Munshi, N. and Avet-Loiseau, H. (2015) 'Genetics of multiple myeloma: Another heterogeneity level?', *Blood*, pp. 1870–1876. doi: 10.1182/blood-2014-10-567370.

Cox, A. D. and Der, C. J. (2010) 'Ras history: The saga continues.', *Small GTPases*, 1(1), pp. 2–27. doi: 10.4161/sgtp.1.1.12178.

Dalakas, M. C. (2008) 'B cells as therapeutic targets in autoimmune neurological disorders.', *Nature clinical practice. Neurology*, 4(10), pp. 557–67. doi: 10.1038/ncpneuro0901.

Dickover, M., Hegarty, J. M., Ly, K., Lopez, D., Yang, H., Zhang, R., Tedeschi, N., Hsiai, T. K. and Chi, N. C. (2014) 'The atypical Rho GTPase, RhoU, regulates cell-adhesion molecules during cardiac morphogenesis', *Developmental Biology*, 389(2), pp. 182–191. doi: 10.1016/j.ydbio.2014.02.014.

Eddy, S., Ketkar, A., Zafar, M. K., Maddukuri, L., Choi, J.-Y. and Eoff, R. L. (2014) 'Human Rev1 polymerase disrupts G-quadruplex DNA.', *Nucleic acids research*, 42(5), pp. 3272–85. doi: 10.1093/nar/gkt1314.

Fairfax, K. A., Kallies, A., Nutt, S. L. and Tarlinton, D. M. (2008) 'Plasma cell development: From B-cell subsets to long-term survival niches', *Seminars in Immunology*, pp. 49–58. doi: 10.1016/j.smim.2007.12.002.

Faure, S. and Fort, P. (2011) 'Atypical RhoV and RhoU GTPases control development of the neural crest', *Small GTPases*, 2(6), pp. 310–313. doi: 10.4161/sgtp.18086.

Fonseca, R. (2007) 'Strategies for risk-adapted therapy in myeloma.', *Hematology*, pp. 304–10. doi: 10.1182/asheducation-2007.1.304.

Fonseca, R., Barlogie, B., Bataille, R., Bastard, C., Bergsagel, P. L., Chesi, M., Davies, F. E., Drach, J., Greipp, P. R., Kirsch, I. R., Kuehl, W. M., Hernandez, J. M., Minvielle, S., Pilarski, L. M., Shaughnessy, J. D., Stewart, A. K. and Avet-Loiseau, H. (2004) 'Genetics and Cytogenetics of Multiple Myeloma: A Workshop Report', in *Cancer Research*, pp. 1546–1558. doi: 10.1158/0008-5472.CAN-03-2876.

Fort, P., Guémar, L., Vignal, E., Morin, N., Notarnicola, C., Barbara, P. de S. and Faure, S. (2011) 'Activity of the RhoU/Wrch1 GTPase is critical for cranial neural crest cell migration', *Developmental Biology*, 350(2), pp. 451–463. doi: 10.1016/j.ydbio.2010.12.011.

Fritz, G. and Henninger, C. (2015) 'Rho GTPases: Novel Players in the Regulation of the DNA Damage Response?', *Biomolecules*, 5(4), pp. 2417–2434. doi: 10.3390/biom5042417.

Fritz, R. D. and Pertz, O. (2016) 'The dynamics of spatio-temporal Rho GTPase signaling: formation of signaling patterns', *F1000Research*, 5, pp. 749–761. doi: 10.12688/f1000research.7370.1.

Gazdar, A. F., Oie, H. K., Kirsch, I. R. and Hollis, G. F. (1986) 'Establishment and characterization of a human plasma cell myeloma culture having a rearranged cellular myc proto-oncogene.', *Blood*, 67(6), pp. 1542–9. Available at: http://www.ncbi.nlm.nih.gov/pubmed/2423157.

Gileadi, C., Yang, X., Papagrigoriou, E., Elkins, J., Zhao, Y., Bray, J., Gileadi, O., Umeano, C., Ugochukwu, E., Uppenberg, J., Bunkoczi, G., von Delft, F., Pike, A. C. ., Phillips, C., Savitsky, P., Fedorov, O., Edwards, A., Weigelt, J., Arrowsmith, C. ., Sundstrom, M. and Doyle, D. A. (2007) 'The crystal structure of RhoU in the GDP-bound state.', *The Protein Data Bank*. doi: 10.2210/PDB2Q3H/PDB.

Gozuacik, D., Chami, M., Lagorce, D., Faivre, J., Murakami, Y., Pock, O., Biermann, E., Knippers, R., Bréchot, C. and Paterlini-Bréchot, P. (2003) 'Identification and functional characterization of a new member of the human Mcm protein family: hMcm8', *Nucleic Acids Research*, pp. 570–579. doi: 10.1093/nar/gkg136.

Guirguis, A. A. and Ebert, B. L. (2015) 'Lenalidomide: Deciphering mechanisms of action in myeloma, myelodysplastic syndrome and beyond', *Current Opinion in Cell Biology*. Elsevier Ltd,

37, pp. 61–67. doi: 10.1016/j.ceb.2015.10.004.

van Helden, S. F. G., Anthony, E. C., Dee, R. and Hordijk, P. L. (2012) 'Rho GTPase expression in human myeloid cells', *PLoS ONE*, 7(8). doi: 10.1371/journal.pone.0042563.

Henninger, E. E. and Pursell, Z. F. (2014) 'DNA polymerase ε and its roles in genome stability', *IUBMB Life*, pp. 339–351. doi: 10.1002/iub.1276.

Hideshima, T., Bergsagel, P. L., Kuehl, W. M. and Anderson, K. C. (2004) 'Advances in biology of multiple myeloma : clinical applications', *Blood*, 104(3), pp. 607–618. doi: 10.1182/blood-2004-01-0037.

Hodge, R. G. and Ridley, A. J. (2016) 'Regulating Rho GTPases and their regulators', *Nature Reviews Molecular Cell Biology*. Nature Publishing Group, 17(8), pp. 496–510. doi: 10.1038/nrm.2016.67.

Huang, D. W., Lempicki, R. a and Sherman, B. T. (2009) 'Systematic and integrative analysis of large gene lists using DAVID bioinformatics resources.', *Nature Protocols*, 4(1), pp. 44–57. doi: 10.1038/nprot.2008.211.

Iliopoulos, D., Jaeger, S. A., Hirsch, H. A., Bulyk, M. L. and Struhl, K. (2010) 'STAT3 Activation of miR-21 and miR-181b-1 via PTEN and CYLD Are Part of the Epigenetic Switch Linking Inflammation to Cancer', *Molecular Cell*, 39(4), pp. 493–506. doi: 10.1016/j.molcel.2010.07.023.

Iqbal, M. S., Otsuyama, K. I., Shamsasenjan, K., Asaoku, H. and Kawano, M. M. (2010) 'CD56 expression in human myeloma cells derived from the neurogenic gene expression: Possible role of the SRY-HMG box gene, SOX4', *International Journal of Hematology*, 91(2), pp. 267–275. doi: 10.1007/s12185-009-0474-3.

Irizarry, R. A., Hobbs, B., Collin, F., Beazer-Barclay, Y. D., Antonellis, K. J., Scherf, U. and Speed, T. P. (2003) 'Exploration, normalization, and summaries of high density oligonucleotide array probe level data', *Biostatistics*, 4(2), pp. 249–264. doi: 10.1093/biostatistics/4.2.249.

Jeong, S.-J., Kim, H.-J., Yang, Y.-J., Seol, J.-H., Jung, B.-Y., Han, J.-W., Lee, H.-W. and Cho, E.-J. (2005) 'Role of RNA polymerase II carboxy terminal domain phosphorylation in DNA damage response.', *Journal of microbiology (Seoul, Korea)*, 43(6), pp. 516–22. Available at: http://www.ncbi.nlm.nih.gov/pubmed/16410768.

Kaiser, U., Auerbach, B. and Oldenburg, M. (1996) 'The neural cell adhesion molecule NCAM in multiple myeloma', *Leukemia & Lymphoma*, 20(5–6), pp. 389–395. doi: 10.3109/10428199609052420.

Kim, H., Fonseca, C. and Stumpff, J. (2014) 'A unique kinesin-8 surface loop provides specificity for chromosome alignment.', *Molecular biology of the cell*, 25(21), pp. 3319–3329. doi: 10.1091/mbc.E14-06-1132.

Klungland, A. and Bjelland, S. (2007) 'Oxidative damage to purines in DNA: Role of mammalian Ogg1', *DNA Repair*, 6(4), pp. 481–488. doi: 10.1016/j.dnarep.2006.10.012.

Kumar, S. K., Lee, J. H., Lahuerta, J. J., Morgan, G., Richardson, P. G., Crowley, J., Haessler, J., Feather, J., Hoering, A., Moreau, P., LeLeu, X., Hulin, C., Klein, S. K., Sonneveld, P., Siegel, D., Bladé, J., Goldschmidt, H., Jagannath, S., Miguel, J. S., Orlowski, R., Palumbo, A., Sezer, O., Rajkumar, S. V and Durie, B. G. M. (2012) 'Risk of progression and survival in multiple myeloma relapsing after therapy with IMiDs and bortezomib: a multicenter international myeloma working group study.', *Leukemia*, 26(1), pp. 149–57. doi: 10.1038/leu.2011.196.

Kumar, S. K., Rajkumar, S. V., Dispenzieri, A., Lacy, M. Q., Hayman, S. R., Buadi, F. K.,

Zeldenrust, S. R., Dingli, D., Russell, S. J., Lust, J. A., Greipp, P. R., Kyle, R. A. and Gertz, M. A. (2008) 'Improved survival in multiple myeloma and the impact of novel therapies', *Blood*, 111(5), pp. 2516–2520. doi: 10.1182/blood-2007-10-116129.

Kumar, S., Kimlinger, T. and Morice, W. (2010) 'Immunophenotyping in multiple myeloma and related plasma cell disorders', *Best Practice and Research: Clinical Haematology*, pp. 433–451. doi: 10.1016/j.beha.2010.09.002.

Landgren, O., Kyle, R. A., Pfeiffer, R. M., Katzmann, J. A., Caporaso, N. E., Hayes, R. B., Dispenzieri, A., Kumar, S., Clark, R. J., Baris, D., Hoover, R. and Rajkumar, S. V. (2009) 'Monoclonal gammopathy of undetermined significance (MGUS) consistently precedes multiple myeloma: A prospective study', *Blood*, 113(22), pp. 5412–5417. doi: 10.1182/blood-2008-12-194241.

Latif, T., Chauhan, N., Khan, R., Moran, A. and Usmani, S. Z. (2012) 'Thalidomide and its analogues in the treatment of Multiple Myeloma', *Experimental Hematology & Oncology*, 1(1), p. 27. doi: 10.1186/2162-3619-1-27.

Li, D., Das, S., Yamada, T. and Samuels, H. H. (2004) 'The NRIF3 family of transcriptional coregulators induces rapid and profound apoptosis in breast cancer cells', *Molecular and cellular ...*, 24(9), pp. 3838–3848. doi: 10.1128/MCB.24.9.3838.

Löffler, D., Brocke-Heidrich, K., Pfeifer, G., Stocsits, C., Hackermüller, J., Kretzschmar, A. K., Burger, R., Gramatzki, M., Blumert, C., Bauer, K., Cvijic, H., Ullmann, A. K., Stadler, P. F. and Horn, F. (2007) 'Interleukin-6 dependent survival of multiple myeloma cells involves the Stat3-mediated induction of microRNA-21 through a highly conserved enhancer', *Blood*, 110(4), pp. 1330–3. doi: 10.1182/blood-2007-03-081133.

López-Corral, L., Corchete, L. A., Sarasquete, M. E., Mateos, M. V., García-Sanz, R., Fermiñán, E., Lahuerta, J. J., Bladé, J., Oriol, A., Teruel, A. I., Martino, M. L., Hernández, J., Hernández-Rivas, J. M., Burguillo, F. J., San Miguel, J. F. and Gutiérrez, N. C. (2014) 'Transcriptome analysis reveals molecular profiles associated with evolving steps of monoclonal gammopathies', *Haematologica*, 99(8), pp. 1365–1372. doi: 10.3324/haematol.2013.087809.

Matsuoka, Y., Moore, G., Yagi, Y. and Pressman, D. (1967) 'Production of free light chains of immunoglobulin by a hematopoietic cell line derived from a patient with multiple myeloma', *Proc Soc Exp Biol Med*, 125(4), pp. 1246–1250.

McDonald, J. A. (2014) 'Canonical and Noncanonical Roles of Par-1/MARK Kinases in Cell Migration', *International Review of Cell and Molecular Biology*, 312, pp. 169–199. doi: 10.1016/B978-0-12-800178-3.00006-3.

Morgan, G. J., Walker, B. a and Davies, F. E. (2012) 'The genetic architecture of multiple myeloma.', *Nature reviews. Cancer*, 12, pp. 335–48. doi: 10.1038/nrc3257.

Nilsson, K., Bennich, H., Johansson, S. G. and Pontén, J. (1970) 'Established immunoglobulin producing myeloma (IgE) and lymphoblastoid (IgG) cell lines from an IgE myeloma patient.', *Clinical and experimental immunology*, 7(4), pp. 477–89. Available at: http://www.pubmedcentral.nih.gov/articlerender.fcgi?artid=1712861&tool=pmcentrez&rendertype=abstract.

Noonan, K. and Borrello, I. (2011) 'The immune microenvironment of myeloma', *Cancer Microenvironment*, pp. 313–323. doi: 10.1007/s12307-011-0086-3.

Ocio, E. M., Richardson, P. G., Rajkumar, S. V, Palumbo, A., Mateos, M. V, Orlowski, R., Kumar, S., Usmani, S., Roodman, D., Niesvizky, R., Einsele, H., Anderson, K. C., Dimopoulos, M. A., Avet-Loiseau, H., Mellqvist, U.-H., Turesson, I., Merlini, G., Schots, R., McCarthy, P.,

Bergsagel, L., Chim, C. S., Lahuerta, J. J., Shah, J., Reiman, A., Mikhael, J., Zweegman, S., Lonial, S., Comenzo, R., Chng, W. J., Moreau, P., Sonneveld, P., Ludwig, H., Durie, B. G. M. and Miguel, J. F. S. (2014) 'New drugs and novel mechanisms of action in multiple myeloma in 2013: a report from the International Myeloma Working Group (IMWG).', *Leukemia*. Nature Publishing Group, 28(3), pp. 525–42. doi: 10.1038/leu.2013.350.

Orjalo, A. V, Arnaoutov, A., Shen, Z., Boyarchuk, Y., Zeitlin, S. G., Fontoura, B., Briggs, S., Dasso, M., Forbes, D. J., Mains, P. E., Sulston, I. A. and Wood, W. B. (2006) 'The Nup107-160 Nucleoporin Complex Is Required for Correct Bipolar Spindle Assembly', *Molecular Biology of the Cell*, 17(9), pp. 3806–3818. doi: 10.1091/mbc.E05-11-1061.

Ory, S., Brazier, H. and Blangy, A. (2007) 'Identification of a bipartite focal adhesion localization signal in RhoU/Wrch-1, a Rho family GTPase that regulates cell adhesion and migration.', *Biology of the cell / under the auspices of the European Cell Biology Organization*, 99, pp. 701–716. doi: 10.1042/BC20070058.

Osman, F. and Whitby, M. C. (2013) 'Emerging roles for centromere-associated proteins in DNA repair and genetic recombination.', *Biochemical Society transactions*, 41(6), pp. 1726–1730. doi: 10.1042/BST20130200.

Paíno, T., Paiva, B., Sayagués, J. M., Mota, I., Carvalheiro, T., Corchete, L. A., Aires-Mejía, I., Pérez, J. J., Sanchez, M. L., Barcena, P., Ocio, E. M., San-Segundo, L., Sarasquete, M. E., García-Sanz, R., Vidriales, M.-B., Oriol, A., Hernández, M.-T., Echeveste, M.-A., Paiva, A., Blade, J., Lahuerta, J.-J., Orfao, A., Mateos, M.-V., Gutiérrez, N. C. and San-Miguel, J. F. (2015) 'Phenotypic identification of subclones in multiple myeloma with different chemoresistant, cytogenetic and clonogenic potential', *Leukemia*, 29(5), pp. 1186–1194. doi: 10.1038/leu.2014.321.

Pajic, M., Herrmann, D., Vennin, C., Conway, J. R., Chin, V. T., Johnsson, A.-K. E., Welch, H. C. and Timpson, P. (2015) 'The dynamics of Rho GTPase signaling and implications for targeting cancer and the tumor microenvironment', *Small GTPases*, 6(2), pp. 123–133. doi: 10.4161/21541248.2014.973749.

Palumbo, A. and Anderson, K. (2011) 'Multiple myeloma.', *The New England journal of medicine*, 364(11), pp. 1046–1060. doi: 10.1056/NEJMra1011442.

Pieper, K., Grimbacher, B. and Eibel, H. (2013) 'B-cell biology and development', *Journal of Allergy and Clinical Immunology*, pp. 959–971. doi: 10.1016/j.jaci.2013.01.046.

Platani, M., Santarella-Mellwig, R., Posch, M., Walczak, R., Swedlow, J. R. and Mattaj, I. W. (2009) 'The Nup107-160 nucleoporin complex promotes mitotic events via control of the localization state of the chromosome passenger complex.', *Molecular biology of the cell*, 20(24), pp. 5260–75. doi: 10.1091/mbc.E09-05-0377.

Podar, K., Chauhan, D. and Anderson, K. C. (2009) 'Bone marrow microenvironment and the identification of new targets for myeloma therapy.', *Leukemia*, 23(1), pp. 10–24. doi: 10.1038/leu.2008.259.

Pollok, S., Stoepel, J., Bauerschmidt, C., Kremmer, E. and Nasheuer, H.-P. (2003) 'Regulation of eukaryotic DNA replication at the initiation step.', *Biochemical Society transactions*, 31, pp. 266–269. doi: 10.1042/.

Raftopoulou, M. and Hall, A. (2004) 'Cell migration: Rho GTPases lead the way', *Developmental Biology*, pp. 23–32. doi: 10.1016/j.ydbio.2003.06.003.

Ramsay, A. G., Evans, R., Kiaii, S., Svensson, L., Hogg, N. and Gribben, J. G. (2013) 'Chronic lymphocytic leukemia cells induce defective LFA-1-directed T-cell motility by altering Rho

GTPase signaling that is reversible with lenalidomide.', *Blood*, 121(14), pp. 2704–2714. doi: 10.1182/blood-2012-08-448332.

Rickert, R. C. (2013) 'New insights into pre-BCR and BCR signalling with relevance to B cell malignancies.', *Nature reviews. Immunology*, 13(8), pp. 578–91. doi: 10.1038/nri3487.

Risse, S. L., Vaz, B., Burton, M. F., Aspenström, P., Piekorz, R. P., Brunsveld, L. and Ahmadian, M. R. (2013) 'SH3-mediated targeting of Wrch1/RhoU by multiple adaptor proteins', *Biological Chemistry*, 394(3), pp. 421–432. doi: 10.1515/hsz-2012-0246.

Roset, R., Inagaki, A., Hohl, M., Brenet, F., Lafrance-Vanasse, J., Lange, J., Scandura, J. M., Tainer, J. A., Keeney, S. and Petrini, J. H. J. (2014) 'The Rad50 hook domain regulates DNA damage signaling and tumorigenesis', *Genes and Development*, 28(5), pp. 451–462. doi: 10.1101/gad.236745.113.

Roy, N., Bagchi, S. and Raychaudhuri, P. (2012) 'Damaged DNA binding protein 2 in reactive oxygen species (ROS) regulation and premature senescence', *International Journal of Molecular Sciences*, 13(9), pp. 11012–11026. doi: 10.3390/ijms130911012.

Saito, Y. and Komatsu, K. (2015) 'Functional Role of NBS1 in Radiation Damage Response and Translesion DNA Synthesis', *Biomolecules*, 5(3), pp. 1990–2002. doi: 10.3390/biom5031990.

Schiavone, D., Dewilde, S., Vallania, F., Turkson, J., Di Cunto, F. and Poli, V. (2009) 'The RhoU/Wrch1 Rho GTPase gene is a common transcriptional target of both the gp130/STAT3 and Wnt-1 pathways.', *The Biochemical journal*, 421, pp. 283–292. doi: 10.1042/BJ20090061.

Schust, J., Sperl, B., Hollis, A., Mayer, T. U. and Berg, T. (2006) 'Stattic : A Small-Molecule Inhibitor of STAT3 Activation and Dimerization', *Chemistry & Biology*, 13, pp. 1235–1242. doi: 10.1016/j.chembiol.2006.09.018.

Shutes, A., Berzat, A. C., Cox, A. D. and Der, C. J. (2004) 'Atypical mechanism of regulation of the Wrch-1 rho family small GTPase', *Current Biology*, 14(22), pp. 2052–2056. doi: 10.1016/j.cub.2004.11.011.

Smithers, C. C. and Overduin, M. (2016) 'Structural Mechanisms and Drug Discovery Prospects of Rho GTPases', *Cells*, 5(26), pp. 1–15. doi: 10.3390/cells5020026.

Song, H., Park, J. E. and Jang, C. Y. (2015) 'DDA3 targets Cep290 into the centrosome to regulate spindle positioning', *Biochemical and Biophysical Research Communications*, 463(1–2), pp. 88–94. doi: 10.1016/j.bbrc.2015.05.028.

Strasser, K. and Ludwig, H. (2002) 'Thalidomide treatment in multiple myeloma', *Blood Reviews*, pp. 207–215. doi: 10.1016/S0268-960X(02)00031-0.

Tao, W., Pennica, D., Xu, L., Kalejta, R. F. and Levine, A. J. (2001) 'Wrch-1, a novel member of the Rho gene family that is regulated by Wnt-1', *Genes and Development*, 15(14), pp. 1796–1807. doi: 10.1101/gad.894301.

Thomas, Y., Coux, O. and Baldin, V. (2010) 'βTrCP-dependent degradation of CDC25B phosphatase at the metaphase-anaphase transition is a pre-requisite for correct mitotic exit', *Cell Cycle*, 9(21), pp. 4338–4350. doi: 10.4161/cc.9.21.13593.

Todoerti, K., Agnelli, L., Fabris, S., Lionetti, M., Tuana, G., Mosca, L., Lombardi, L., Grieco, V., Bianchino, G., D'Auria, F., Statuto, T., Mazzoccoli, C., De Luca, L., Petrucci, M. T., Morabito, F., Offidani, M., Raimondo, F. Di, Falcone, A., Omede, P., Tassone, P., Boccadoro, M., Palumbo, A., Neri, A. and Musto, P. (2013) 'Transcriptional characterization of a prospective series of primary plasma cell leukemia revealed signatures associated with tumor progression and poorer outcome', *Clinical Cancer Research*, 19(12), pp. 3247–3258. doi: 10.1158/1078-0432.CCR-12-

3461.

Tusher, V. G., Tibshirani, R. and Chu, G. (2001) 'Significance analysis of microarrays applied to the ionizing radiation response.', *Proceedings of the National Academy of Sciences of the United States of America*, 98(9), pp. 5116–21. doi: 10.1073/pnas.091062498.

Vega, F. M. and Ridley, A. J. (2008) 'Rho GTPases in cancer cell biology', *FEBS Letters*, pp. 2093–2101. doi: 10.1016/j.febslet.2008.04.039.

Vetter, I. R. and Wittinghofer, a (2001) 'The guanine nucleotide-binding switch in three dimensions.', *Science (New York, N.Y.)*, 294(5545), pp. 1299–1304. doi: 10.1126/science.1062023.

Wang, J. Y., Yu, P., Chen, S., Xing, H., Chen, Y., Wang, M., Tang, K., Tian, Z., Rao, Q. and Wang, J. (2013) 'Activation of Rac1 GTPase promotes leukemia cell chemotherapy resistance, quiescence and niche interaction', *Molecular Oncology*, 7(5), pp. 907–916. doi: 10.1016/j.molonc.2013.05.001.

Wäsch, R., Robbins, J. a and Cross, F. R. (2010) 'The emerging role of APC/CCdh1 in controlling differentiation, genomic stability and tumor suppression.', *Oncogene*, 29(1), pp. 1–10. doi: 10.1038/onc.2009.325.

Weisz Hubsman, M., Volinsky, N., Manser, E., Yablonski, D. and Aronheim, A. (2007) 'Autophosphorylation-dependent degradation of Pak1, triggered by the Rho-family GTPase, Chp.', *The Biochemical journal*, 404(3), pp. 487–497. doi: 10.1042/BJ20061696.

Wennerberg, K., Rossman, K. L. and Der, C. J. (2005) 'The Ras superfamily at a glance', *Journal of Cell Science*, 118, pp. 843–846. doi: 10.1242/jcs.094300.

Wu, J., Lu, L. Y. and Yu, X. (2010) 'The role of BRCA1 in DNA damage response', *Protein and Cell*, pp. 117–123. doi: 10.1007/s13238-010-0010-5.

Xiong, Q., Zhong, Q., Zhang, J., Yang, M., Li, C., Zheng, P., Bi, L. J. and Ge, F. (2012) 'Identification of novel miR-21 target proteins in multiple myeloma cells by quantitative proteomics', *Journal of Proteome Research*, 11(4), pp. 2078–2090. doi: 10.1021/pr201079y.

Xu, Y., Li, J., Ferguson, G. D., Mercurio, F., Khambatta, G., Morrison, L., Lopez-Girona, A., Corral, L. G., Webb, D. R., Bennett, B. L. and Xie, W. (2009) 'Immunomodulatory drugs reorganize cytoskeleton by modulating Rho GTPases', *Blood*, 114(2), pp. 338–345. doi: 10.1182/blood-2009-02-200543.

Yang, F. C., Atkinson, S. J., Gu, Y., Borneo, J. B., Roberts, A. W., Zheng, Y., Pennington, J. and Williams, D. A. (2001) 'Rac and Cdc42 GTPases control hematopoietic stem cell shape, adhesion, migration, and mobilization.', *Proceedings of the National Academy of Sciences of the United States of America*, 98(10), pp. 5614–8. doi: 10.1073/pnas.101546898.

Yang, L., Wang, L., Geiger, H., Cancelas, J. A., Mo, J. and Zheng, Y. (2007) 'Rho GTPase Cdc42 coordinates hematopoietic stem cell quiescence and niche interaction in the bone marrow.', *Proceedings of the National Academy of Sciences of the United States of America*, 104(12), pp. 5091–6. doi: 10.1073/pnas.0610819104.

FEATURED PUBLICATIONS

SCIENTIFIC ARTICLES

Mandato E., Zaffino F., Casellato A., Pizzi M., Macaccaro P., Vitulo N., **Canovas Nunes S.**, Quotti Tubi L., Zumerle S., Manni S., Filhol-Cochet O., Boldyreff B., Siebel C., Rugge M., Viola A., Valle G., Trentin L., Semenzato G., PiazzaF.
CK2 regulates B cell commitment and the germinal center reaction counteracting NOTCH2 and sustaining the BCR signaling in mice
Blood, *submitted.*

Manni S., Carrino M., Manzoni M., Gianesin K., **Canovas Nunes S.**, Costacurta M., Quotti Tubi L., Macaccaro P., Taiana E., Cabrelle A., Barilà G., Martines A., Zambello R., Bonaldi L., Trentin L., Neri A., Semenzato G., Piazza F.
Inactivation of CK1α in multiple myeloma empowers drug cytotoxicity by affecting AKT and β-catenin survival signaling pathways.
Oncotarget. 2017 Jan 14. doi: 10.18632/oncotarget.14654. [Epub ahead of print]

Quotti Tubi L., **Canovas Nunes S.**, Brancalion A., Doriguzzi Breatta E., Manni S., Mandato E., Zaffino F., Macaccaro P., Carrino M., Gianesin K., Trentin L., Binotto G., Zambello R. Semenzato G., Gurrieri C., Piazza F.
Protein kinase CK2 regulates AKT, NF-κB and STAT3 activation, stem cell viability and proliferation in acute myeloid leukemia.
Leukemia. 2016 Sep 2. doi: 10.1038/leu.2016.209. [Epub ahead of print]

CONFERENCE PRESENTATIONS

Canovas Nunes S., Carrino M., Mandato E., Quotti Tubi L., Zaffino F., Manni S., Semenzato G., Piazza F.
The role of RhoU GTPase in the cross-talk between neoplastic plasma cells and bone marrow microenvironment in multiple myeloma.
XIV National SIES Congress - Italian Society of Experimental Haematology, Rimini (IT) 2016

Carrino M., Manni S., **Canovas Nunes S**., Macaccaro P., Gianesin K., Quotti Tubi L., Cabrelle A., Semenzato G., Piazza F.
CK1α inactivation triggers autophagy in multiple myeloma.
XIV National SIES Congress - Italian Society of Experimental Haematology, Rimini (IT) 2016

Quotti Tubi L., **Canovas Nunes S.**, Doriguzzi Breatta E., Zaffino F., Mandato E., Macaccaro P., Manni S., Boldyreff B., Filhol-Cochet O., Gurrieri C. and Piazza F.
Knockout of Csnk2b during hematopoiesis results in mid/late gestation lethality mainly due to impaired fetal erythropoiesis.

XIII National SIES Congress - Italian Society of Experimental Haematology, Rimini (IT) 2014

CONFERENCE POSTERS

Canovas Nunes S., Mandato E., Carrino M., Manni M., Manzoni M., Neri A., Piazza F.
Role of the atypical GTPase RhoU in Plasma Cell malignancies
International retreat of PhD students in immunology, Napoli (IT) 2016

Mandato E., Zaffino F., Pizzi M., Macaccaro P., **Canovas Nunes S.**, Quotti Tubi L., Filhol-Cochet O., Boldyreff B., Siebel C., PiazzaF.
Protein kinase CK2beta orchestrates mature B cell commitment, plasma cell generation and antibody response
International retreat of PhD students in immunology, Napoli (IT) 2016

Canovas Nunes S., Carrino M., Mandato E., Quotti Tubi L., Zaffino F., Manni S., Semenzato G., Piazza F.
RhoU GTPase: a novel potential target to disrupt multiple myeloma plasma cell interaction with protective bone marrow niches.
21st Congress of the European Hematology Association (EHA), Copenhagen (DK) 2016

Manni S., Carrino M., **Canovas Nunes S**., Gianesin K., Macaccaro P., Quotti Tubi L., Cabrelle A., Semenzato G., Piazza F.
Protein kinase CK1α inactivation in multiple myeloma empowers lenalidomide induced cytotoxicity and cell cycle arrest.
21st Congress of the European Hematology Association (EHA), Copenhagen (DK) 2016

Carrino M., Manni S., **Canovas Nunes S**., Macaccaro P., Gianesin K., Quotti Tubi L., Cabrelle A., Semenzato G., Piazza F.
Targeting protein kinase CK1α in the bone marrow microenvironment: a new possible therapeutic approach for multiple myeloma therapy?
21st Congress of the European Hematology Association (EHA), Copenhagen (DK) 2016

Canovas Nunes S., Carrino M., Mandato E., Quotti Tubi L., Zaffino F., Manni S., Semenzato G., Piazza F.
RhoU expression changes in multiple myeloma reveal a possible correlation with bone marrow microenvironment dependence.
EMBO|EMBL Symposium: Tumour Microenvironment and Signalling, Heidelberg (DE) 2016

Carrino M., Manni S., **Canovas Nunes S**., Macaccaro P., Gianesin K., Quotti Tubi L., Cabrelle A., Semenzato G., Piazza F.
CK1α inactivation overcomes bone marrow microenvironment protection inducing multiple myeloma cell death.

EMBO|EMBL Symposium: Tumour Microenvironment and Signalling, Heidelberg (DE) 2016

Quotti Tubi L., **Canovas Nunes S**., Casellato A., Mandato E., Zaffino F., Brancalion A., Filhol-Cochet O., Boldyreff B., Manni S., Semenzato G., Piazza F.
Csnk2β knockout during hematopoiesis results in lethality at mid/late gestation mostly due to impaired fetal erythropoiesis.
56th ASH annual meeting, San Francisco (USA) 2014.

Canovas Nunes S., Quotti Tubi L., Mandato E., Carrino M., Zaffino F., Manni S., Zambello R., Adami F., Trentin L., Semenzato G., Piazza F.
Analysis of RhoU and RhoV expression in Multiple Myeloma reveals a possible correlation with bone marrow dependence.
20th Congress of the European Hematology Association (EHA), Vienna (AT) 2015

Mandato E., Zaffino F., Casellato A., Macaccaro P., **Canovas Nunes S.**, Pizzi M., Trentin L., Semenzato G., Piazza F.
Protein kinase CK2 in Diffuse Large B-cell Lymphoma: Defining its role to shape new therapies.
20th Congress of the European Hematology Association (EHA), Vienna (AT) 2015

AKNOWLEDGMENTS

First of all, I want to thank my mother for always pushing me forward and teaching me never to give up. I owe her my thirst for knowledge and the desire to be always better in what I do.

There are many people whose direction, advice, support and contributions have brought me here. For this reason I want to thank all my colleges and my supervisor that help me realize every day the kind of scientist I want to become (and the one I'll be sure never to).

Thank you to our collaborators in Milan for the help and support with the analysis of the gene expression profiling data; and to the pathologist of our department who helped with the acquisition of IHC pictures.

Last but not least, to my partner without whom I would have never started this PhD. And to all my friends and family (near or far), without them cutting this finish line would not taste the same.

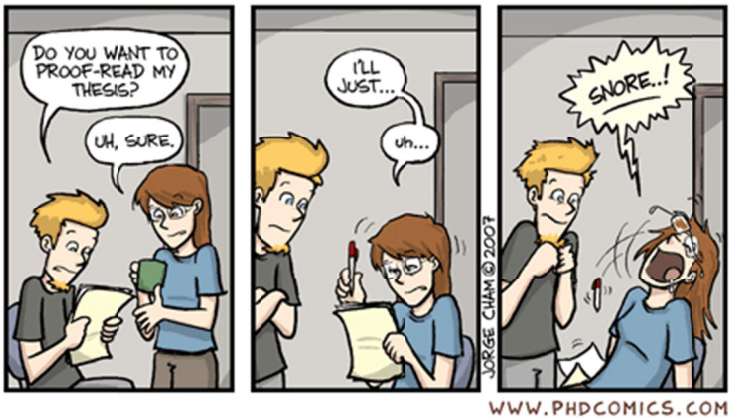

P.S. A special thanks goes to those who have proof-red my thesis.